VERIFICATION AND LOCAL CALIBRATION/VALIDATION OF THE MEPDG PERFORMANCE MODELS FOR USE IN GEORGIA

Calibration of the MEPDG Transfer Functions in Georgia

Task Order 2 Report

Submitted to:

Office of Research and Office of Materials Testing
15 Kennedy Drive
Forest Park, Georgia 30297

Submitted by:

Harold L. Von Quintus, P.E.
Michael I. Darter, P.E.
Biplab B. Bhattacharya, P.E.
Leslie Titus-Glover
Applied Research Associates, Inc.
100 Trade Center Drive, Suite 200
Champaign, IL, 61820

October 28, 2014
Revised: March 28, 2015

Notice

This document is disseminated under the sponsorship of the Georgia Department of Transportation (DOT) and the U.S. Department of Transportation in the interest of information exchange. The Georgia DOT and U.S. Government assume no liability for the use of the information contained in this document. This report does not constitute a standard, specification, or regulation.

The Georgia DOT or U.S. Government does not endorse products or manufacturers. Trademarks or manufacturers' names appear in this report only because they are considered essential to the objective of the document.

Quality Assurance Statement

The Georgia DOT and Federal Highway Administration (FHWA) provide high-quality information to serve Government, industry, and the public in a manner that promotes public understanding. Standards and policies are used to ensure and maximize the quality, objectivity, utility, and integrity of its information. Georgia DOT the FHWA periodically review quality issues and adjusts its programs and processes to ensure continuous quality improvement.

TECHNICAL DOCUMENTATION PAGE

1. Report No. FHWA/GA-014-11-17	2. Government Accession No.	3. Recipient's Catalog No.
4. Title and Subtitle Calibration of the MEPDG Transfer Functions in Georgia		5. Report Date October 28, 2014 Revised: March 28, 2015
		6. Performing Organization Code
7. Author(s) Mr. Harold L. Von Quintus, P.E., Dr. Michael I. Darter, P.E., Dr. Biplab Bhattacharya, P.E., and Mr. Leslie Titus-Glover		8. Performing Organization Report No.
9. Performing Organization Name and Address Applied Research Associates, Inc. 100 Trade Centre Blvd., Suite #200 Champaign, Illinois 61820		10. Work Unit No. (TRAIS) 11. Contract or Grant No. TOOMRPRO130020
12. Sponsoring Agency Name and Address Georgia Department of Transportation One Georgia Center, 19th Floor 600 West Peachtree Street, NW Atlanta, Georgia 30308		13. Type of Report and Period Covered Task 4 Interim Report – Task Order #2 14. Sponsoring Agency Code
15. Supplementary Notes The Contracting Officer's Technical Representative (COTR) was Mr. Steve Pahno		

16. Abstract

The Georgia Department of Transportation (GDOT) currently uses the empirical 1972 AASHTO Interim Guide for Design of Pavement Structures as their standard pavement design procedure. However, GDOT plans to transition to the Mechanistic Empirical Pavement Design Guide (MEPDG) for designing new and rehabilitated highway pavements. As a part of the transitioning process, GDOT has sponsored an implementation project. One part of the implementation project is to verify the MEPDG global distress transfer functions and calibrate these functions to local conditions, if determined to be necessary. The Georgia Long-Term Pavement Performance (LTPP) and non-LTPP roadway segments were used for this verification-calibration process.

As noted above, one objective of the implementation project was to verify or confirm that the MEPDG transfer functions and global calibration coefficients derived from NCHRP project 1-40D reasonably predict distresses and smoothness in Georgia. The Task 2 interim report focused on using the Georgia LTPP test sections to confirm the applicability of the global calibration coefficients. The Task 2 interim report concluded some of the transfer functions exhibited significant bias between the measured and predicted distress and require local calibration.

This report documents the local calibration of the transfer functions using LTPP and non-LTPP roadway segments. The calibration process follows the procedure presented in the 2010 AASHTO MEPDG Local Calibration Guide. Local calibration coefficients were derived to remove that bias for the rutting, fatigue cracking, and thermal cracking transfer functions of flexible pavements, and the faulting and fatigue cracking transfer functions of rigid pavements. The global coefficients of the smoothness degradation regression equation for flexible and rigid pavements were also checked for their applicability to Georgia conditions.

17. Key Words Mechanistic-Empirical Pavement Design Guide, ME Design, Transfer Functions, Fatigue Cracking, Rutting, Thermal Cracking, Faulting, Mid-Slab Cracking, IRI.		18. Distribution Statement No restrictions.	
19. Security Classification of this report: Unclassified	20. Security Classification (of this page): Unclassified	21. No. of Pages 112	22. Price

Form DOT F 1700.7 (8-72) Reproduction of completed page authorized

SI* (MODERN METRIC) CONVERSION FACTORS

APPROXIMATE CONVERSIONS TO SI UNITS

Symbol	When You Know	Multiply By	To Find	Symbol
		LENGTH		
in	inches	25.4	millimeters	mm
ft	feet	0.305	meters	m
yd	yards	0.914	meters	m
mi	miles	1.61	kilometers	km
		AREA		
in^2	square inches	645.2	square millimeters	mm^2
ft^2	square feet	0.093	square meters	m^2
yd^2	square yard	0.836	square meters	m^2
ac	acres	0.405	hectares	ha
mi^2	square miles	2.59	square kilometers	km^2
		VOLUME		
fl oz	fluid ounces	29.57	milliliters	mL
gal	gallons	3.785	liters	L
ft^3	cubic feet	0.028	cubic meters	m^3
yd^3	cubic yards	0.765	cubic meters	m^3
	NOTE: volumes greater than 1000 L shall be shown in m^3			
		MASS		
oz	ounces	28.35	grams	g
lb	pounds	0.454	kilograms	kg
T	short tons (2000 lb)	0.907	megagrams (or "metric ton")	Mg (or "t")
		TEMPERATURE (exact degrees)		
^oF	Fahrenheit	5 (F-32)/9 or (F-32)/1.8	Celsius	^oC
		ILLUMINATION		
fc	foot-candles	10.76	lux	lx
fl	foot-Lamberts	3.426	$candela/m^2$	cd/m^2
		FORCE and PRESSURE or STRESS		
lbf	poundforce	4.45	newtons	N
lbf/in^2	poundforce per square inch	6.89	kilopascals	kPa

APPROXIMATE CONVERSIONS FROM SI UNITS

Symbol	When You Know	Multiply By	To Find	Symbol
		LENGTH		
mm	millimeters	0.039	inches	in
m	meters	3.28	feet	ft
m	meters	1.09	yards	yd
km	kilometers	0.621	miles	mi
		AREA		
mm^2	square millimeters	0.0016	square inches	in^2
m^2	square meters	10.764	square feet	ft^2
m^2	square meters	1.195	square yards	yd^2
ha	hectares	2.47	acres	ac
km^2	square kilometers	0.386	square miles	mi^2
		VOLUME		
mL	milliliters	0.034	fluid ounces	fl oz
L	liters	0.264	gallons	gal
m^3	cubic meters	35.314	cubic feet	ft^3
m^3	cubic meters	1.307	cubic yards	yd^3
		MASS		
g	grams	0.035	ounces	oz
kg	kilograms	2.202	pounds	lb
Mg (or "t")	megagrams (or "metric ton")	1.103	short tons (2000 lb)	T
		TEMPERATURE (exact degrees)		
^oC	Celsius	1.8C+32	Fahrenheit	^oF
		ILLUMINATION		
lx	lux	0.0929	foot-candles	fc
cd/m^2	$candela/m^2$	0.2919	foot-Lamberts	fl
		FORCE and PRESSURE or STRESS		
N	newtons	0.225	poundforce	lbf
kPa	kilopascals	0.145	poundforce per square inch	lbf/in^2

*SI is the symbol for the International System of Units. Appropriate rounding should be made to comply with Section 4 of ASTM E380.
(Revised March 2003)

Table of Contents

LIST OF FIGURES

Figure Number **Page No.**

LIST OF TABLES

Table Number **Page No.**

ABBREVIATIONS

AADTT	Average Annual Daily Truck Traffic
AASHTO	American Association of State and Highway Transportation Officials
AC	Asphalt Concrete
ARA	Applied Research Associates, Inc.
ATB	Asphalt Treated Base
AVC	Automated Vehicle Classification
CRCP	Continuously Reinforced Concrete Pavement
CTB	Cement Treated Base
CTE	Coefficient of Thermal Expansion
DCP	Dynamic Cone Penetrometer
DOT	Department of Transportation
FHWA	Federal Highway Administration
FWD	Falling Weight Deflectometer
GDOT	Georgia Department of Transportation
GPS	General Pavement Study and Global Positioning System
HMA	Hot Mix Asphalt
ICM	Integrated Climate Model
IRI	International Roughness Index
JPCP	Jointed Plain Concrete Pavement
LTPP	Long Term Pavement Performance
MAF	Monthly Adjustment Factor
NALS	Normalized Axle Load Spectra
NCAT	National Center for Asphalt Technology
PCC	Portland Cement Concrete
RAP	Recycled Asphalt Pavement
SEE	Standard Error of the Estimate
SPS	Special Pavement Study
TTC	Truck Traffic Classification
WIM	Weigh-In-Motion

CALIBRATION OF THE MECHANISTIC-EMPIRICAL PAVEMENT DESIGN GUIDE IN GEORGIA

I. INTRODUCTION

1.1 Background

Many highway agencies, including the Georgia Department of Transportation (GDOT), are transitioning from empirical design procedures to the Mechanistic-Empirical Pavement Design Guide (MEDPG) procedure for designing new and rehabilitated pavements.[1] The MEPDG is a part of the American Association of State Highway and Transportation Officials (AASHTO) software *Pavement ME Design* and uses mechanistic-empirical (ME) principles. This procedure is a significant departure from the existing empirical procedures (such as the 1972 and 1993 AASHTO procedures). GDOT currently uses the 1972 AASHTO Interim Guide for Design of Pavement Structures as its standard pavement design procedure.

The MEPDG distress transfer functions and prediction methodology were calibrated using data from the Long Term Pavement Performance (LTPP) program under National Cooperative Highway Research Program (NCHRP) projects 1-37A and 1-40D (NCHRP, 2004 and 2006). A transfer function is defined as a mathematical relationship that transfers computed mechanistic pavement responses (stresses, strains, and/or deflections) into what is observed or measured on the pavement surface.

The global calibration effort, however, cannot consider all potential factors that can occur throughout all agencies, materials, design strategies, and climates found in North America. Factors such as maintenance strategies, construction specifications, aggregate and binder type, mixture design procedures, and material specifications can result in performance differences – all other factors being equal. In fact, small differences in some of the above factors can cause large differences in performance.

The overall objective of the implementation process was to validate and re-calibrate, if necessary, the transfer functions. In other words, adjusting the distress and smoothness prediction models or transfer functions so that they accurately represent the performance of GDOT roadways. Local calibration will enable GDOT to use the MEPDG with confidence for the design of new and rehabilitated pavements.

The implementation process also integrates GDOT's operational policies, material and construction specifications, truck traffic, and climate to streamline the design process for day-to-day use. As such, another objective of the implementation study was to ensure that all of the input parameters are adequately defined and can be determined with no to minimal changes in GDOT day-to-day procedures so that it is practical.

The proposed work plan to implement the MEPDG into GDOT's day-to-day practice consisted of seven tasks grouped into three task orders:

[1] Task 1 Interim Report: Literature Search and Synthesis; Verification and Local Calibration/Validation of the MEPDG Performance Models for Use in Georgia, Report #GADOT-TO-01-Task 1, July 16, 2013.

- Task Order #1:
    - Task 1—Literature Search/ Synthesis and Two Draft Verification Work Plans
    - Task 2—Verification using LTPP Test Sections located in Georgia
- Task Order #2:
    - Task 3—Development of a Sampling Matrix and Selection of Non-LTPP Sites for Calibration
    - Task 4—Calibration of the Distress Transfer Functions
- Task Order #3:
    - Task 5—Validation of the Distress Transfer Functions
    - Task 6—Design Manual
    - Task 7—Final Report

Results from the Task 2 work found significant bias for some of the distress transfer functions. This report is based on the Task 2 verification report.[2] It addresses Tasks 3 through 5 using the LTPP and non-LTPP test sections located in Georgia to calibrate and validate the distress transfer functions included in the MEPDG software and Manual of Practice (AASHTO, 2008).

1.2 Objective

The objective of Tasks 3 to 5 was to determine the local calibration coefficients of the MEPDG transfer functions to eliminate the bias found and reported in the verification report (Task 2). The calibration process followed the procedure presented in the AASHTO MEPDG Local Calibration Guide (AASHTO, 2010). This report documents use of the LTPP and non-LTPP sites in Georgia and determination of the Georgia calibration coefficients to accurately predict distress and smoothness using the MEPDG.

1.3 Scope of Work

As stated above, it is impossible to account for all factors in developing a global distress/performance simulation model. All models have errors because of simplifying assumptions, so it is good practice to evaluate the applicability of any conceptual and/or statistical model on a limited basis prior to full-scale use.

The LTPP test sections were used to determine if there are significant differences between the measured and predicted distresses using the global calibration factors of the MEPDG conceptual models or transfer functions. The global calibration coefficients for each transfer function are included in Section 5 of the MEPDG Manual of Practice (AASHTO, 2008).

Significant bias was found in some of the transfer functions for both flexible and rigid pavements, which is reported in the verification task of this project. In addition, an initial sampling matrix was developed to eliminate the bias for a range of pavement features and site conditions considered important to and defined by GODT.

[2] Task 2 Interim Report: Validation of the MEPDG Transfer Functions Using the LTPP Test Sections in Georgia, Report #GADOT-TO-01-Task 2, July 16, 2013

The scope of work for this portion of the project was to define the local or Georgia calibration coefficients and consisted of the following activities:

- *Continue to Review Results from GDOT Sponsored Studies:* This activity is a continuation of Task Order No. 1 to review the results from on-going or recently completed projects sponsored by GDOT and other agencies.
- *Prepare Sampling Matrix:* This task was completed under Work Order No. 1, and the sampling matrices for flexible and rigid pavements were included in the Task 2 Interim Report. The sampling matrices for flexible and rigid pavements, however, were reviewed and revised in terms of specific non-LTPP roadway segments selected for use in calibrating the MEPDG software to Georgia conditions and materials.
- *Identify Differences between LTPP and Non-LTPP Distress Data:* Any difference in distress magnitudes found between the LTPP and non-LTPP roadway segments needs to be explained and eliminated. The impact of any difference between the way FHWA/LTPP and GDOT measure distress will increase the residual and standard errors of the transfer functions. This difference, if any is found, needs to be identified and accounted for as part of the local calibration process.
- *Select Non-LTPP Roadway Segments:* The original scope of services for this project was to minimize any field and laboratory testing. Field investigations, however, are needed to determine the layer properties of the non-LTPP segments, and also confirm the data extracted from the project construction files. Field investigations were also used to categorize and define the type of cracking exhibited along each calibration section.
- *Execute ME Design Software using Data Recovered from Project Files:* The *Pavement ME Design*™ software was used to predict the distress and performance of each non-LTPP roadway segment based on data recovered from the project files and other available information. The result from this activity was used to prioritize the sites for the field investigations.
- *Laboratory Testing of Selected Materials:* Selected volumetric properties of the asphalt concrete mixtures were measured in the laboratory.
- *Execute ME Design Software for the LTPP and Non-LTPP Sites:* The appropriate input parameters for each of the LTPP and non-LTPP segments were determined for each calibration site. This activity was used to determine the Georgia default input values or confirm the applicability of the global default input values that were unavailable from GDOT's construction files or the LTPP database.
- *Compare and Evaluate the Residual Errors*: The measured and predicted distresses were compared and evaluated in accordance with the appropriate sampling matrix or template. The residual errors (difference between the measured and predicted distress) were investigated as to whether the errors were dependent on the primary tiers or factors of the sampling matrix and other factors (for example; LTPP versus non-LTPP sections). The residual errors and their dependency on or independence from the primary factors were used to determine the Georgia calibration coefficients.

II. SAMPLING MATRICES AND FACTORIALS

The distress transfer functions and IRI regression equations were calibrated using a wide range of pavement sections located across North America. Global models, however, require confirmation at the local level to ensure their accuracy and unbiasedness to local conditions and operational or management policies. A verification or confirmation study was performed under Task Order 1 to determine if significant differences exist between the global calibration factors and those applicable to Georgia conditions and materials. The verification study in Task Order 1 was limited to the FHWA LTPP test sections located in Georgia.[3]

Significant differences were found and reported in the Task 2 interim report between the predicted and measured performance indicators (individual distresses and smoothness as measured by the International Roughness Index [IRI]). The factors causing the difference need to be identified so adjustments can be made to the global calibration coefficients. This section of the report presents the sampling matrices, as well as the LTPP and non-LTPP roadway segments identified for use to determine the Georgia calibration coefficients.

2.1 LTPP Test Sections

Preliminary sampling matrices or factorials were prepared for the flexible and rigid pavements using the LTPP sections. The preliminary factorials are provided in Tables 1 and 2 for flexible and rigid pavements, respectively, but mostly represent past GDOT design practices and material specifications. Figure 1 shows the geographic distribution of the LTPP sites in Georgia, while Table 3 provides the global positioning system (GPS) coordinates and other location information for these sites. In summary, there are an insufficient number of sites for local calibration when limited to the LTPP test sections, especially for the rigid pavements.

The following summarizes the items that have a significant impact on pavement performance but were not included as features/factors in the Georgia LTPP test sections but do represent typical construction practice in Georgia.

- Polymer modified asphalt (PMA) mixtures and mixtures with varying amounts of recycled asphalt pavement (RAP). The use of PMA mixtures and mixtures with high RAP contents has a significant impact on performance that is well documented in the literature.
    - GDOT typically uses less than 20 percent RAP in their mixtures, but half of the Special Pavement Study (SPS) 5 experimental test sections included mixtures with 30+ percent RAP. GDOT revised its material specifications during the period when Superpave mixture system was being adopted because the performance of mixtures with higher RAP contents exhibited inferior performance. Thus, RAP was excluded as a primary factor in the sampling

[3] Note: Task Order #1 did not include the non-FHWA LTPP calibration sections which are included the Georgia LTPP Project which was specifically established for future calibration efforts of the MEPDG in Georgia. The Georgia LTPP project was established and is being completed through a study being conducted by the School of Electrical and Computer Engineering, Georgia Institute of Technology; Contact is Yi-Ching Wu.

matrix or template but does represent a potential confounding factor embedded in the flexible pavement sampling template.

- PMA mixtures are typically used in Georgia on higher volume roadways, while neat (unmodified) mixtures are used in lower volume roadways. Multiple studies have concluded that PMA mixtures provide enhanced performance which is not properly accounted for by the MEPDG distress prediction methodology. Thus, it was included as a primary factor in the flexible pavement sampling template.

Table 1—Number of LTPP Test Sections: Flexible or Semi-Rigid Pavements, New Construction and Rehabilitations

Flexible Pavement Type			Number of Test Sections			
			With Full Time Series Data		With Only One or Two Observations	
			Site ID	Number	Site ID	Number
New Construction	Flexible Pavement	Conventional	1001, 1004, 1005, 4111	4		0
		Full Depth or Deep Strength	1031, 4112, 4113, 4119	4	SPS-5 Sections	15[1]
	Semi-Rigid Pavement		4092, 4093, 4096, 4420	4		0
Rehabilitation	HMA Overlay of Flexible Pavement		SPS-5 Sections[2]	15		0
			1031, 4112; 4113	3		0
	HMA Overlay of Semi-Rigid Pavement		4096, 4420	2		0
TOTAL			**32**		**15**	

NOTES:
1. Although there are 15 sections with performance data, these sections only represent one project.
2. There are 15 individual test sections which represent only 4 calibration projects (RAP versus non-RAP or virgin mixtures or thin versus thick overlays).

- Pavement preservation treatments were not included on any of the LTPP test sections for both types of pavements. GDOT has implemented and used pavement preservation program to extend pavement service life for Portland cement concrete (PCC) and hot mix asphalt (HMA) pavements. The program was found to be very beneficial. Calibration of the MEPDG should consider or include this benefit, but the MEPDG does not have the capability to directly consider the impact of different pavement preservation methods. Most preservation methods do not add structural value to the existing pavement. Thus, another confounding factor of the sampling template is pavement preservation because of the potential difference in performance between LTPP and non-LTPP sections. A calibration issue is how to handle the extended use of different pavement preservation treatment methods in Georgia, which is discussed below.

The Montana Department of Transportation (MDOT) is the only agency where pavement preservation methods were considered within the calibration process to date (Von Quintus and Moulthrop, 2007). It is expected that a similar type of procedure be used to eliminate bias in the predictions of distress and consider the impact of preservation methods on enhancing performance. Michigan DOT is identifying methods to account for or consider the benefit of using aggressive preservation programs in terms of the MEPDG (Von Quintus and Perera, 2011). Arizona DOT has sufficient performance data on preservation methods and investigated how that data can be used to adjust or determine their local calibration coefficients (Darter, et al., 2014). The key issue is how to determine the standard error of the estimate when these methods are placed at different times under different existing pavement conditions. The issue is not related to missing data or information, but rather how to use and apply that information in calibrating the transfer functions. As such, application of pavement preservation treatments was excluded as a primary or secondary tier in the sampling matrices, but it may represent a confounding factor for both sampling templates.

Table 2—Number of LTPP Test Sections: Rigid Pavements, New Construction and Rehabilitations

Rigid Pavement Type			**Number of Test Sections With Time Series Data**				
			Site ID	**Number**	**Dowel Diameter (in.)**	**Joint Spacing (feet)**	**PCC-Base Contact Friction (months)**
New Construction	Jointed Plain Concrete Pavement (JPCP)	Granular	3007	2	1.125	20	Full, entire design life
			3019		1.125	20	Full, entire design life
		Asphalt Treated Base (ATB)	3011	3	No dowels	Random, 18.5 ft to 22.5 ft	Full, entire design life
			3015		1.25	20	Full, entire design life
			3016		1.25	20	Full, entire design life
		Cement Treated Base (CTB)	3017	3	No dowels	Random, 18.5 ft to 22.5 ft	Partial, 120 months
			3018		No dowels	21	Partial, 120 months
			3020		1.125	20	Partial, 120 months
	Continuously Reinforced Concrete Pavement (CRCP)		5023	1	None	None	None
Rehabilitation	CRCP	HMA Overlay	None	0	None	None	None
	JPCP	HMA Overlay	7028	1	1.25	15	Full, entire design life
		CRCP Overlay	4118	1	None	None	None
TOTAL SITES			**11**				

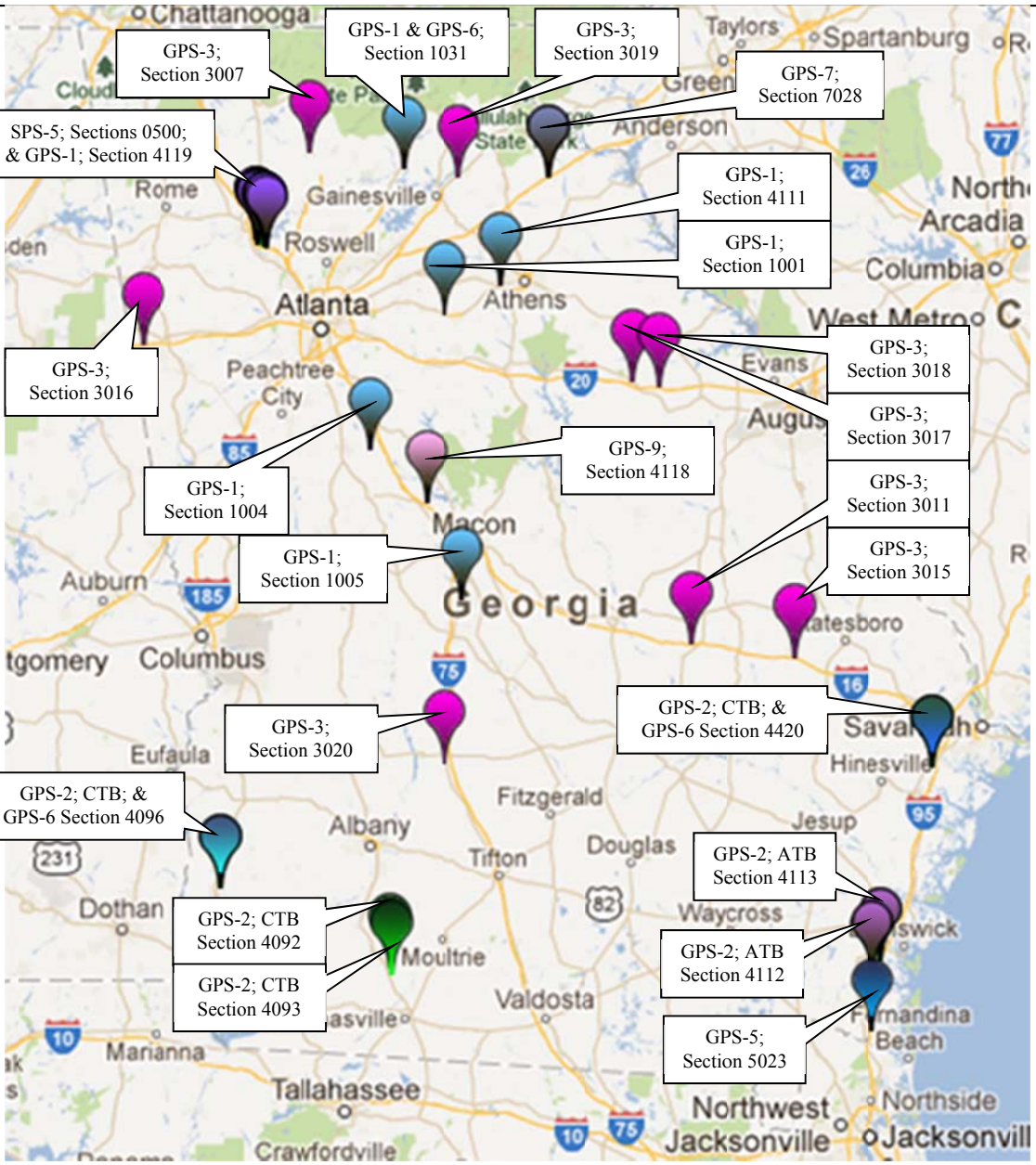

Legend:

- General Pavement Study (GPS)-1; flexible pavement, AC over aggregate base
- GPS-2; flexible pavement; AC over ATB or full-depth
- GPS-2; flexible pavement; AC over CTB or soil cement, semi-rigid

Legend:

- GPS-6; AC overlay of flexible pavement
- SPS-5; AC overlay of flexible pavement
- GPS-3; rigid pavement, JPCP
- GPS-5; rigid pavement, CRCP
- GPS-7; AC overlay of rigid pavement
- GPS-9; PCC overlay of rigid pavement

Figure 1—Location of LTPP Sites in Georgia

Table 3—Location Information for the Georgia Calibration Sections

LTPP ID No.	Pavement Type	County	Route	Elevation, ft	Longitude, deg	Latitude, deg	Constr. Year
0502 to 0566	HMA Overlay; Deep Strength	Bartow	I-401	815	-84.7265	34.1005	June 1993
1001	Flexible	Walton	SR 10	905	-83.7900	33.8075	Sept 1986
1004	Flexible	Spalding	SR 16	760	-84.1688	33.2381	June 1983
1005	Flexible	Houston	SR 247	452	-83.6999	32.6154	June 1986
1031	Flexible	Dawson	SR 247C	120	-84.005	34.4036	June 1981
1031	HMA Overlay; Flexible	Dawson	SR 247C	120	-84.005	34.4036	June 1997
3007	JPCP	Pickens	SR 5	1422	-84.4634	34.4733	Dec 1981
3011	JPCP	Treutlen	I-16	248	-82.567	32.4285	Dec 1975
3015	JPCP	Candler	I-16	178	-82.0424	32.3734	Sept 1978
3016	JPCP	Haralson	I-20	1218	-85.2932	33.6814	Dec 1977
3017	JPCP	Taliaferro	I-20	583	-82.8635	33.5185	Dec 1973
3017	JPCP	Taliaferro	I-20	583	-82.8635	33.5185	May 2001
3018	JPCP	Warren	I-20	550	-82.7273	33.5034	July 1973
3019	JPCP	Hall	US-23	1042	-83.7264	34.3731	Dec 1981
3020	JPCP	Crisp	SR 300	307	-83.7887	31.9234	Sept 1985
3020	JPCP	Crisp	SR 300	307	-83.7887	31.9234	June 2006
4092	Semi-Rigid	Thomas	SR 300	278	-84.0583	31.0225	June 1986
4093	Semi-Rigid	Thomas	SR 300	350	-84.071	31.0529	June 1986
4096	Semi-Rigid	Early	SR 62C	270	-84.9171	31.3944	June 1985
4096	HMA Overlay; Semi-Rigid	Early	SR 62C	270	-84.9171	31.3944	Apr 2001
4111	Flexible	Oconee	US-78	735	-83.5134	33.9224	Nov 1980
4112	Full Depth	Camden	I-95	13	-81.6565	31.0261	June 1987
4112	HMA Overlay; Full Depth	Camden	I-95	13	-81.6565	31.0261	Sept 1998
4113	Full Depth	Camden	I-95	13	-81.6143	31.0818	June 1987
4113	HMA Overlay; Full Depth	Camden	I-95	13	-81.6143	31.0818	Sept 1998
4118	CRCP Overlay of JPCP	Monroe	I-401	750	-83.8845	33.0149	June 1963
4119	HMA with ATB	Bartow	I-401	815	-84.706	34.0886	June 1978
4420	Semi-Rigid	Bryan	US-17	17	-81.3633	31.9042	Apr 1984
4420	HMA Overlay; Semi-Rigid	Bryan	US-17	17	-81.3633	31.9042	Oct 1992
5023	CRCP	Camden	I-95	25	-81.6561	30.7787	June 1974
7028	HMA Overlay; JPCP	Franklin	I-85	850	-83.2783	34.3684	Nov 1986
7028	2nd HMA Overlay; JPCP	Franklin	I-85	850	-83.2783	34.3684	July 1998

- Various design features for jointed plain concrete pavements (JPCP) were not adequately covered from the LTPP sections. Gaps between these LTPP sections and current Georgia design practice were noted in joint spacing, use of dowels, base types, and shoulders. In addition, asphalt interlayers are used in JPCP construction. Of the 11 LTPP rigid pavement test sections, test section 3016 was the only one with an asphalt interlayer. Thus, base type and other JPCP design features were added to the sampling template. Base types of rigid pavements that are typically used in Georgia include: granular aggregate base (GAB), chemically stabilized base, and asphalt interlayers.

- Continuously reinforced concrete pavement (CRCP) was included for only two LTPP projects. Additional projects are needed to determine the calibration coefficients for CRCP. Relatively few CRCP projects have been constructed that are over 10 years in age of service. Thus, CRCP was excluded from the sampling template of rigid pavements.

- Very few JPCP unbonded overlays have been constructed in Georgia. In fact, there was only one unbonded JPCP overlay of existing JPCP included in the LTPP program in Georgia. The primary rehabilitation strategy of JPCP is asphalt concrete (AC) overlays. Thus, JPCP unbonded overlays were excluded as a primary factor in the sampling template.

- Soil type is more important relative to flexible pavement performance in comparison to rigid pavement performance. A higher percentage of the Georgia LTPP sites are located above the "fall line," for which the soils are classified as fine-grained. To investigate whether the soil is properly accounted for in the MEPDG design methodology, coarse-grained versus fine-grained soils and stabilized versus non-stabilized soils were added to the sampling template for flexible pavements.

2.2 Non-LTPP Test Sections

The preliminary sampling matrices (see Tables 1 and 2) were revised to include other factors and current GDOT design practices and materials, as discussed above. Tables 4 and 5 represent the expanded sampling templates or matrices. Table 4 is for new JPCP pavements and contains 30 cells, while Table 5 is for new flexible and rehabilitated pavements and contains 46 cells. Table 4 excludes the overlay and CRCP test sections listed in Table 2.

The first step to select non-LTPP roadway segments was to identify as many potential projects as possible that could be used to satisfy the recommendations presented above and populate the sampling templates. Non-LTPP sites were selected considering two criteria: (1) filling as many of the cells in the sampling matrix as possible to achieve a balanced factorial, and (2) include segments exhibiting higher levels of distress that are consistent with GDOT threshold values or design criteria. The Task 2 interim report documented that the LTPP test sections were exhibiting distress levels or magnitudes far below typical threshold values. The non-LTPP sites were selected to include higher levels of distress.

Table 4—Sampling Template or Matrix for Validation of New JPCP Transfer Function

PCC Thickness, in	Doweled Pavement	Edge Support	Subgrade Type					
			Coarse (A-1 through A-3)			Fine (A-4 through A-7)		
			Base Type					
			Aggr. Base	Chemically Stabilized*	Asphalt Interlayer	Aggr. Base	Chemically Stabilized*	Asphalt Interlayer
≤ 10	Non-doweled	None		3017	3: I-20	3019	3018	4: I-475 5: I-85
		Tied PCC and or widened lanes	X		X			X
	Doweled	None	6: I-985	3020		3007		
		Tied PCC and or widened lanes	12: SR127		7: SR-207		2: SR-316	
> 10	Non-doweled	None		3011				
		Tied PCC and or widened lanes						
	Doweled	None		3015		X		X
		Tied PCC and or widened lanes	10: I-75 11: SR-158		8: I-20 9: I-965		1: I675	3016
TOTAL SITES			**4**	**4**	**4**	**2**	**3**	**3**

Dark Shaded Cells – Indicate that these designs are not used on State Routes or the primary system.
*Chemically stabilized base = lean concrete base, soil cement, or cement treated base
X – Identifies cells to be filled for a partial or fractional factorial that were not filled with an in-service pavement.

An additional 19 roadway segments were identified and included in the sampling matrix for flexible pavements, while an additional 9 segments were included in the rigid pavement sampling matrix. Figures 2 and 3 show the general location for these non-LTPP roadway segments for flexible and rigid pavements, respectively.

By combining the LTPP and non-LTPP sites results in a total of 20 rigid pavement sections and 38 flexible pavement sections for calibrating the distress transfer functions and smoothness regression equations. This number of rigid sites are considered borderline, while the number of flexible pavement sections are considered sufficient for determining the Georgia calibration coefficients.

Appendix A includes a listing of the material type and layer thickness for the LTPP and non-LTPP test sections located in Georgia. These test sections were categorized by the general pavement groups identified in Tables 4 and 5, as defined by the MEPDG Manual of Practice. The number of individual projects for each pavement type is considered the minimum required for confirming the accuracy of the transfer functions in accordance with the MEPDG Local Calibration Guide (AASHTO, 2010).

Table 5—Sampling Template or Matrix for Validation of New and Rehabilitated Flexible Pavements and HMA Overlays

HMA Thickness	Binder Type	Soil Type		Pavement Structure					
				New Construction			Rehabilitation[1]		
				Flexible; Conv.	Deep Strength	Semi-Rigid	HMA Overlay with & without Milling		
							Flexible Conv.	Deep Strength	Semi-Rigid
<7	Neat	Coarse-Grained		10:SR144	Cells not likely found.	11:SR14092; 4093; 4094; 4096; 4420 13:SR38	10:SR144 18:SR57	Cells not likely found.	4096; 4420
		Fine-Grained	None	1004			X		
			Stabilized						
	PMA	Coarse-Grained							
		Fine-Grained	None						
			Stabilized						
7 to 10	Neat	Coarse-Grained		1005 1:SR15			1:SR15		
		Fine-Grained	None	1001; 4111	X		18:SR3		
			Stabilized					X	
	PMA	Coarse-Grained		19:I520		X	4:SR6	8:SR54	X
		Fine-Grained	None	3:SR11	X		3:SR11		
			Stabilized	X				X	
>10	Neat	Coarse-Grained			0501; 1031; 4112; 4113			SPS-5[2]; 1031; 4112; 4113	
		Fine-Grained	None		4119				
			Stabilized						
	PMA	Coarse-Grained			2:SR280			2:SR280	
		Fine-Grained	None	12:I95			12:I95	9:I85	
			Stabilized		X				
TOTAL SITES				**9**	**6**	**7**	**7**	**7**	**2**

Definitions Used in Table:

- **Dark Shaded Cells** – Indicate that these designs are not used on State Routes or the primary system.
- **X** – Identifies cells to be filled for a partial or fractional factorial that were not filled with an in-service pavement.
- **Conv.** = Conventional; flexible pavements with a relatively thin HMA surface and thick crushed stone or aggregate base layer.
- **Deep Strength** = For this sampling matrix, deep-strength asphalt pavements include very thick asphalt base mixtures with relatively thin aggregate base layers and also includes the category of full-depth HMA pavements.
- **Semi-Rigid** = Includes HMA pavements with a soil-cement subgrade or cement treated base layer.

NOTES:

- **NOTE 1**: Three categories of overlay thickness will be included; less than 2.5 inches, 2.5 to 5 inches, and greater than 5.0 inches.
- **NOTE 2**: The SPS-5 project represents 4 calibration test sections.

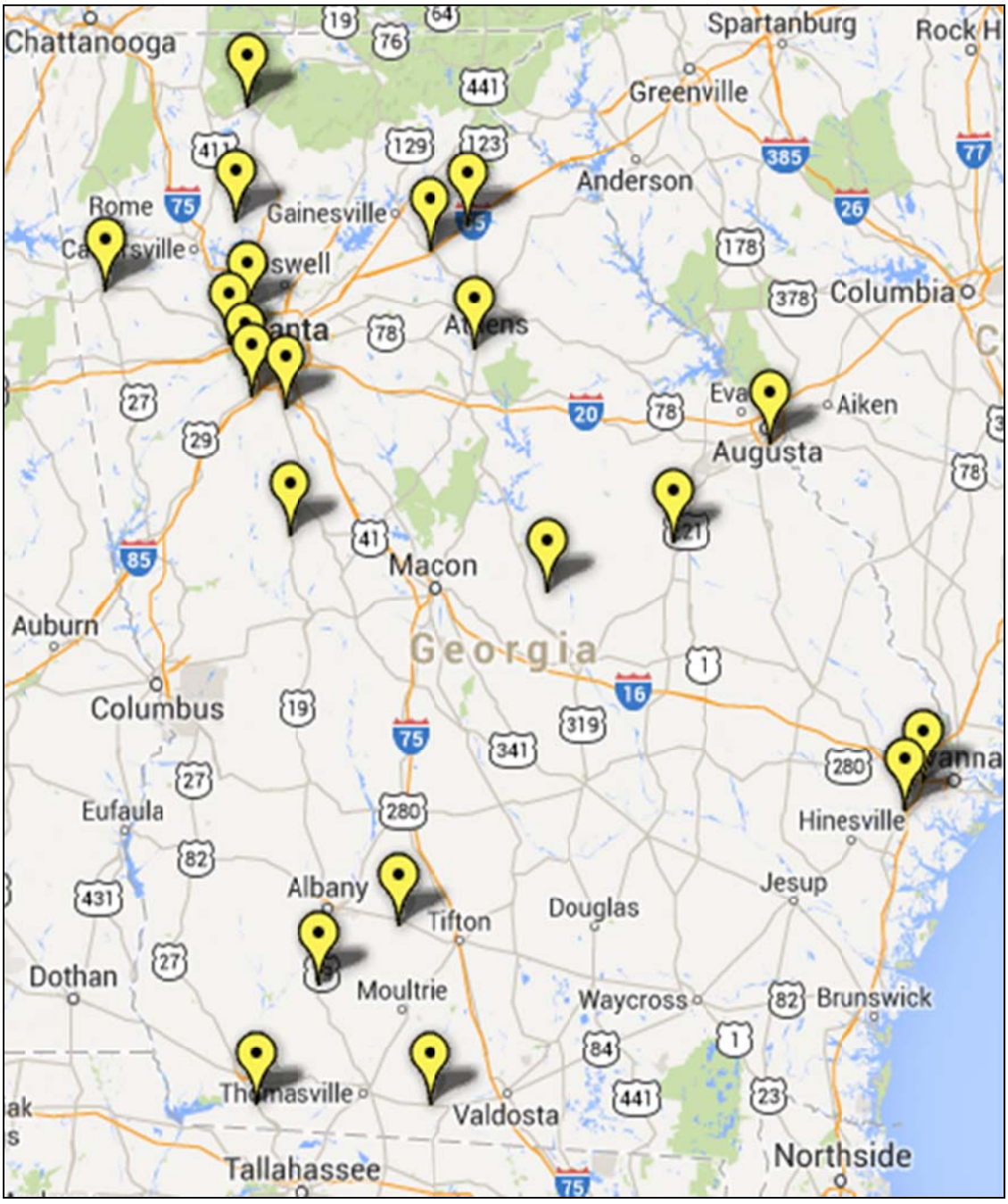

Figure 2—Location of Non-LTPP Flexible Pavement Calibration Sites in Georgia

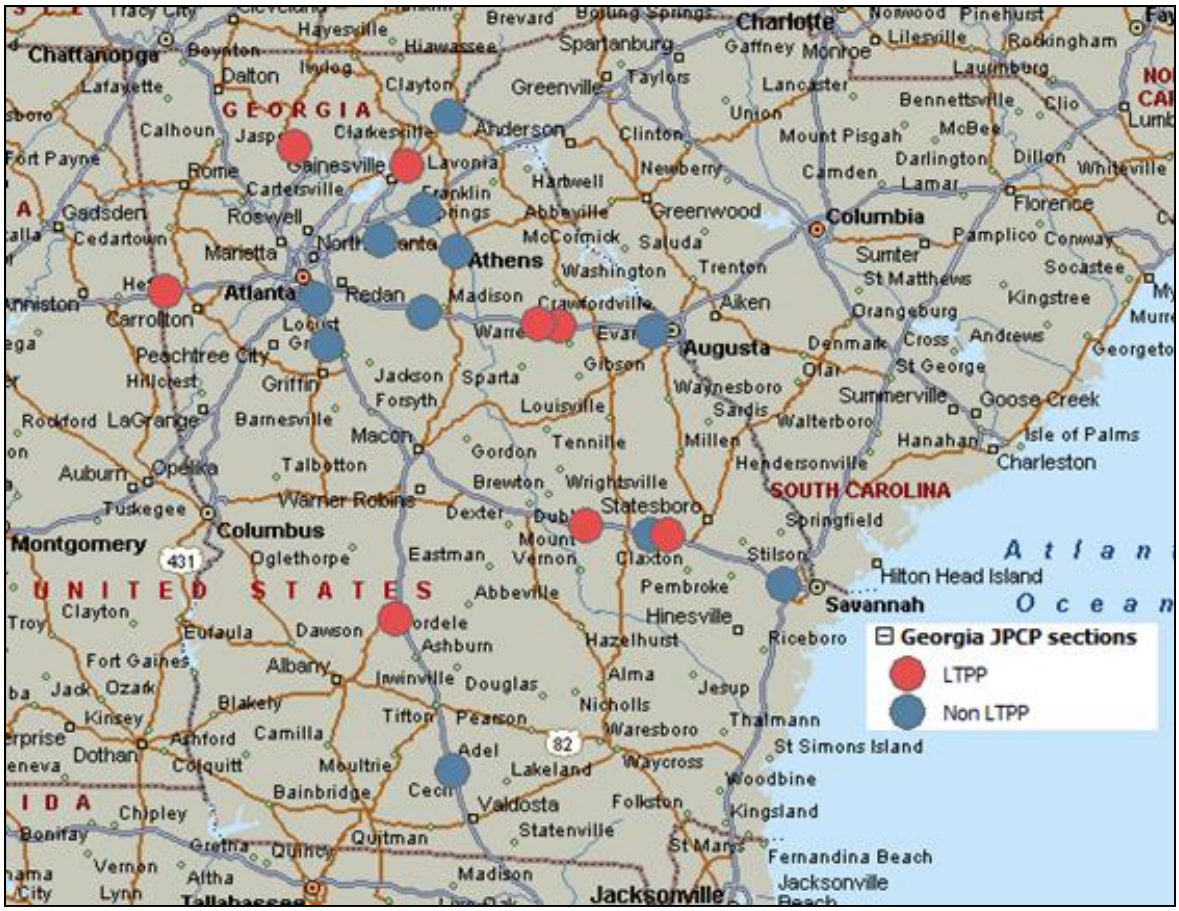

Figure 3—Location of LTPP and Non-LTPP Rigid Pavement Calibration Sites in Georgia

III. FIELD INVESTIGATIONS

The Georgia LTPP test sections represent the "best" candidates for the local calibration of the distress transfer functions in the MEPDG software package. The number of test sections, however, was found to be insufficient to cover the range of materials, pavement structures, and other design features commonly used by GDOT. As such, non-LTPP roadway segments were designated for use to supplement the LTPP test sections in calibrating the *Pavement ME Design*™ software to Georgia materials, conditions, and operational policies.

Both new and rehabilitated roadway projects were identified for the local calibration experimental factorials or sampling templates (see Tables 4 and 5). All layer and material property inputs needed for *Pavement ME Design*™ were extracted from construction files and as-built construction plans. The accuracy of the as-built plans and construction files, however, were believed to be insufficient. Field investigations were planned and conducted to measure selected layer properties and confirm the data extracted from the construction files.

3.1 Field Testing

Applied Research Associates (ARA) and the National Center for Asphalt Technology (NCAT) performed field testing during the spring and summer of 2014. Most of the testing took place from March to June of 2014. The field testing program included: (1) condition surveys made in accordance with the FHWA/LTPP Distress Identification Manual [FHWA, 2003], (2) Falling Weight Deflectometer (FWD) deflection basin testing, (3) Dynamic Cone Penetrometer (DCP) tests of the base and subgrade, and (4) drilling cores. ARA coordinated traffic control, took GPS encrypted pictures of all of the core locations, filled out pavement distress surveys, and assisted NCAT with DCP testing. ARA and NCAT performed the FWD deflection testing, while NCAT was primarily responsible for the coring operation and DCP testing.

Once traffic control had the test site closed down, the specific test section was marked. The length of the test sections varied from 500 to 700 feet, depending on the location. Three cores were located within cracked areas of the pavement. In most cases, the cores of cracked areas were taken directly over the cracks to determine whether the cracks initiated at the surface or bottom of the HMA layers. FWD deflection basin measurements were made every 50 feet over the length of the section within the right wheel path (see Figure 4).

Distress surveys were completed in accordance with the FHWA Distress Identification Manual to measure the magnitude and identify the severity level of distress observed along the segment. Figure 5 shows some examples of pavement distress along one of the non-LTPP sections. The amount of cracking along this segment, as well as other non-LTPP segments, was a lot higher than for the Georgia LTPP test sections.

After FWD testing was completed, nine 6-inch diameter cores were drilled through the depth of the pavement. The nine cores from each test location were spaced over the length of the section. Three cores were taken in distressed areas and the other six were selected randomly in areas without cracking (see Figure 6). The cores were photographed by a special GPS camera provided by GDOT. Figure 7 includes photographs of selected asphalt concrete and

PCC cores recovered from a couple of the non-LTPP segments. All cores were labeled and bagged for transport to the laboratory for measuring thickness and volumetric properties.

Figure 4—FWD Deflection Testing in Right Wheel Path

Figure 5—Examples of Distressed Pavement with Higher Amounts of Cracking

DCP measurements were performed at three core holes over the length of the section. Figure 8 includes some examples showing the results from the DCP testing. The DCP penetration rates were used to establish the in place resilient modulus for the unbound layers in comparison to the backcalculated values from the FWD deflection basins. After all work was completed along the site, all core holes were patched by NCAT.

Figure 6—Cutting Cores from Pavement in Cracked and Un-Cracked Areas

3.2 Laboratory Testing

Once the cores were recovered from the field projects and shipped to the laboratory, core thicknesses and individual layer heights were measured. The base and surface layers were sawed or separated into individual layers using a wet saw. The bulk specific gravity of each layer was measured in accordance with AASHTO T 166, "Bulk Specific Gravity (G_{mb}) of Compacted Hot Mix Asphalt (HMA) Using Saturated Surface-Dry Specimens." The maximum specific gravity of each layer was measured in accordance with AASHTO T 209, "Theoretical Maximum Specific Gravity (G_{mm}) and Density of Hot Mix Asphalt (HMA)." The asphalt content was measured for selected layers near the bottom of the pavement using the NCAT ignition oven.

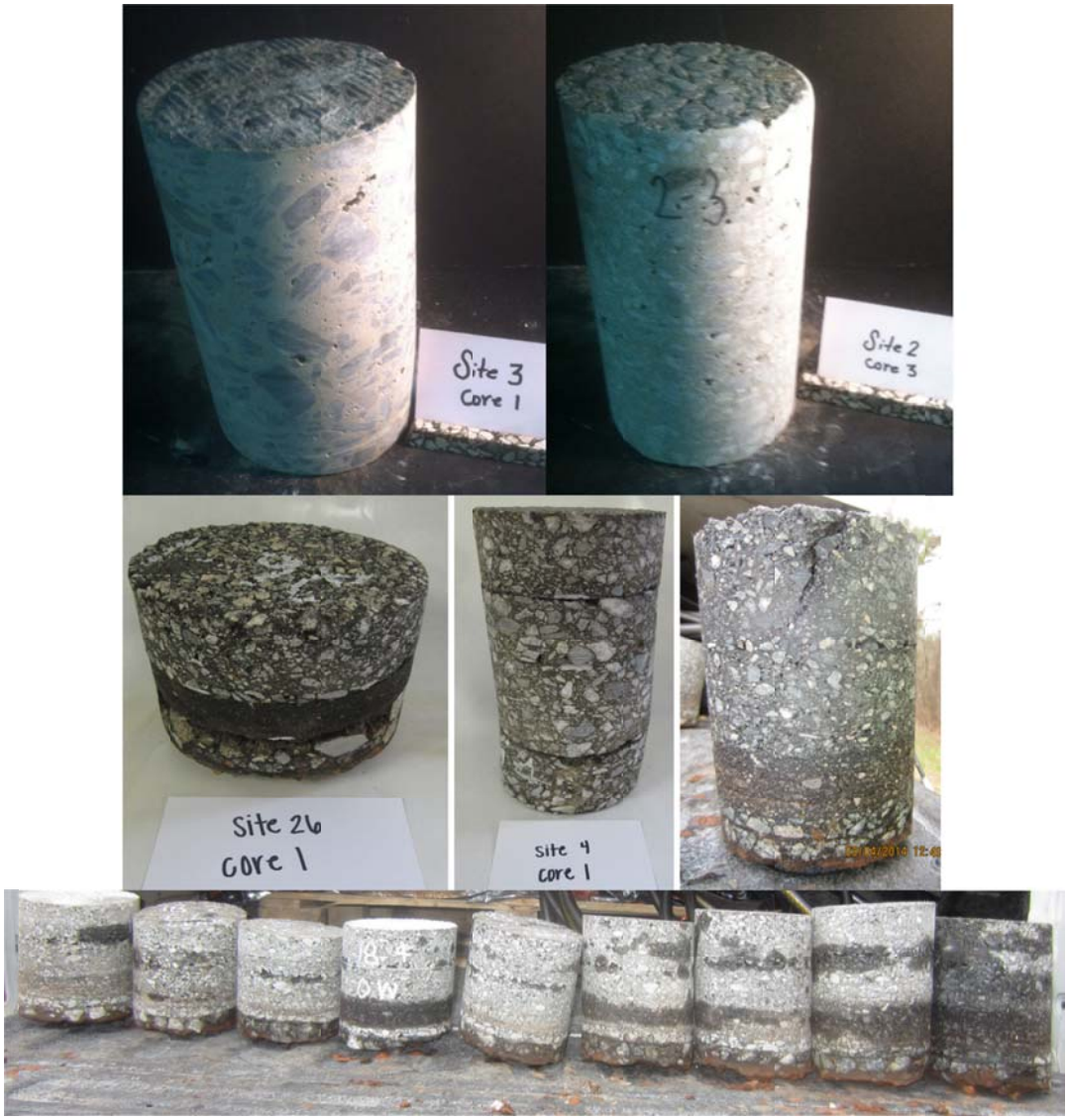

Figure 7—Photographs of Selected Asphalt Concrete and PCC Cores

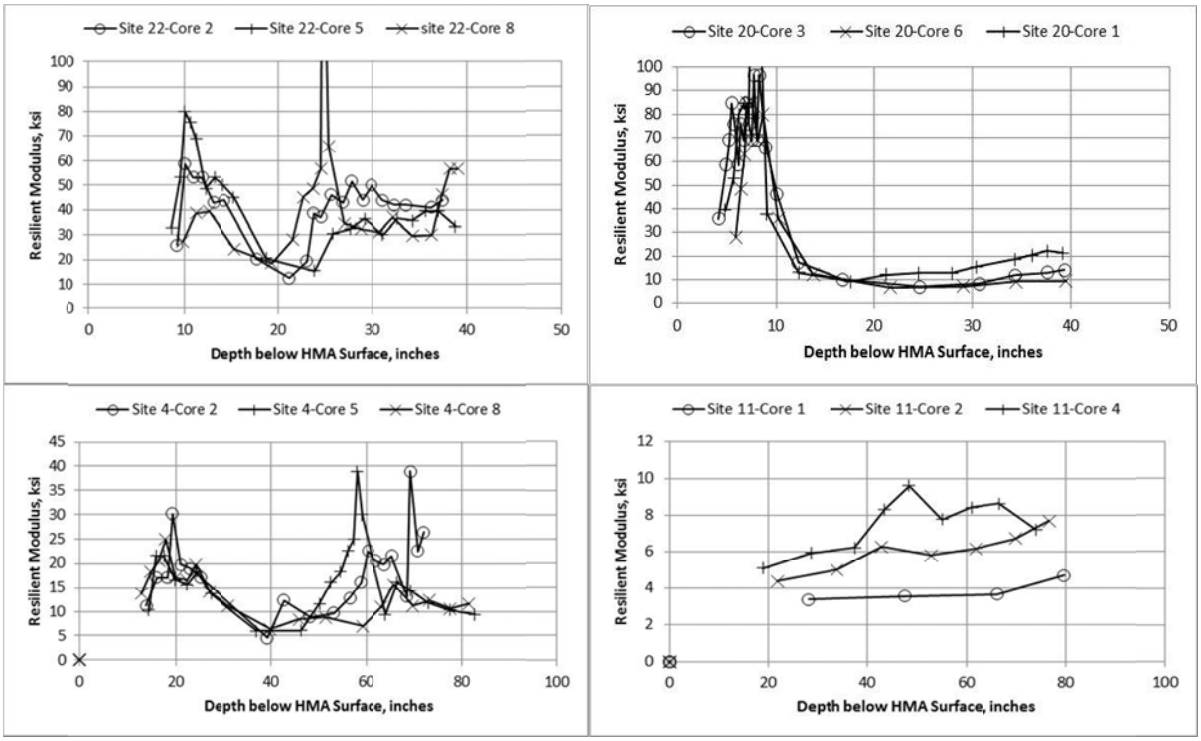

Figure 8— Results from DCP Testing for Selected Non-LTPP Sites

IV. SITE CONDITIONS AND DESIGN FEATURES

The sampling templates and calibration sections were presented in Section II of this report. This section documents selected site conditions and design features and determination of some of the input parameters for the LTPP and non-LTPP roadway segments. The Task 2 interim report for the verification included detailed discussion and documentation of the different input parameters for the LTPP test sections that were used in the verification process. Most of the input parameters determined for the non-LTPP segments follow those same procedures, so this section basically summarizes how the input parameters were determined.

4.1 Climate/Weather Stations

The MEPDG requires the location of a project be defined by its longitude, latitude, and elevation in order to develop project specific climate data. The GPS coordinates were included in Table 3. The climate specific data for each project was generated using the closest weather station. The closest weather station to each LTPP project site is included in Table 6. Typically, each weather station had 96 to 116 months of climate data.

Two other site condition features are required by the MEPDG: (1) the water table depth, and (2) the depth to a rigid layer. The 20-foot boring drilled in the shoulder area at each LTPP site was reviewed to estimate the depth to a rigid layer, a saturated layer, or free water. Wet soil strata or water was observed during the drilling process and recorded on the boring log for some of the sites. Similarly, refusal or presence of weathered rock was recorded on the boring log for some of the sites. The depth to water table and/or a hard or rigid layer are included in Table 6. If water or wet soils or refusal was not recorded on the boring log, the following assumptions were made in setting up the pavement structure in the MEPDG.

- If free water or wet soils were not recorded on the boring log, the depth to the water table was assumed to be:
  - 20-feet for higher elevations or mountainous areas.
  - 15-feet for the northern counties, north of the fall line.
  - 10-feet for the southern counties, south of the fall line.
  - 6-feet for the coastal areas or counties.
- If a hard pan layer was not encountered or refusal was not recorded on the boring log, the thickness of the subgrade soil was assumed to be infinite.

4.2 Truck Traffic

Many of the truck traffic inputs for the Georgia LTPP sections are at level 1 since volume and portable weigh-in-motion (WIM) data were available for all LTPP sites in Georgia. The Georgia WIM study, however, recommended the portable WIM data not be used because of potential errors in the data, except for a couple of sites. The truck axle weight data were processed under the WIM study, and a detailed description of all traffic data for the LTPP WIM sites in Georgia is presented within the WIM study documents (Selezneva, 2014). Table 7 summarizes the functional classes and MEPDG truck traffic classification (TTC) groups for each site. The subsections that follow discuss the different truck traffic inputs and the values used for determining Georgia's calibration coefficients.

Table 6—Weather Station and Other Climate Data for the Georgia Calibration Sites

LTPP ID No.	Weather Station	Water Table		Hard Layer	
		Depth, ft.	Description	Depth, ft.	Description
0500	Cartersville, GA	---	None except as noted	---	None except as noted
0502		---		8.5	Weathered Rock
0504, 0505, 0506, 0507		---		5.5	
0563		---		3	
0565		---		5	
0503		8.5	Seasonal	19.5	Refusal; Hard Layer
4119	Cartersville, GA	15	High Moisture; Seasonal	4	Weathered Rock Pieces
1001	Athens, GA	12	Seasonal; Gravel Seam	---	
1004	Atlanta, GA	12	Water Table	---	
1005	Macon, GA	16	Seasonal	---	
1031	Gainesville, GA	---		---	
3007	Cartersville, GA	12	Moist; Seasonal	---	
3011	Alma, GA	9	Water Table	---	
3015	Savannah, GA	10	Water Table	---	
3016	Anniston, AL	---		5	Weathered Rock
3017	Athens, GA	---		12	Weak Rock
3018	Athens, GA	---		---	
3019	Gainesville, GA	---		---	
3020	Albany, GA	12	Wet Soil; Seasonal	---	
4092	Albany, GA	15	Very Wet Soil; Seasonal	---	
4093	Albany, GA	---		13	Refusal
4096	Dothan, AL	---		---	
4111	Athens, GA	---		---	
4112	Brunswick, GA	5	Water Table	---	
4113	Brunswick, GA	10	Water Table	---	
4118	Macon, GA	---		---	
4420	Savannah, GA	10	Water Table	---	
5023	Jacksonville, FL	4	Water Table	---	
7028	Athens, GA	15	Wet Soil; Seasonal	---	

Table 7—Basic Truck Traffic Information for the Georgia Calibration Sites

LTPP ID No.	County	Route	Functional Class	MEPDG TTC Group	Initial AADTT (LTPP Lane)	Growth Function	Growth Rate
0502 to 0566	Bartow	I-401	Rural Interstate	8	5330	None	---
1001	Walton	SR 10	Rural Principal Arterial	12	690	None	---
1004	Spalding	SR 16	Rural Minor Arterial	8	140	Linear	14.8
1005	Houston	SR 247	Rural Major Collector	14	400	Linear	3.6
1031 New	Dawson	SR 247C	Rural Principal Arterial	12	125	Compound	6.0
1031 Rehab	Dawson	SR 247C	Rural Principal Arterial	12	275	Compound	6.0
3007	Pickens	SR 5	Rural Principal Arterial	12	190	Linear	8.0
3011	Treutlen	I-16	Rural Interstate	7	590	Linear	4.7
3015	Candler	I-16	Rural Interstate	11	500	Linear	7.0
3016	Haralson	I-20	Rural Interstate	1	1230	Compound	4.2
3017	Taliaferro	I-20	Rural Interstate	6	610	Compound	5.4
3017	Taliaferro	I-20	Rural Interstate	6	2730	Compound	5.4
3018	Warren	I-20	Rural Interstate	9	950	Compound	4.3
3019	Hall	US-23	Rural Principal Arterial	14	270	Compound	6.5
3020 New	Crisp	SR 300	Rural Principal Arterial	4	200	Linear	7.5
3020 Rehab	Crisp	SR 300	Rural Principal Arterial	4	600	Linear	7.5
4092	Thomas	SR 300	Rural Principal Arterial	14	300	Compound	5.5
4093	Thomas	SR 300	Rural Principal Arterial	14	300	Compound	5.5
4096	Early	SR 62C	Rural Minor Collector	8	50	Compound	7.0
4096	Early	SR 62C	Rural Minor Collector	8	180	Compound	7.0
4111	Oconee	US-78	Rural Minor Collector	17	500	None	---
4112	Camden	I-95	Rural Interstate	8	2400	Linear	2.1
4112	Camden	I-95	Rural Interstate	8	3600	Linear	2.1
4113	Camden	I-95	Rural Interstate	11	1300	Compound	5.0
4113	Camden	I-95	Rural Interstate	11	4100	Compound	5.0
4118	Monroe	I-401	Rural Interstate	5	4500	Linear	0.7
4119	Bartow	I-401	Rural Interstate	8	5330	None	---

Table 7— Basic Truck Traffic Information for the Georgia Calibration Sites (continued)

LTPP ID No.	County	Route	Functional Class	MEPDG TTC Group	Initial AADTT (LTPP Lane)	Growth Function	Growth Rate
4420	Bryan	US-17	Rural Principal Arterial	11	140	Compound	4.0
4420	Bryan	US-17	Rural Principal Arterial	11	200	Compound	4.0
5023	Camden	I-95	Rural Interstate	12	1100	Compound	5.7
7028	Franklin	I-85	Rural Interstate	8	1900	Linear	7.2
7028	Franklin	I-85	Rural Interstate	8	3536	Linear	7.2

4.2.1 Initial AADTT and Truck Growth Factors

The two-way average annual daily truck traffic (AADTT) is an important input parameter to the MEPDG, as well as the truck traffic growth over time. Truck traffic volume data are available for all of the sites, but for some of the sites, AADTT is only available many years after construction. For the cases where AADTT was unavailable at construction, the starting value was backcasted to the year of construction. The AADTT values included in the LTPP and GDOT databases were also used to estimate the growth rate and function of truck traffic for each site.

Figures 9 and 10 include examples of the backcasting method to determine the initial AADTT and growth throughout the monitoring period for four of the Georgia calibration sites. These four sites were selected to illustrate the process used for varying discrepancies between the historical and monitoring data included in the LTPP database. Table 7 listed the initial AADTT, as well as the growth rate for each roadway segment. The following summarizes the assumptions applied to the historical and monitoring data related to each of these sites.

- LTPP Site 13-1001 (Figure 9) – There is a significant discrepancy between the historical and monitored data sets for this site. For the LTPP sites that exhibit this type of discrepancy between the historical and monitored data sets, the monitored data was used to estimate the initial AADTT, and to determine the growth rate and function.
- LTPP Site 13-1004 (Figure 9) – The historical and monitored data sets show similar increases in truck traffic or AADTT over time. For this case, the historical data set exhibits slightly lower AADTT values than the monitored data set. For the LTPP sites that exhibit this type of trend between the historical and monitored data sets, both sets of data were used to estimate the growth rate and function, but only the monitored data set was used to backcast the initial AADTT.
- LTPP Site 13-3018 (Figure 10) – The historical and monitored data set have a lot of dispersion in the AADTT value reported over time, but exhibit similar trends and growth in the AADTT. For other sites that exhibit this type of trend between the historical and monitored data sets, both sets of data were used to backcast the initial AADTT and estimate the growth rate and function.

- LTPP Site 13-4118 (Figure 10) – The historical data set has a value much higher than the monitored data set. For cases where the historical data sets were slightly higher or lower than the monitored data set and only contained a few data points, the monitored data was used to backcast the initial AADTT and estimate the growth rate and function.

Table 8 lists some of the other truck traffic inputs for each calibration site in Georgia. The following discusses some of the truck traffic input parameters that are segment or project specific and used for the calibration process. The global default values recommended for use in the 2008 MEPDG Manual of Practice were used for all other truck traffic inputs.

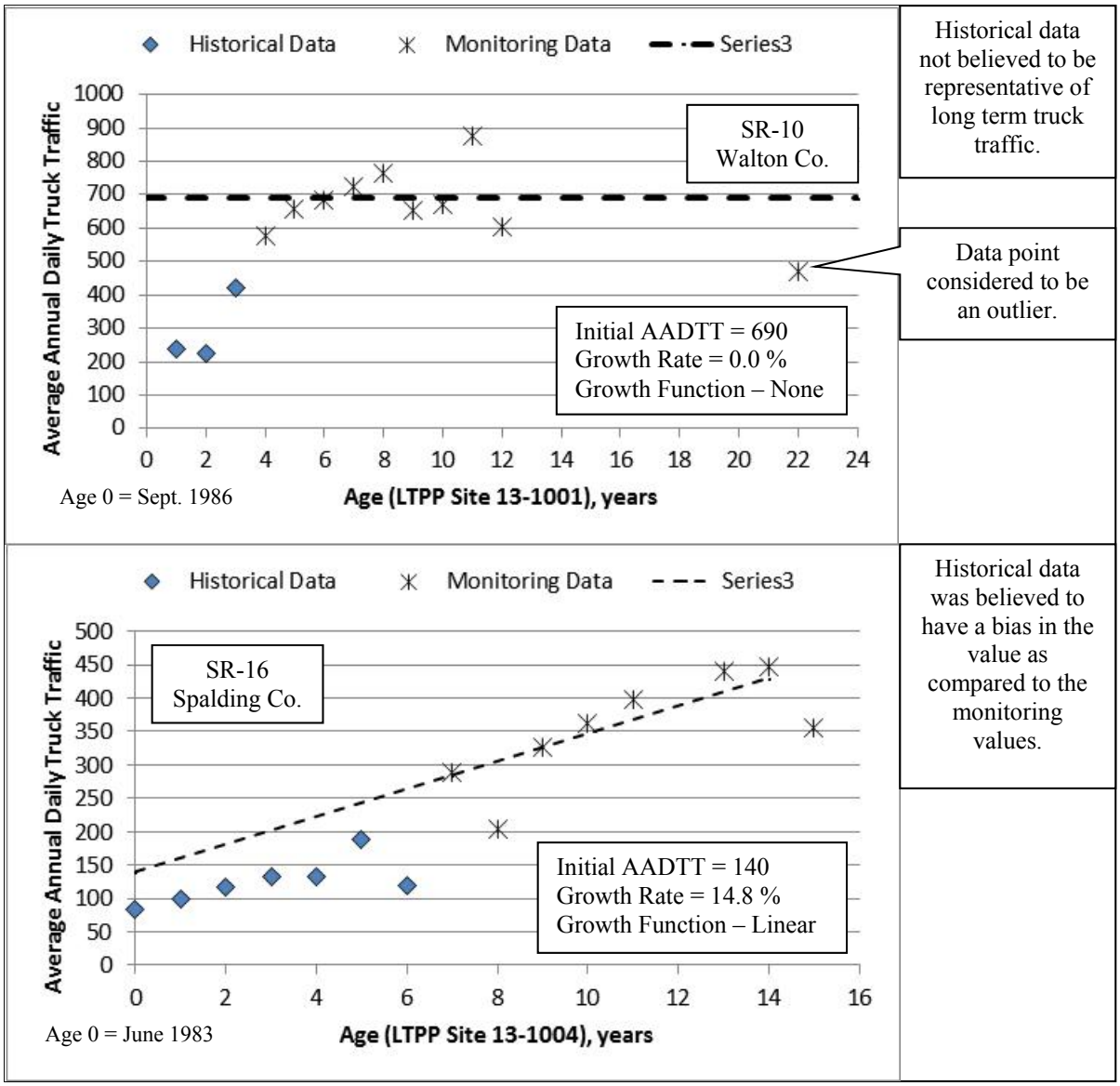

Figure 9—Illustration of the Process used to Backcast the Initial AADTT for some LTPP Flexible Pavement Sections

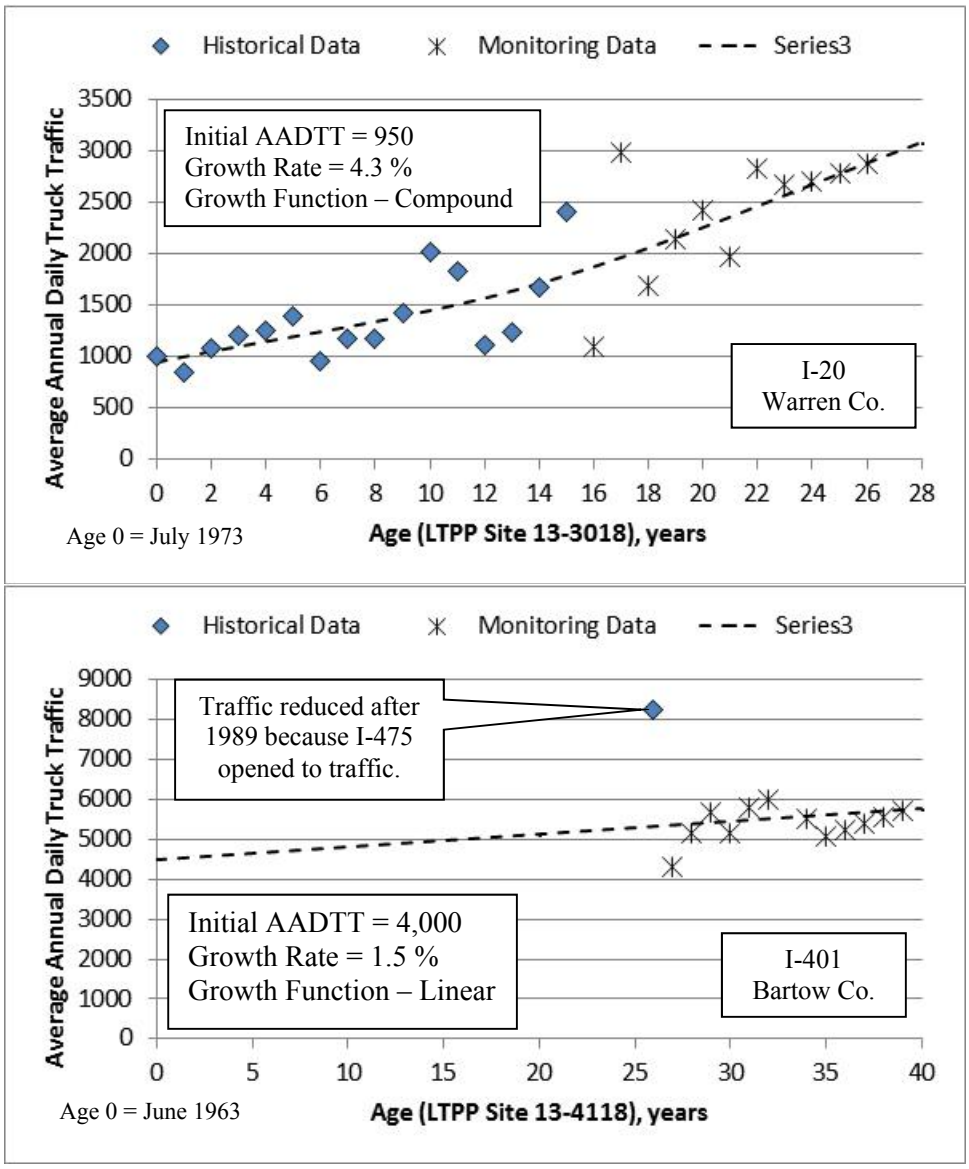

Figure 10—Illustration of the Process used to Backcast the Initial AADTT for some LTPP Rigid Pavement Sections

4.2.2 Normalized Vehicle Class Volume Distribution

The normalized vehicle class volume distribution was computed using automated vehicle classifier (AVC) and WIM data available in LTPP for all the sections used in the analysis. A summary of the data is presented in Table 9. These values represent the average normalized volume distribution for each site. For a few sites, significant deviations in the normalized truck class distribution were observed in the data. Any anomalies or outliers were removed from the data set used to determine the average values listed in Table 9.

Table 8—Summary of Predominant Truck Traffic Seasonal Distribution and Normalized Axle Load Distribution used in the Calibration Process

LTPP ID No.	County	Route	Functional Class	MAF Seasonal	NALS Designation
0502 to 0566	Bartow	I-401	Rural Interstate	Independent	H1
1001	Walton	SR 10	Rural Principal Arterial	Dependent	H1
1004	Spalding	SR 16	Rural Minor Arterial	Dependent	GA-U&R-MA
1005	Houston	SR 247	Rural Major Collector	Dependent	H1
1031	Dawson	SR 247C	Rural Principal Arterial	Independent	H1
3007	Pickens	SR 5	Rural Interstate	Independent	GA-RI-MA
3011	Treutlen	I-16	Rural Interstate	Independent	175-0247-3-1
3015	Candler	I-16	Rural Interstate	Independent	175-0247-3-1
3016	Haralson	I-20	Rural Interstate	Dependent	175-0196-3-1
3017	Taliaferro	I-20	Rural Interstate	Dependent	M
3018	Warren	I-20	Rural Interstate	Dependent	M
3019	Hall	US-23	Rural Principal Arterial	Independent	H2
3020	Crisp	SR 300	Rural Principal Arterial	Dependent	M
4092	Thomas	SR 300	Rural Principal Arterial	Dependent	081-0347-7-1
4093	Thomas	SR 300	Rural Principal Arterial	Dependent	081-0347-7-1
4096	Early	SR 62C	Rural Minor Collector	Dependent	081-0347-7-1
4111	Oconee	US-78	Rural Minor Collector	Independent	M
4112	Camden	I-95	Rural Interstate	Independent	GA-RI-MA
4113	Camden	I-95	Rural Interstate	Independent	GA-RI-MA
4118	Monroe	I-401	Rural Interstate	Independent	H1
4119	Bartow	I-401	Rural Interstate	Independent	H1
4420	Bryan	US-17	Rural Principal Arterial	Independent	H1
5023	Camden	I-95	Rural Interstate	Dependent	H1
7028	Franklin	I-85	Rural Interstate	Independent	GA-RI-MA

4.2.3 Monthly Volume Adjustment Factors

Sufficient data to determine the monthly adjustment factor (MAF) information was unavailable for many of the LTPP sites in Georgia. Two MAF data sets were determined for use in the validation study using the LTPP sites. These MAF values are provided in Tables 10 and 11. Table 10 includes the MAF values for sites that exhibit seasonally dependent truck traffic, while Table 11 includes the MAF values for seasonally independent truck traffic.

4.2.4 Axle Load Distribution Factors

The MEPDG requires single, tandem, tridem, and quad normalized axle load spectra (NALS) factors for analysis. The Georgia WIM project analyzed the axle weight data collected at all LTPP sites and other non-LTPP sites (almost 90 portable WIM sites were analyzed under the WIM project). For all sections analyzed, the single and tandem NALS factors were developed using WIM data obtained from the LTPP sites. Most of the data collected over a short time period with the use of portable devices were considered not reliable. For these cases, default NALS were recommended for use for the LTPP sites from the Georgia WIM

study. Table 8 lists the default or local NALS that were used in predicting pavement distress for each of the Georgia calibration sites. The NALS were defined in the Task 2 interim report.

Table 9—Average Normalized Truck Class Volume Distribution

LTPP ID	Truck or Vehicle Class									
	4	5	6	7	8	9	10	11	12	13
0500	9.653	14.318	5.935	1.669	13.936	46.607	1.009	3.709	0.714	2.451
1001	8.467	41.581	5.191	0.199	12.041	29.920	0.791	0.908	0.314	0.588
1004	5.753	14.107	9.287	0.442	17.557	42.357	2.099	0.247	0.021	8.130
1005	7.344	55.807	4.697	0.085	11.870	20.068	0.085	0.043	0.000	0.000
1031	5.510	46.803	12.636	0.728	11.351	20.029	1.119	0.266	0.182	1.377
3007	7.243	34.269	5.626	0.465	16.945	31.585	1.163	0.280	0.261	2.164
3011	4.167	23.788	4.706	0.150	23.799	40.375	0.842	1.499	0.362	0.312
3015	10.070	18.658	5.849	0.951	25.365	32.998	1.417	1.526	0.386	2.780
3016	3.095	5.802	0.900	0.004	12.769	70.227	0.549	4.514	2.141	0.000
3017	1.067	37.318	1.902	0.612	5.751	49.139	1.818	1.530	0.706	0.158
3018	0.829	36.680	3.085	5.166	6.864	40.554	4.784	1.208	0.649	0.180
3019	2.866	72.163	3.701	0.277	4.470	15.907	0.263	0.091	0.027	0.236
3020	2.866	72.163	3.701	0.277	4.470	15.907	0.263	0.091	0.027	0.236
4092	1.788	70.756	6.339	0.339	6.352	12.406	0.461	0.309	0.122	1.128
4093	1.902	66.707	7.640	0.490	7.184	13.865	0.545	0.254	0.117	1.297
4096	2.933	10.126	5.013	21.416	13.730	39.959	2.914	0.120	0.452	3.337
4111	16.866	26.414	12.313	7.301	16.764	13.618	2.075	0.709	0.565	3.376
4112	5.889	16.970	3.941	0.300	20.630	46.954	0.710	3.031	0.740	0.834
4113	9.845	22.147	4.833	1.123	19.512	35.168	1.146	2.776	0.563	2.888
4118	7.279	10.651	8.899	2.212	20.458	44.150	1.644	3.041	1.114	0.552
4119	9.653	14.318	5.935	1.669	13.936	46.607	1.009	3.709	0.714	2.451
4420	5.756	19.062	19.796	3.235	10.335	24.775	5.811	0.316	0.117	10.797
5023	12.90	43.58	2.68	0.39	11.50	25.62	0.61	1.66	0.40	0.65
7028	8.222	17.023	3.425	0.263	13.366	49.079	1.332	4.042	1.011	2.237

Table 10—Monthly Adjustment Factors for Roadways with Heavy Seasonally Dependent Truck Traffic

Month	Truck Classification									
	4	5	6	7	8	9	10	11	12	13
January	0.17	0.11	0.79	1.6	0.22	0.22	1.94	0.16	0.51	1.12
February	0.23	0.06	0.74	1.53	0.28	0.39	2.06	0.39	0.67	0.65
March	0.74	0.56	0.91	0.89	0.91	0.84	1.42	0.74	0.86	0.74
April	1.41	1.26	1.08	0.6	1.29	1.34	0.65	1.28	1.07	0.81
May	1.71	1.65	1.08	0.12	1.51	1.45	0.36	1.61	1.26	0.57
June	1.54	1.97	1.08	0.12	1.53	1.5	0.24	1.72	1.32	0.57
July	1.49	2.14	1.02	0.12	1.4	1.4	0.19	1.46	1.07	0.65
August	1.41	1.95	1.19	0.12	1.52	1.63	0.25	1.63	1.3	0.96
September	1.46	1.2	1.03	0.56	1.54	1.55	0.42	1.61	1.56	1.11
October	1.29	0.78	1.15	1.19	1.18	1.17	1	1.01	1.13	2.18
November	0.33	0.16	1.08	2.87	0.39	0.34	1.93	0.28	0.79	1.28
December	0.22	0.16	0.85	2.28	0.23	0.17	1.54	0.11	0.46	1.36

Table 11—Monthly Adjustment Factors for Roadways with Heavy Seasonally Independent Truck Traffic

Month	Truck Classification									
	4	5	6	7	8	9	10	11	12	13
January	0.6	0.84	1.56	0.96	0.96	1.06	1.32	0.96	1.08	1.32
February	0.72	0.96	1.2	0.96	1.08	1.06	1.2	0.96	1.14	0.96
March	0.96	1.08	0.96	0.6	1.08	1.06	0.96	0.96	1.14	0.96
April	1.44	1.2	0.96	0.48	1.08	0.96	0.96	0.96	1.08	0.84
May	1.08	0.96	0.84	0.48	1.08	0.96	0.96	0.96	0.84	0.48
June	1.08	1.08	0.72	0.6	1.08	0.96	0.96	1.08	0.96	0.6
July	0.72	0.84	1.08	1.08	0.96	0.84	0.84	0.96	0.84	0.6
August	0.84	0.72	0.96	1.32	1.08	0.96	0.84	1.08	0.96	0.84
September	0.84	0.84	0.84	1.32	0.84	0.96	0.96	1.08	0.96	0.84
October	1.44	1.32	0.96	1.44	0.96	1.06	0.96	1.08	1.08	1.32
November	1.32	1.2	0.96	1.44	0.96	1.06	0.96	0.96	1.08	1.44
December	0.96	0.96	0.96	1.32	0.84	1.06	1.08	0.96	0.84	1.8

4.3 Layer/Material Properties

4.3.1 HMA Layers/Mixtures

All of the input parameters for the hot mix asphalt (HMA) layers are documented in the Task 2 interim report and defined in the MEPDG Manual of Practice. The following discusses how some of the properties were estimated that were not included in the LTPP database and GDOT construction files.

The air voids and density at construction (bulk specific gravity) change over time and the values at construction were unavailable for most of the LTPP and non-LTPP flexible pavement sites. The air void at construction was backcast using the average air voids measured at the pavement's age of sampling and the densification function shown below.

$$V_a(t) = (D + V_d)10^{-a\left(\frac{t}{5}\right)^b} \quad (1)$$

Where:

- $V_a(t)$ = Air voids at time or age t.
- V_d = Design air voids for selecting the asphalt content, %
- t = Time or age of HMA mixture after construction, years.
- D = Regression constant; expected maximum change or decrease in air voids and defined at the age or time of sampling.
- a, b = Regression constants fitting the decrease in air voids over time (a=0.1 and b=0.25). These regression coefficients for typical dense graded mixtures (estimated from previous projects).

Figures 11 and 12 illustrate use of the densification function for backcasting the initial HMA air voids for four of the LTPP sites. This same process was used for the non-LTPP segments. The air voids at construction are included in the Task 2 interim report. Figure 13 shows a comparison between the total asphalt content by weight for all of the sections included in the calibration process. As shown, no specific relationship was found in terms of confirming the initial air voids with another volumetric property.

The global default values recommended for use in the 2008 MEPDG Manual of Practice were assumed for the thermal and volumetric properties not measured or included in the LTPP or GDOT construction databases.

4.3.2 PCC Layers/Mixtures

All of the input parameters for the PCC layers are documented in the Task 2 interim report and defined in the MEPDG Manual of Practice. Most of the inputs were extracted from the LTPP database or from other GDOT sponsored projects and/or construction records, so input levels 1 and 2 were used for the verification of the rigid pavement transfer functions. Key inventory, design, materials, and construction data were assembled for each project. The data were reviewed for identification and elimination of outliers and anomalies, and eventual inclusion in the GDOT MEPDG database for GDOT default input values. The global default values recommended in the 2008 MEPDG Manual of Practice were used for most of the PCC layer or material properties.

The long-term compressive strength and elastic modulus were available, for some of the Georgia's LTPP sections, while 28-day strengths were only available for the non-LTPP sites. The initial compressive strength and elastic modulus were backcast to the time at construction for the LTPP sections using the laboratory measured strengths at the age of the pavement when the samples were recovered. The strength-modulus gain or growth model included in the MEPDG was used to backcast the strength and modulus of typical Georgia PCC mixtures. The average 28-day flexural strengths ranged from 600 to 800 psi, and the 28-day elastic modulus ranged from 3,000,000 to 5,000,000 psi. An important observation from the 28-day elastic modulus data is that no modulus values were found with the mid-range (4,000,000 psi).

Coefficient of thermal expansion (CTE) values were obtained from the NCHRP project 20-07 corrected values for the Georgia LTPP test sections (Sachs, 2014), as well as from the values measured by Kim for standard Georgia mixtures (Kim, 2012). Average CTE values were selected based on the aggregate type for the non-LTPP sections. The CTE values used in the local calibration process ranged from 4 to 6 in./in./°F.

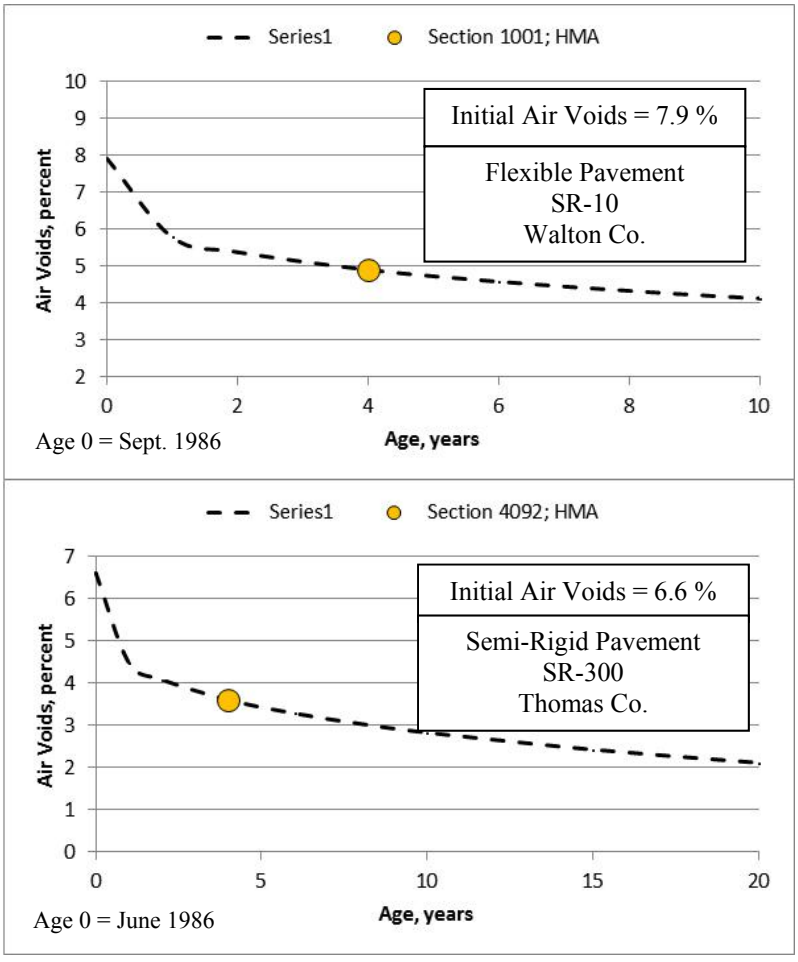

Figure 11—Illustration of the Process used to Backcast the Initial Air Voids of HMA Layers with Adequate Compaction

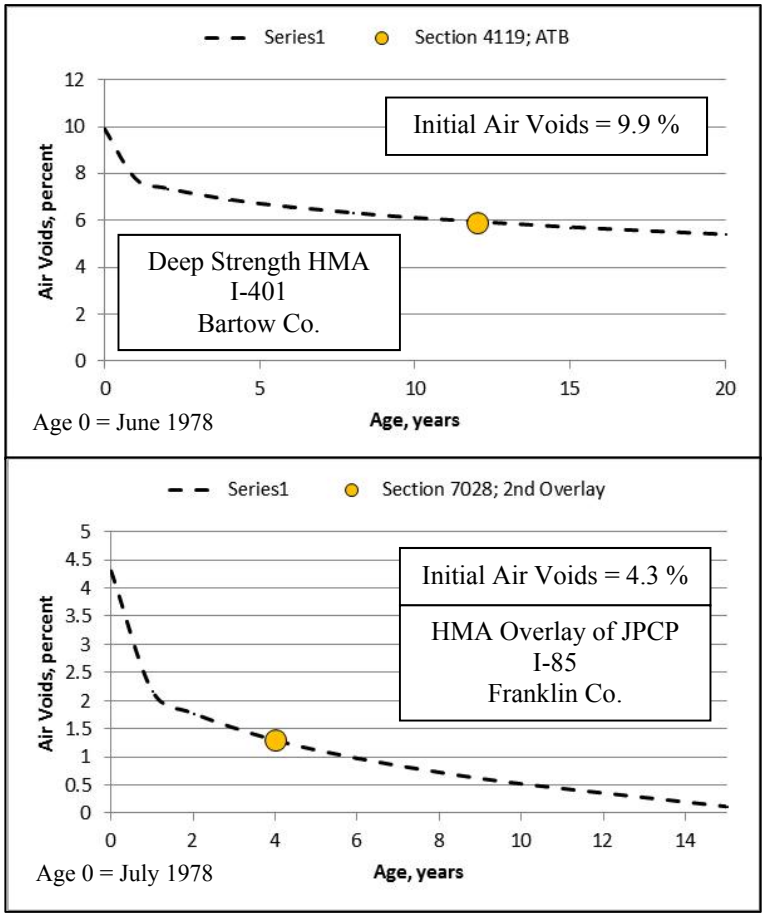

Figure 12—Illustration of the Process used to Backcast the Initial Air Voids of HMA Layers with Under and Over Compaction

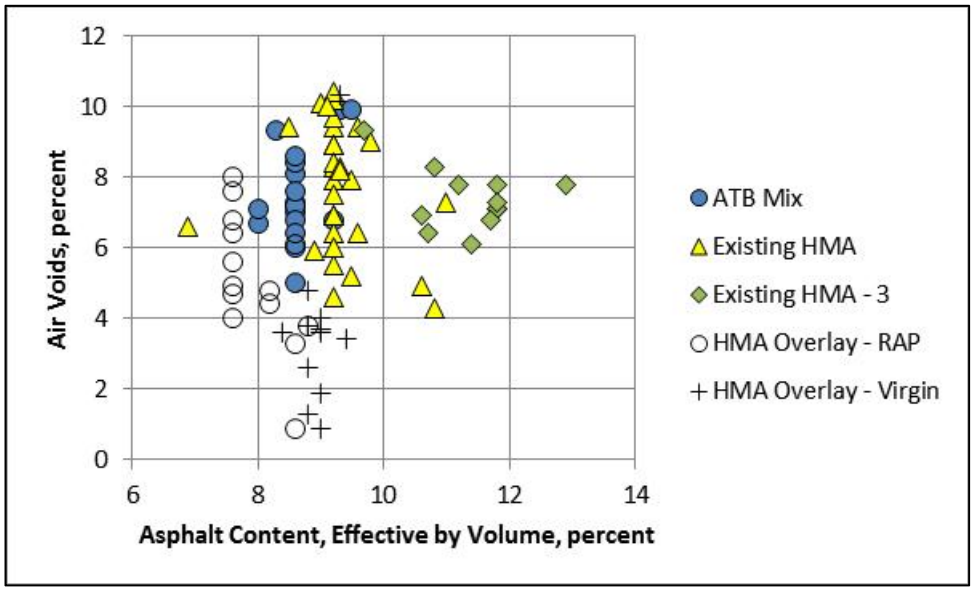

Figure 13—Initial Air Voids compared to the Effective Asphalt Content by Volume for the HMA Dense-Graded Mixtures

4.3.3 Unbound Aggregate Base and Soil Layers/Materials

The inputs for all unbound aggregate base layers, embankments, and subgrades were listed in the Task 2 interim report. The gradation, Atterberg limits, optimum water content, and maximum dry density test results are included in the LTPP database for a specific section of roadway. Figure 14 provides a comparison between the optimum water content and maximum dry unit weight for all unbound layers of the Georgia calibration sites. These values are an important input to the MEPDG to estimate the change in resilient modulus over time.

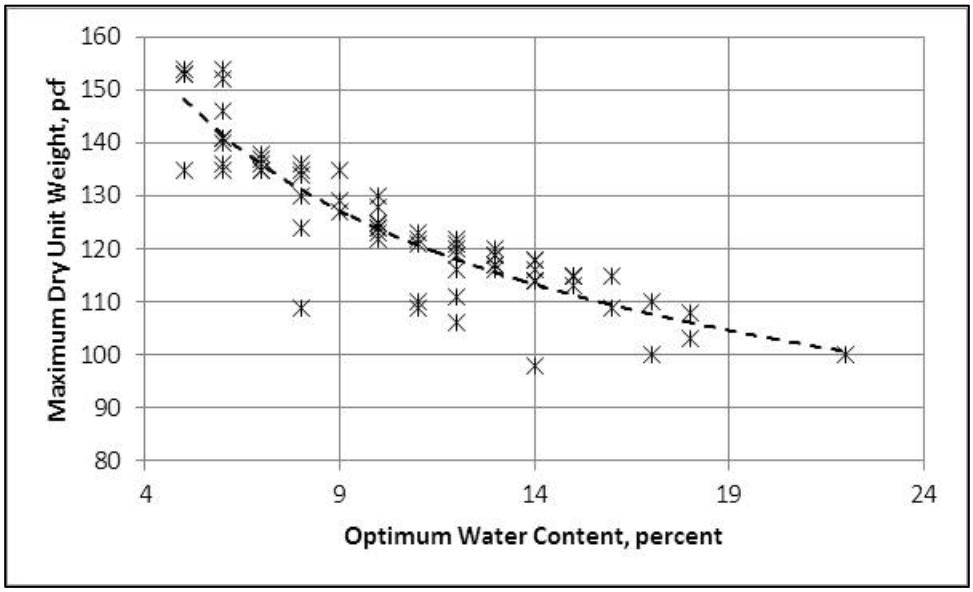

Figure 14—Relationship between Optimum Water Content and Maximum Dry Unit Weight for all Unbound Materials and Soils for the Georgia Sites

The resilient modulus, however, was not always measured on specimens prepared at optimum conditions. The water content and dry density reported for the resilient modulus tests for all unbound layers were entered as input level 1. The average values for a specific soil type were assumed to be applicable for the non-LTPP segments for the cases or sites when the in place water content was unavailable.

Two approaches were used to determine the resilient modulus at the time of construction: (1) laboratory repeated load resilient modulus tests, and (2) backcalculation of elastic modulus from deflection basins. The backcalculated modulus value adjusted to laboratory conditions is the preferred technique for rehabilitation design because the resulting layer modulus is an equivalent value of the materials that vary horizontally and vertically. The laboratory resilient modulus test represents a discrete specimen in the horizontal and vertical direction. More importantly, unbound layers and foundations that contain large boulders or aggregates are difficult or impossible to test in the laboratory.

Multiple backcalculation programs provide the elastic layer modulus typically used for pavement evaluation and rehabilitation design. ASTM D 5858, *Standard Guide for Calculating In Situ Equivalent Elastic Moduli of Pavement Materials Using Layered Elastic Theory* is a procedure for analyzing deflection basin test results to determine layer elastic moduli (i.e., Young's modulus). The backcalculation program *EVERCALC* was used to determine the in place elastic modulus for all structural layers.

Repeated load resilient modulus lab test results are included in the LTPP database for most unbound layers. The laboratory resilient modulus at optimum moisture content is the specified input when the Integrated Climate Model (ICM) is used to determine the seasonal effects over time. The laboratory resilient modulus of the subgrade soil is used to backcalculate a k-value for each month which is used in to calculate the stresses and deflections used to compute the damage in JPCP. LTPP does not provide the required subgrade laboratory resilient modulus at optimum moisture content for all sites. Thus, FWD data from the LTPP database were used to backcalculate the in place subgrade resilient modulus and k-value as appropriate for the flexible and rigid LTPP, as well as non-LTPP sections.

The point in time chosen for the backcalculation was selected to represent the time at which the soils and materials were sampled. This time was selected so the laboratory measured resilient modulus at an equivalent stress state below the pavement surface was determined under the same conditions during which the deflection basins were measured with the FWD. Estimating both of these values at the same time or subsurface condition, permits the AASHTO C-factor to be determined and compared to the values recommended for use in the MEPDG Manual of Practice. The procedure summarized by Von Quintus and Killingsworth was used to estimate the in place resilient modulus for each site (1997).

The Task 2 interim report included the laboratory measured resilient modulus at equivalent in place stress states, backcalculated resilient modulus, dry density and water content for the unbound layers of each site in comparison to the default values. Figures 15 and 16 include a graphical comparison of the laboratory derived resilient modulus and backcalculated derived elastic modulus values. As shown, there is a lot of variability between the laboratory and in place modulus values. Table 12 summarizes the average C-factors for the different types of structures, in comparison to the values recommended in the MEPDG Manual of Practice. These average values for the c-factor were used for the non-LTPP sites.

Figure 17 includes a comparison between the water contents measured on bulk or undisturbed samples of the subgrade soil and aggregate base material and the optimum water content. In summary, the specimen and in place water content for many of the aggregate base layers and fine-grained subgrade soil is slightly greater than the optimum water content (materials with the higher optimum water contents). The poorly graded sands and other high permeability coarse-grained materials are the predominant material where the in place water content is lower than the optimum water content (lower optimum water contents).

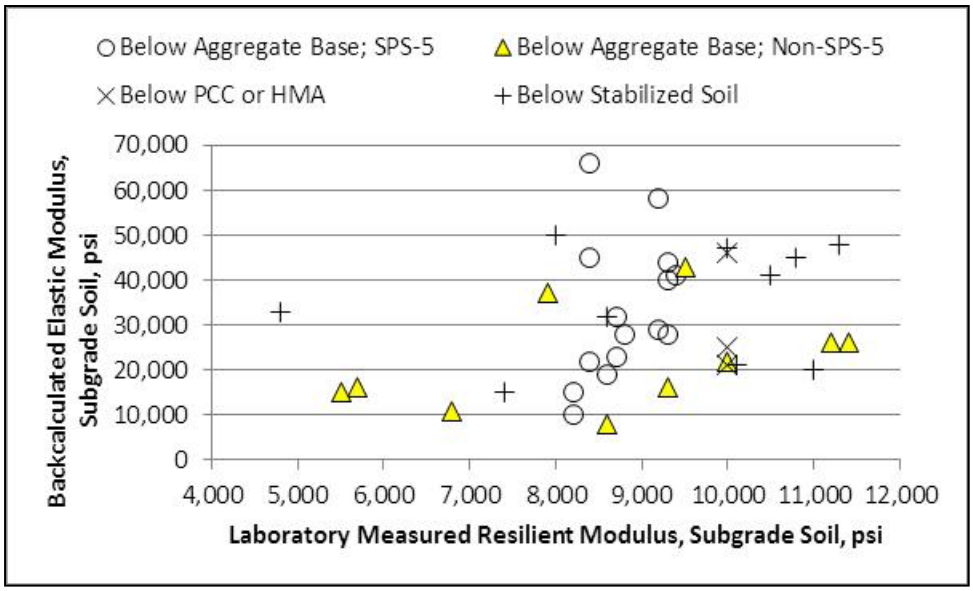

Figure 15—Laboratory Derived Resilient Modulus Values compared to the Field Derived Backcalculated Elastic Modulus Values for the Georgia Subgrade Soils

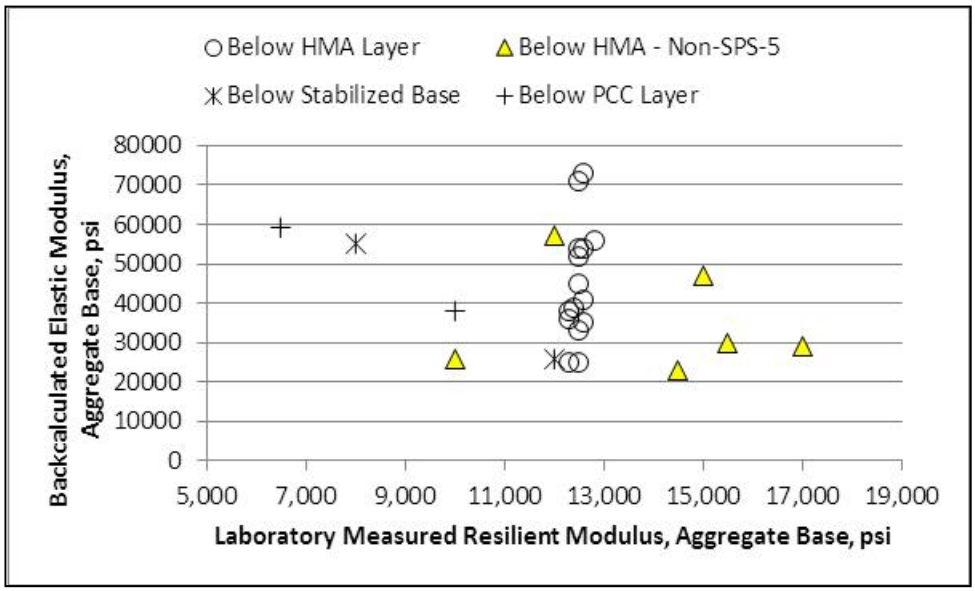

Figure 16—Laboratory Derived Resilient Modulus Values compared to the Field Derived Backcalculated Elastic Modulus Values for the Aggregate Bases in Georgia

Table 12—Average AASHTO c-Factors for the Georgia Unbound Layers

Layer Type	Location	C-Value or M_r/E_{FWD} Ratio	
		MEPDG MOP	Georgia LTPP Sites
Aggregate Base/Subbase	Between a Stabilized & HMA Layer	1.43	0.303
	Below a PCC Layer	1.32	0.187
	Below an HMA Layer	0.62	0.373
Subgrade-Embankment	Below a Stabilized Subgrade/Embankment	0.75	0.304
	Below an HMA or PCC Layer	0.52	0.365
	Below an Unbound Aggregate Base	0.35	0.404

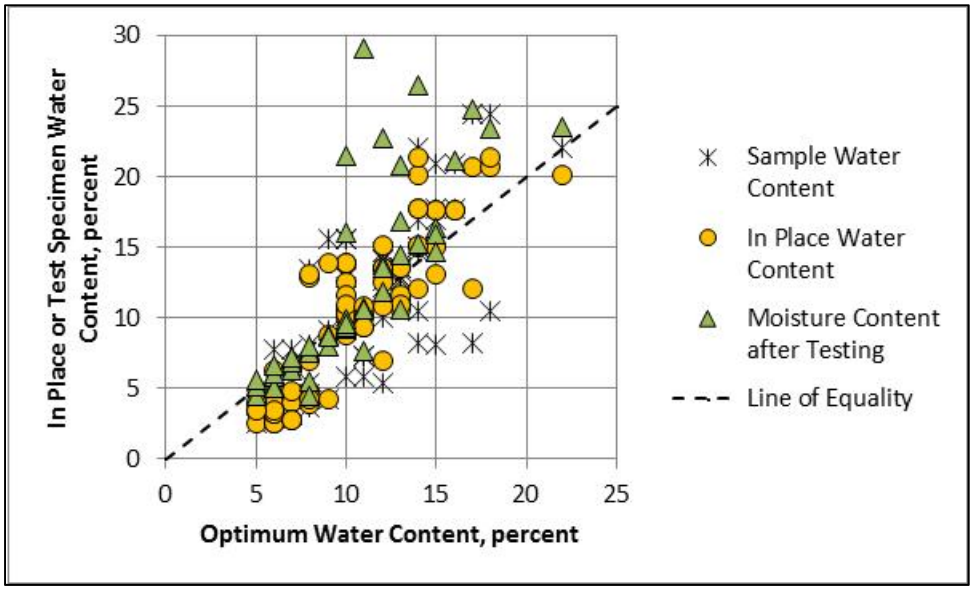

Figure 17—In Place Water Content compared to the Optimum Water Content for Georgia Soils

4.4 Initial Smoothness

The initial IRI is a required input to the MEPDG, but was only available for a few of the Georgia LTPP test sections. Thus, the initial value was backcasted from the monitored IRI data, similar to the backcasting procedure used for the initial AADTT, with one major exception. Unlike for AADTT, IRI does not change significantly until distresses begin to occur, as illustrated in Figure 18 for a couple of SPS-5 test sections (sections 0503 and 0506). The IRI-time relationship for some time after construction is relatively flat, and only starts to increase after the occurrence of surface distress. The following equation was used to backcast the initial IRI values, which has been used in other studies.

$$IRI_t = IRI_i (e)^{g_1 \left(\frac{t}{20}\right)^{g_2}} \quad (2)$$

Where:

IRI_t = IRI measured at time t.
IRI_i = Initial IRI measured or estimated at time of construction.

t = Time or age of pavement, years.
g_1, g_2 = Regression constants determined from the monitored IRI-time values.

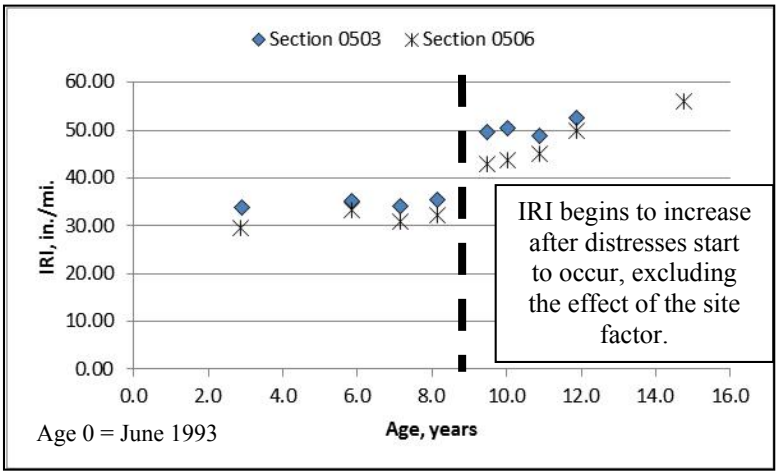

I-401
Bartow Co.
HMA Overlay:
- 0503-Dense graded mix with RAP.
- 0506-Dense graded mix without RAP.

Figure 18—IRI Measured over Time for Two Georgia SPS-5 Flexible Pavement Test Sections

Figures 19 and 20 include examples of using the empirical IRI-time relationship to estimate the initial IRI for the older LTPP test sections. A summary of initial IRI values for all the LTPP sections is presented in Table 13. Sufficient time series data was unavailable for the non-LTPP sections, so the average initial IRI value was used for all of the non-LTPP segments.

4.5 Distress Data

There were two issues or concerns related to the distress data that were used in the calibration process. These two concerns were: (1) potential differences in distress magnitudes between the LTPP and non-LTPP sections, and (2) potential differences in distress definitions and measurement procedures between the Distress Identification Manual and GDOT's PACES and CPACES manuals. This subsection of the report addresses both concerns.

- *Differences in amounts of cracking: LTPP versus non-LTPP segments.* There are significant differences in the amount of cracking between the LTPP and non-LTPP segments. The LTPP sections have relatively low amounts of cracking while the non-LTPP flexible pavement segments exhibit higher amounts of cracking because that is why they were selected. The issue is whether that difference or bias in cracking can be explained through the MEPDG design methodology. Residual errors between LTPP and non-LTPP sections were evaluated to determine if those differences are a result of some confounding factor not properly addressed or considered in the MEPDG transfer functions and prediction methodology. This evaluation is addressed in Section VI.

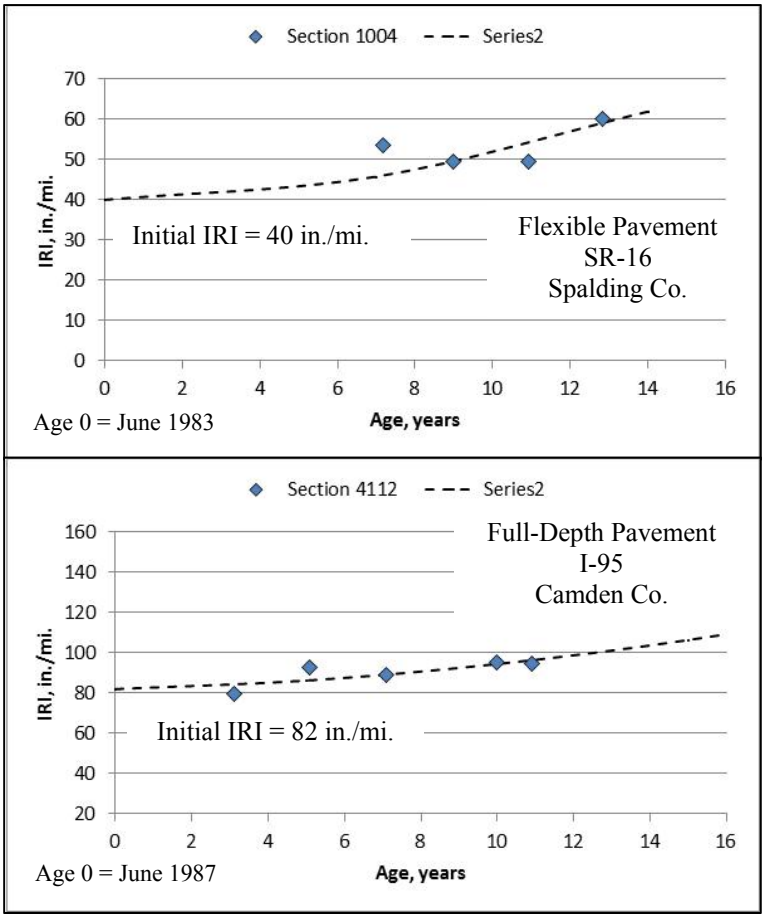

Figure 19—Illustration of the Process used to Backcast the Initial IRI for Two LTPP Flexible Pavement Test Sections

- *Differences in distress definitions and measurement techniques: LTPP versus GDOT procedures.* Distress data were extracted from the LTPP database and were measured in accordance with the FHWA Distress Identification Manual, while the distress data for the non-LTPP segments was extracted from the GDOT PACES and CPACES databases. As part of the field investigations, distress surveys were completed for each of the non-LTPP sections and compared with the distress data extracted from PACES and CPACES. Significant differences were found which potentially restrict use of the historical data from PACES and CPACES, if the two measurement definitions cannot be related. Figure 21 shows the comparison of the total amount of fatigue cracking as defined by LTPP and the Distress Identification Manual versus the total amount of cracking recorded in the GDOT PACES database for comparable times. As shown, there is a relationship so this relationship was used to estimate the amount of fatigue cracking as defined by LTPP from the total amount of cracking recorded in PACES for the time series data.

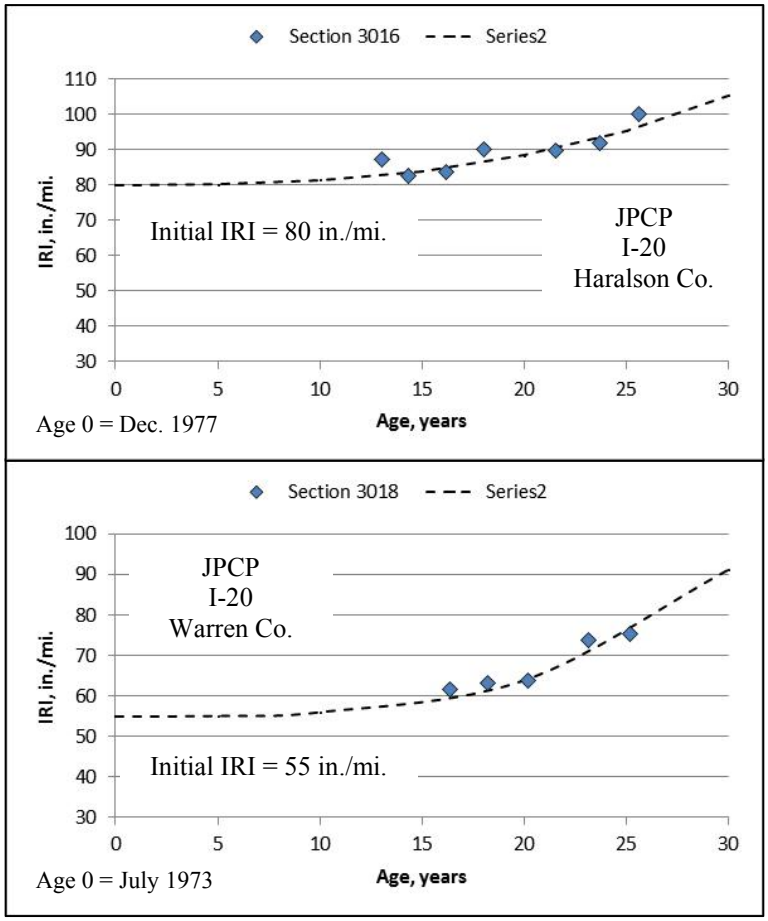

Figure 20—Illustration of the Process used to Backcast the Initial IRI for Two LTPP Rigid Pavement Sections

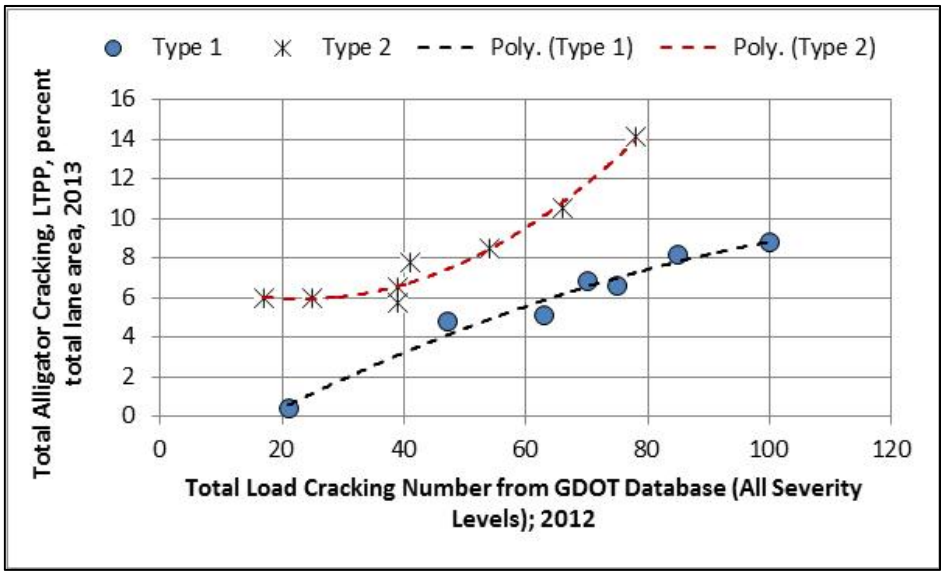

Figure 21—Relationship between Total Load Cracking Number from GDOT PACES Database and LTPP Defined Total Alligator Cracking

Table 13—Initial IRI Estimated for the Georgia LTPP Sections

LTPP Section ID		Initial IRI, in/mi	LTPP Section ID	Initial IRI, in/mi
SPS-5 Test Sections; HMA Overlay	0502	33	3016- JPCP	80
	0503	34	3017- JPCP	78
	0504	30	3017- CPR	38
	0505	34	3018 – JPCP	55
	0506	30	3019 – JPCP	88
	0507	30	3020 – JPCP	84
	0508	42	3020 – HMA Overlay	85
	0509	33	4092 – Semi-Rigid	43
	0560	28	4093 – Semi-Rigid	44
	0561	30	4096 – Semi-Rigid	57
	0562	34	4096 – HMA Overlay	53
	0563	39	4111 – Flexible	45
	0564	30	4112 – Full-Depth	82
	0565	31	4113 – Full-Depth	62
	0566	41	4113 – HMA Overlay	40
1001-Flexible		50	4118 – CRC Overlay	35
1004-Flexible		40	4119 – Flexible	60
1005-Flexible		59	4420 – Semi-Rigid	58
1031-Flexible		42	4420 – HMA Overlay	49
1031-HMA Overlay		34	5023 – CRCP	80
3007-JPCP		110	7028 – HMA Overlay	63
3011-JPCP		65	7028 – HMA Overlay	38
3015 – JPCP		65		

V. CALIBRATION COEFFICIENTS FOR RIGID PAVEMENTS AND PCC OVERLAYS

Verification of the MEPDG global calibration coefficients and standard deviations of the rigid pavement transfer functions for Georgia conditions consisted of running the *Pavement ME Design* software for the Georgia LTPP and other JPCP sections and evaluating goodness of fit and bias. The AASHTO adopted global model or calibration coefficients utilized were those developed under NCHRP project 20-07 (327) to reflect corrections made to the concrete CTE values (Sachs, 2014). The correct CTE values used in the NCHRP project 20-07 (327) were used in evaluating and judging the accuracy of the transfer functions for the Georgia rigid pavement test sections. Thus, proper lab measurements of CTE using AASHTO T336 *Coefficient of Thermal Expansion of Hydraulic Cement Concrete* can be directly input into the design of all PCC pavements and overlays.

Appendix A provides the layer and design details of the 8 LTPP and 12 non-LTPP JPCP sections used in the verification and calibration analysis. A map illustrating the locations of the LTPP and other Georgia JPCP sections was included in Figures 1 and 3. A reasonable spread of sections throughout Georgia and design features was obtained with a concentration in the Atlanta area where many concrete pavements have been constructed. Table 14 includes a summary of the design, age, and traffic characteristics of these sections. The JPCP sections range in age from 6 to 64 years. These pavements were loaded by heavy truck traffic which ranged from 1 to 50 million trucks in the heavily trafficked lane over the life of the pavement.

The design features include a wide range of slab thickness (7.5 to 14 in.), transverse joint spacing (15 to 30 ft.), base types and subgrade soils. Most of the JPCP projects included dowel bars at transverse joints with dowel diameters ranging from 1.00 to 1.50 in.

Table 14—Characteristics of Rigid Pavement Structures Used for Calibration

Pavement Feature	Range	Mean or Typical Value
Age of JPCP	6 to 64 years	31 years
No. of Trucks (Design Lane)	1 to 50 million	16 million
Slab Thickness	7.5 to14.3 in	10.3 in
Joint Spacing*	15 to 30 ft	20 ft
Dowel Bars	None, 1.0 to 1.5 in	1.25 in
Base Type	Aggregate, HMA, HMA/Soil Cement, CTB	ALL
Subgrade Type	Sandy Silt, Sand, Silty Sand, Clayey Sand, Poorly Graded Sand	ALL

*Note: Skewed joints increase the effective joint spacing by 2 ft. Thus, a skewed joint spacing of 16 ft would require an input of 18 ft.
Note: When a thin (1-in) HMA interlayer existed between PCC slab and CTB, it was modeled as a CTB with the additional thickness. This approach matched measured transverse cracking since there was typically a strong bond between layers over many years which resulted in a composite slab.

5.1 JPCP Fatigue Cracking or Mid-Slab Cracking

5.1.1 Transfer Function

Two key models are used to predict mid-slab transverse fatigue cracking: (1) one model for determining the allowable number of loading cycles for a specific condition, and (2) a model for estimating the percentage of cracks slabs from the cumulative damage index. Equation 3 is used to estimate the fatigue life (N) of PCC slabs when subjected to repeated wheel load stresses and curling stresses (at both top and bottom of the slab) for a given flexural bending beam strength. The calibration factors C_1 and C_2 can be modified but since they are based on substantial laboratory and full scale field testing data, the MEPDG Manual of Practice does not recommend changing these coefficients. These values are $C_1 = 1.0$ and $C_2 = -1.22$ which were held constant for the Georgia calibration process.

$$\log\left(N_{i,j,k,l,m,n}\right) = C_1 \cdot \left(\frac{MR_i}{\sigma_{i,j,k,l,m,n}}\right)^{C_2} \quad (3)$$

The transfer function with appropriate model coefficients is the S-shaped curve giving the relationship between the measured fatigue cracking and accumulated fatigue damage (DF) at top and bottom of the JPCP slabs. Calibration coefficients C_4 and C_5 in equation 4 can be adjusted to remove bias and improve the goodness of fit with field data.

$$CRK = \frac{1}{1 + C_4\left(DI_F\right)^{C_5}} \quad (4)$$

Values derived for the global calibration coefficients are listed below and were obtained from NCHRP 20-07 (327) (Sachs, et al., 2014). These values were evaluated for adequacy against the measured Georgia JPCP cracking data:

$C_4 = 0.52$
$C_5 = -2.17$

5.1.2 Verification of the Global Calibration Coefficients

The majority of the LTPP JPCP sections have little to no measured transverse fatigue cracking (see Task 2 interim report). Figure 22 compares the predicted and measured percent slabs cracked, while Figure 23 compares the calculated concrete fatigue damage index accumulated over time to the measured percent slabs cracked. Predicted cracking versus the residual error (predicted minus measured values) are included in Figure 24 and confirms bias in the model. The main cause of for poor goodness of fit and bias in the global model, however, is probably due to a lack of measured cracking data in the higher range as illustrated in Figure 23.

Some measured data show significant increase in transverse cracking over a short time interval, while the transfer function (predicted cracking) does not exhibit this increase. As a result, the transfer function significantly under predicts transverse cracking. A few measured

data are believed to be outliers and are considered suspicious data. An example of suspicious data point is illustrated in Figure 23. The site investigations or forensic evaluations of those pavement sections did not explain or reveal the actual cause of the high amount of cracking. The distress survey was checked and it was confirmed the cracking magnitude was not in error. This large difference between the measured and predicted values is a reason why more test sections need to be included in the local calibration process. More test sections and data points reduce the erroneous impact one outlier or suspicious data, that cannot be explained, can have on calibration factors.

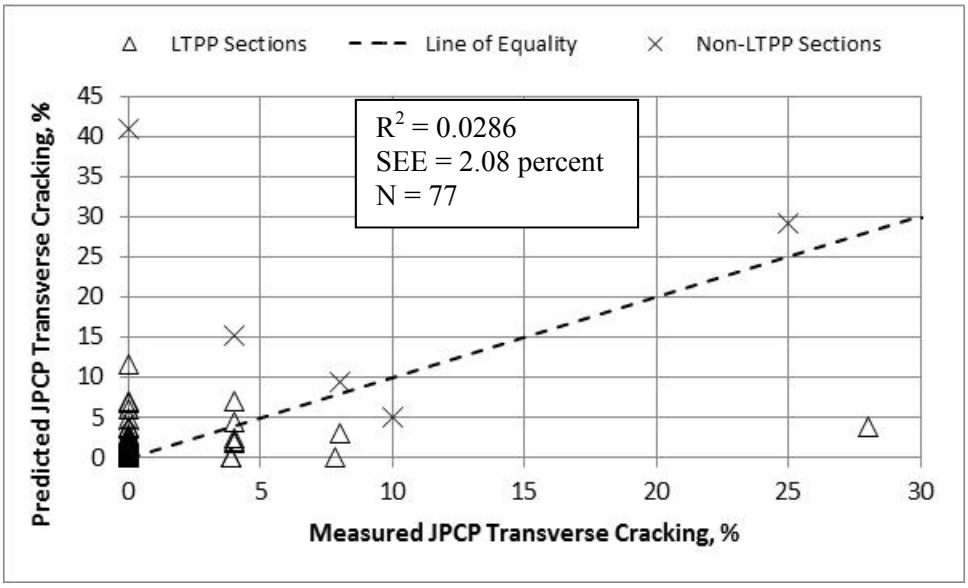

Figure 22—Predicted versus Measured Percent Slabs Cracked

Table 15 summarizes the statistical analysis between the predicted and measured cracking data. It should be noted that the amount of cracking is very low for the majority of the LTPP sites in Georgia, so the standard error of the estimate (SEE) is only representative of these low amounts of measured cracking. The results are summarized as follows, for the LTPP rigid pavement test sections with low amounts of cracked slabs:

- The intercept of the y= x curve was 1.418 (ranging from 0.928 to 1.907) with a corresponding p-value of <0.0001. The p-value less than 0.05 means the Test 1 null hypothesis was rejected. Thus, the MEPDG predicted cracking did exhibit this aspect of bias.

- The slope of the y equals x curve was 0.199. The corresponding p-value was <0.0001. Thus, the Test 2 null hypothesis was rejected, indicating that the predicted cracking does not equal the measured cracking, and this difference is significant. MEPDG cracking estimates cannot be extrapolated beyond the key inputs used for calibration.

- Finally, the p-value from paired t-test value compares predicted cracking from the MEPDG to the measured cracking value. The t-test value was 0.1836, and suggests the difference between the pairs is insignificant.

Non-LTPP test sections with higher amounts of cracking were identified and selected for use in calibrating the transfer function, as noted in Section II. These additional sites were combined with the LTPP sections to determine the Georgia calibration coefficients for the mid-slab fatigue cracking transfer function.

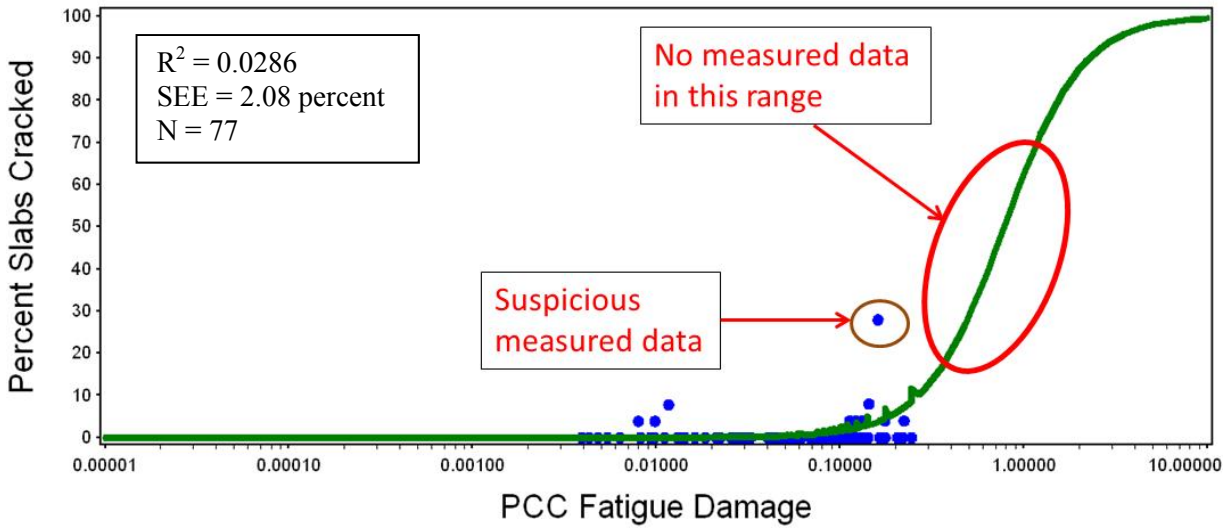

Figure 23—Measured Fatigue Transverse Cracking versus Concrete Fatigue Damage for all Georgia LTPP JPCP Sections

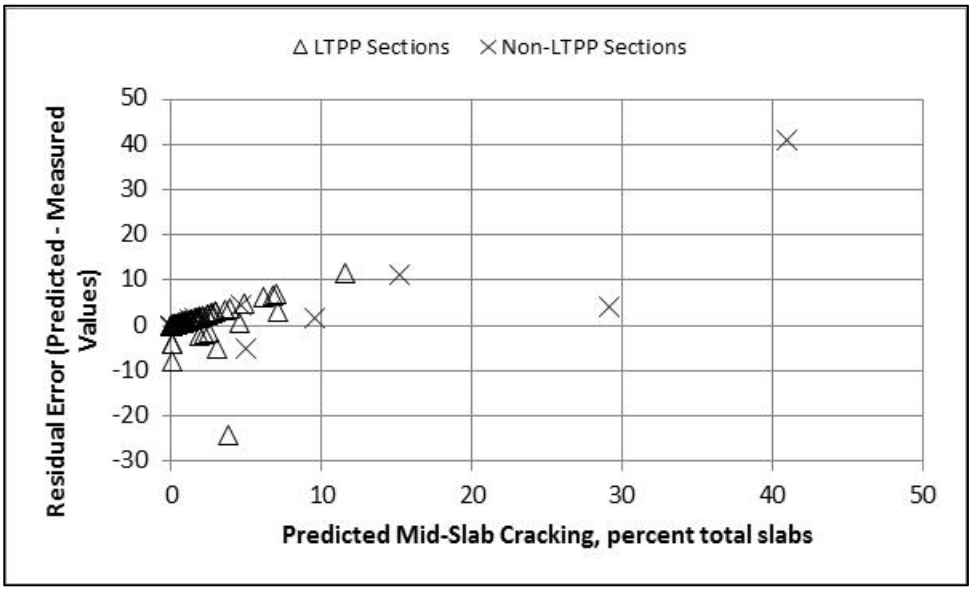

Figure 24—Predicted versus Residuals (Predicted minus Measured Values) for Percent Slabs Cracked

Table 15—Statistical Comparison of Measured and MEPDG Predicted Transverse Cracking

Hypothesis Testing and T-Test				Goodness of Fit	
Test Type	**Value**	**Range**	**p-value**	**R^2**	**SEE, percent**
Hypothesis Test (1): Intercept = 0	1.418	0.928 to 1.907	<0.0001	0.0286	2.08
Hypothesis Test (2): Slope = 1	0.199	0.004 to 0.355	<0.0001		
Paired t-test	—	—	0.1836		

5.1.3 Georgia Calibration Coefficients

Measured transverse cracking trends for all Georgia calibration sections were reviewed and evaluated for reasonableness. There existed some significant variations over time for some sections probably due to variations in field measurements or removal and replacement of slabs not recorded in the LTPP database or GDOT as-built construction records. Whenever there was a significant time sequence aberration in the data, the individual cracking measurements were removed from the analysis when the data point was defined as an outlier.

The analysis utilized the full Georgia JPCP database to establish the goodness of fit and bias in the MEPDG transverse cracking model. Figure 25 shows the concrete fatigue damage accumulated over time along with the measured percent slabs cracked. Figure 26 illustrates good fit of the measured cracking from low damage (newer or more structurally sound pavements) with no fatigue cracking to higher damages (> 0.10) with greater amounts of fatigue cracking. The statistical analysis indicated by adjusting C_4 and C_5 the goodness of fit improved. The values of $C_4 = 0.52$ and $C_5 = -2.17$ are recommended for use in design of JPCP.

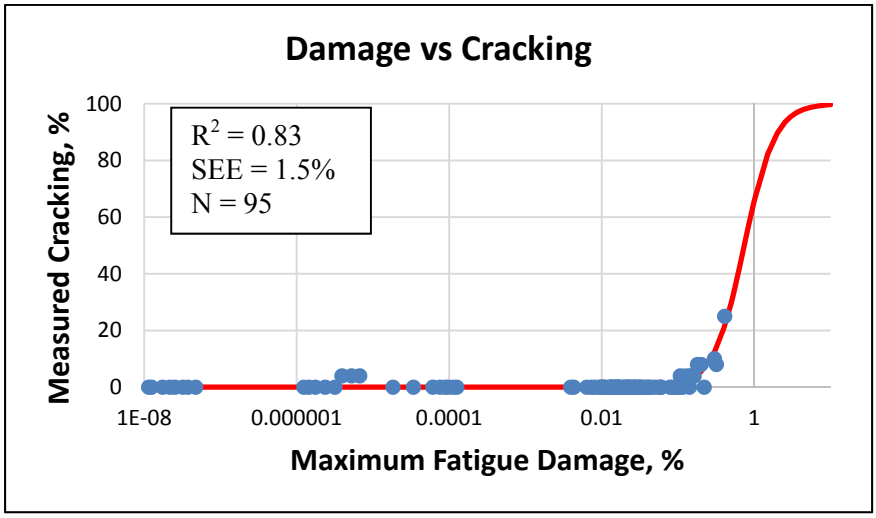

Figure 25—Measured Fatigue Transverse Cracking (percent slabs cracked) versus Fatigue Damage for all Georgia JPCP Sections ($C_4 = 0.52$; $C_5 = -2.17$)

Figure 26 shows a direct comparison of measured and predicted fatigue cracking using the Georgia calibration coefficients. Given the strong correlation between measured cracking and accumulated fatigue damage, the predicted versus measured cracking plot shows excellent goodness of fit (83 percent R^2) and no significant bias.

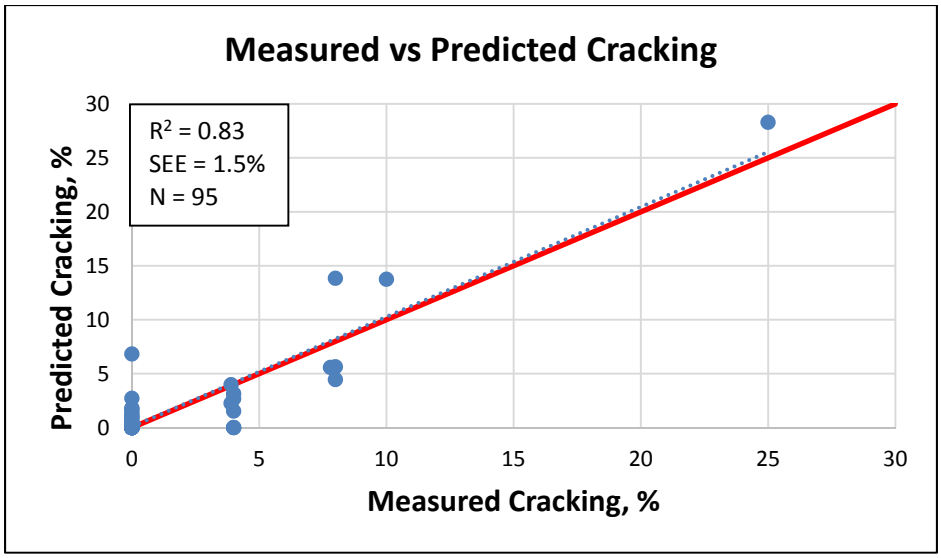

Figure 26—Predicted versus Measured Percent Slabs Cracked (C_4 = 0.52; C_5 = -2.17)

One limitation of the calibration process is that there are only a few sections that had measured transverse cracking more than zero, with the maximum amount being 25 percent. Typical design criteria range from 10 to 25 percent. It would be better if there were more JPCP sections that exhibited even larger amounts of fatigue cracking to better validate the prediction methodology and transfer function. The cracking prediction model does predict fatigue cracking reasonably well up to the 25 percent.

Table 16 summarizes the statistical validation analysis between the predicted and measured cracking data and the results are summarized for the Georgia JPCP pavement sections. There are three statistical tests to validate that the prediction models for cracking:

- The intercept of the y = x curve was -0.08 (ranging from -0.39 to 0.24) with a corresponding p-value of 0.62. The p-value greater than 0.05 means the null hypothesis that the intercept is zero is accepted. Thus, the predicted versus measured cracking line did not exhibit bias related to the intercept.

- The slope of the y = x curve was 1.01 which is very close to 1.00 the null hypothesis. The 95 percent confidence interval ranges from 0.91 to 1.10 which includes 1.00. The corresponding p-value should be > 0.05 (the calculated value appeared to be in error), so the null hypothesis that the slope between predicted and measured cracking is 1.00 is accepted indicating no bias.

- Finally, the p-value from the paired t-test value compares predicted minus measured cracking residual error over the entire database. The paired t-test p-value was 0.64 which exceeded 0.05, so the null hypothesis (that the paired predicted and measured cracking values are equal) was accepted. This indicates no bias related to overall measured and predicted cracking values.

Table 16—Statistical Comparisons of Measured and MEPDG Predicted Transverse Fatigue Cracking to Show that the Cracking Prediction Model is Unbiased (C_4 = 0.52; C_5 = -2.17)

Hypothesis Testing and t-test				Goodness of Fit	
Test Type	**Value**	**Range**	**p-value**	**R^2**	**SEE, percent**
Hypothesis Test (1): Intercept = 0	-0.08	-0.39 to 0.24	0.62	0.83 (Good Fit) N = 95	1.47 (Unusually low due to good fit)
Hypothesis Test (2): Slope = 1	1.01	0.91 to 1.10	NA		
Hypothesis Test (3): Paired t-test Difference = 0	—	—	0.64		

Figure 27 illustrates two of the LTPP projects with higher amounts of fatigue cracking in comparison to the predicted amounts of cracking. As shown, the predicted amounts of cracking fairly well matches the measured cracking over a 25 year time span.

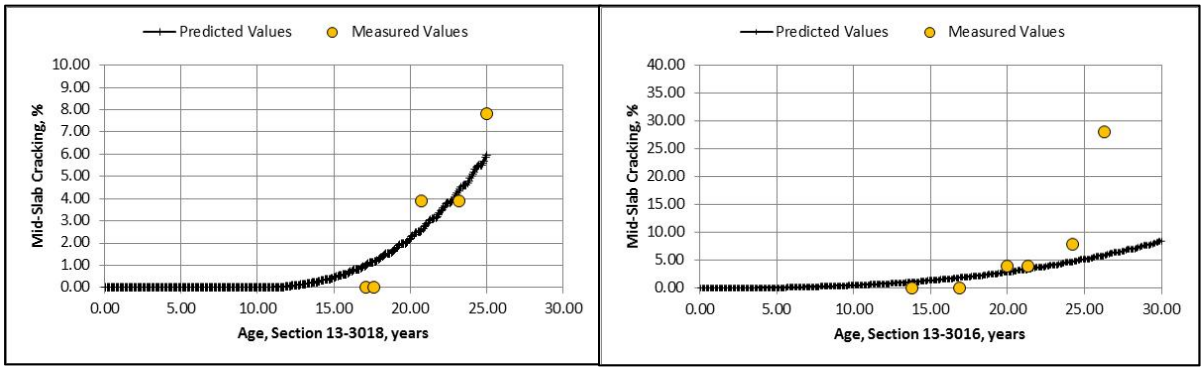

Figure 27—Percent Slabs Cracked over Time for Georgia Sections 13-3016 and 13-3018 (Georgia Calibration Coefficients)

The fatigue cracking SEE derived from the Georgia calibration sections was very low compared to the global standard deviation (1.47 percent slabs cracked versus 4.58 percent from NCHRP 20-07(327)). This outcome will significantly affect the design reliability prediction. A major limitation of this outcome, however, is the few number of actual projects included in the database and the fact that most of them had no cracking. After consideration, it was decided to utilize the global standard deviation equation (standard error of the estimate [SEE]) shown below from NCHRP 20-07 (327):

Standard Deviation Cracking = 3.5522*Pow(CRACK,0.3415)+0.75 (5)

This standard deviation equation will provide a more realistic impact of design reliability on pavement design because it is based on hundreds of JPCP projects around the country. As more data on percent cracked slabs become available over time for these and other calibration sties, GDOT should periodically verify and validate the Georgia calibration coefficients and the standard error of the transfer function.

5.2 JPCP Faulting

5.2.1 Transfer Function

The mean transverse joint faulting is predicted using a complex incremental approach. A detailed description of the faulting prediction process is presented in Section 5 the MEPDG Manual of Practice. MEPDG faulting is predicted using the models presented below:

$$Fault_m = \sum_{i=1}^{m} \Delta Fault_i \tag{6}$$

$$\Delta Fault_i = C_{34} * (FAULTMAX_{i-1} - Fault_{i-1})^2 * DE_i \tag{7}$$

$$FAULTMAX_i = FAULTMAX_0 + C_7 * \sum_{j=1}^{m} DE_j * Log(1 + C_5 * 5.0^{EROD})^{C_6} \tag{8}$$

$$FAULTMAX_0 = C_{12} * \delta_{curling} * \left[Log(1 + C_5 * 5.0^{EROD}) * Log(\frac{P_{200} * WetDays}{p_s}) \right]^{C_6} \tag{9}$$

Where:

$Fault_m$ = Mean joint faulting at the end of month m, in
$\Delta Fault_i$ = Incremental change (monthly) in mean transverse joint faulting during month *i*, in
$FAULTMAX_i$ = Maximum mean transverse joint faulting for month *i*, in
$FAULTMAX_0$ = Initial maximum mean transverse joint faulting, in
$EROD$ = Base/subbase erodibility factor
DE_i = Differential deformation energy accumulated during month *i*. Computed using various inputs including joint LTE and dowel damage
$EROD$ = Base/subbase erodibility factor
$\delta_{curling}$ = Maximum mean monthly slab corner upward deflection PCC due to temperature curling and moisture warping.
P_S = Overburden on subgrade, lb
P_{200} = Percent subgrade soil material passing No. 200 sieve
$WetDays$ = Average annual number of wet days (greater than 0.1 in rainfall)

$$C_{12} = C_1 + C_2 * FR^{0.25} \tag{10}$$

$$C_{34} = C_3 + C_4 * FR^{0.25} \quad (11)$$

FR = Base freezing index defined as percentage of time the top base temperature is below freezing (32°F) temperature.

Dowel joint damage accumulated for the current month is determined from the following equation:

$$\Delta DOWDAM_{tot} = \sum_{j=1}^{N} C_8 * F_j \frac{n_j}{d f_c^*} \quad (12)$$

Where:

$\Delta DOWDAM_{tot}$ = Cumulative dowel damage for the current month.

n_i = Number of axle load applications for current increment and load group *j*.

N = Number of load categories.

f_c^* = PCC compressive stress estimated.

C_8 = Calibration constant.

F_j = Effective dowel shear force induced by axle loading of load category j.

C_1 through C_8 are calibration constants to be established based on field performance.

Faulting model calibration involved determination of the calibration parameters C_1 through C_7 from the above equations and the rate of dowel deterioration parameter, C_8, from the above equation, which minimize the error function, ERR, defined as:

$$ERR(C_1, C_2, ..., C_8) = \sum_{ob=1}^{Nob} \left(FaultPredicted_{ob} - FaultMeasured_{ob}\right)^2 \quad (13)$$

Where:

ERR = Error function

$C_1, C_2, ..., C_8$ = Calibration parameters

$FaultPredicted_{ob}$ = Predicted faulting for observation *ob* in the calibration database

$FaultMeasured_{ob}$ = Measured faulting for observation *ob* in the calibration database

N_{ob} = Number of observation in the calibration database

The global calibration coefficients from NCHRP 20-07(327) are as follows (Sachs, 2014):

C1 = 0.595
C2 = 1.636
C3 = 0.00217
C4 = 0.00444
C5 = 250
C6 = 0.47
C7 = 7.30
C8 = 400

The global faulting model for standard deviation as a function of mean joint faulting is given in equation 14.

$$\text{Standard Deviation (FLT)} = 0.00806 + 0.07162 * (\text{FLT}^{0.368}) \quad (14)$$

5.2.2 Verification of the Global Calibration Coefficients

Only data from the Georgia LTPP sections were available for use on this project. Measured faulting trends for each Georgia section were carefully reviewed. There existed some significant variations over time for nearly all sections probably due to variable curling of the slabs. Whenever there was a significant time sequence aberration in the data, the individual faulting measurements were removed from the analysis; similar to what was done for the JPCP fatigue cracking data.

Figure 28 shows the predicted versus measured faulting using the global calibration coefficients for all data. The plot shows poor goodness of fit along with an obvious bias of under predicted faulting. However, the magnitude of faulting is generally low with the highest values just exceeding the threshold value normally used in design. The reason for the low faulting values is the stabilization of the base and the standard practice by GDOT to use dowels and edge drains on many JPCP projects.

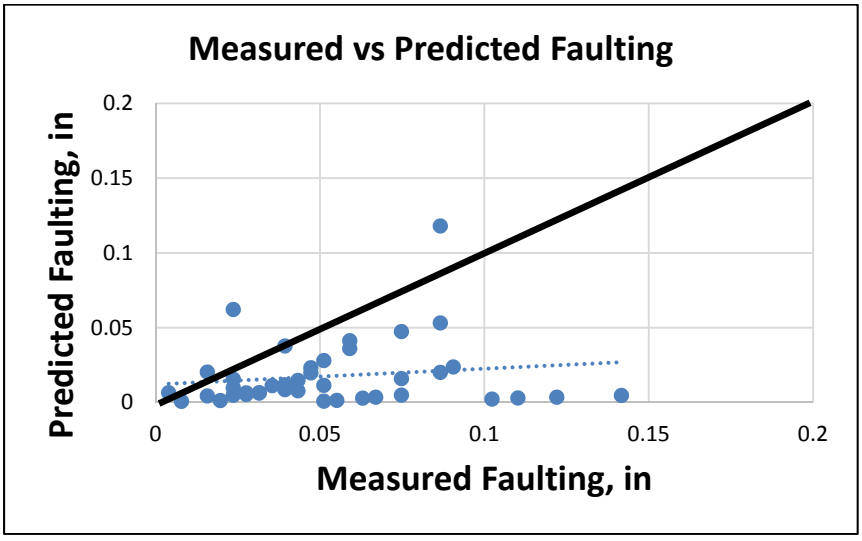

Figure 28—Predicted versus Measured Faulting using NCHRP 20-07(327) Global Calibration Coefficients

The predicted faulting versus the residual faulting error (predicted minus measured value) is included in Figure 29 and shows a tread that confirms bias in the model. The magnitude of faulting, however, is very low. In fact, the magnitude is significantly lower than the threshold value normally used in design. The reason for low faulting values is that GDOT has been doweling JPCP since the 1970's.

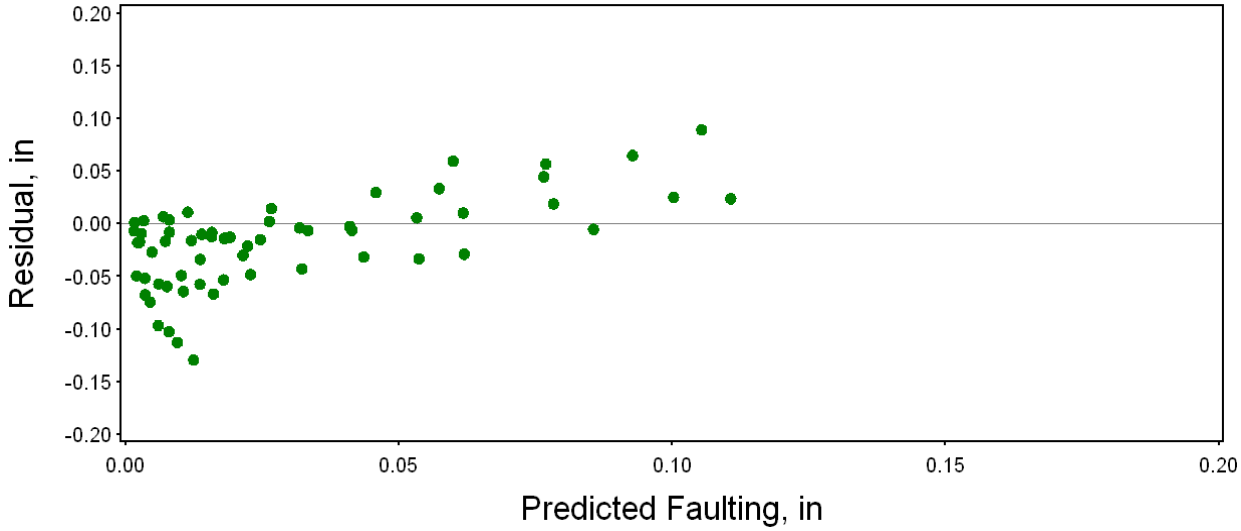

Figure 29—Predicted versus Residuals (Predicted minus Measured Value) for Faulting

Table 17 includes results from the statistical analysis performed in comparing the predicted and measured faulting values. Results from the statistical analysis are summarized below:

- The intercept of the y= x curve was 0.0259 (ranging from 0.013 to 0.039) with a corresponding p-value of 0.0003. The p-value less than 0.05 implied the Test 1 null hypothesis is rejected. Thus, the MEPDG faulting transfer function does exhibit bias.

- The slope of the y= x curve was 0.448. The corresponding p-value was <0.0001. Thus, the Test 2 null hypothesis was rejected, indicating the predicted MEPDG faulting is unequal to the measured faulting, and is significant. MEPDG faulting estimates cannot be extrapolated beyond or outside of the key inputs used for calibration.

- Finally, the p-value from the paired t-test comparing faulting estimated with the MEPDG to the measured faulting was 0.0023. This shows that this aspect of bias was significant.

There are no obvious causes for under prediction of faulting using the NCHRP 20-07 (327) global faulting model coefficients for Georgia. Thus, the global calibration coefficients are inappropriate for Georgia conditions and design features, and local calibration is needed to adjust the model coefficients to match the measured transverse joint faulting data.

Table 17—Statistical Comparison of Measured and MEPDG Predicted Faulting

Hypothesis Testing and T-Test				Goodness of Fit	
Test Type	**Value**	**Range**	**p-value**	**R^2**	**SEE, in**
Hypothesis Test (1): Intercept = 0	0.259	0.013 to 0.039	0.0003	0.0067	0.0298
Hypothesis Test (2): Slope = 1	0.448	0.299 to 0.597	<0.0001		
Paired t-test	—	—	0.1836		

5.2.3 Georgia Calibration Coefficients

As stated above, GDOT has been doweling JPCP since the 1970's and low faulting was expected. The measured faulting trends for all calibration sections were reviewed and evaluated for reasonableness. Most of the faulting time series data exhibited reasonable trends. As such, adjustments were made to the global calibrations coefficients to account for this difference or bias between the measured and predicted values. Local calibration was performed using these data, and the final set of Georgia specific local joint faulting model coefficients are summarized below:

C1 = 0.611
C2 = 0.00838
C3 = 0.00147
C4 = 0.008345
C5 = 5999
C6 = 0.8404
C7 = 5.9293
C8 = 400

The standard deviation of the transverse joint faulting equation was determined using GDOT data as shown in equation 15. This standard deviation equation is similar to the nationally derived model and is believed to provide a reasonable assessment of variation for joint faulting prediction.

$$\text{Standard Deviation (Faulting)} = 0.0097*FAULT)^{0.5721} + 0.01 \quad (15)$$

Where: *FAULT* = Predicted mean joint faulting, in.

Figure 30 shows the predicted versus measured faulting using the Georgia local calibration coefficients. The plot shows reasonable goodness of fit (R^2 = 0.60 and SEE = 0.03 in) along with no obvious bias of under or over prediction of faulting.

One limitation of the calibration is that there are only a few sections with measured transverse joint faulting above 0.12 inches and the maximum was 0.15 inches. Typical design criteria range from 0.10 to 0.20 inches and it would be better if there were more JPCP sections that exhibit higher faulting to provide better validation. However, the faulting prediction model does predict reasonably well up to the 0.15 inches. When properly sized dowel bars are used the amount of joint faulting is typically very low as shown by these data.

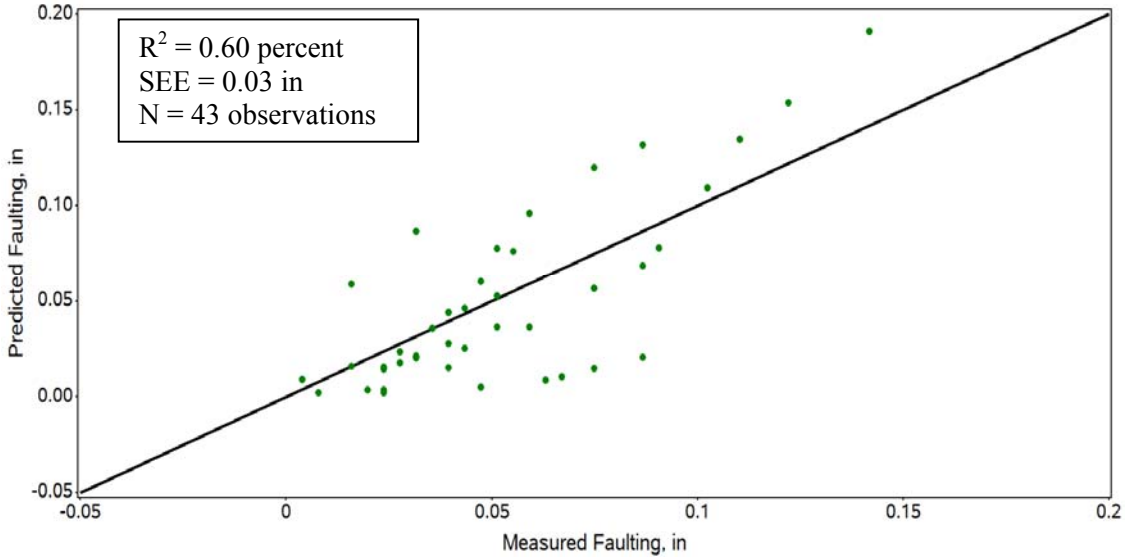

Figure 30—Measured versus Predicted Joint Faulting using Georgia JPCP Calibration Coefficients

Table 18 summarizes the statistical validation analysis between the predicted and measured faulting data for the JPCP pavement sections. The outcome of the three statistical tests to validate that the prediction models for the faulting transfer function is not biased:

- The intercept of the y= x curve was -0.01 (95 percent confidence interval ranges from -0.03 to 0.01) which includes the null hypothesis of 0.00 with a corresponding p-value of >0.05. The p-value greater than 0.05 means the null hypothesis that the intercept is zero is accepted. Thus, the predicted versus measured faulting line did not exhibit bias related to the intercept.

- The slope of the y= x curve was 1.00 which is equal to the null hypothesis slope of 1.00. The 95 percent confidence interval ranges from 0.84 to 1.14 which includes 1.00. Thus, the null hypothesis was accepted, indicating that the slope between predicted and measured faulting is close to 1.00 indicating no bias.

- Finally, a direct comparison of measured and predicted faulting for each section was made across the entire database using the paired t-test. The p-value from paired t-testing was > 0.05 value and thus the null hypothesis (that the mean difference between predicted and measured cracking across all observations are equal) was accepted. This indicates no bias related to predicted and measured values over the entire database.

These results suggest that the Georgia calibrated joint faulting transfer function and prediction methodology is not biased in over or under predicting faulting on average over the

entire database. It is recommended that the Georgia faulting transfer function be used for design of JPCP.

Table 18—Statistical Comparison of Measured and MEPDG Predicted Faulting

Hypothesis Testing and T-Test				Goodness of Fit	
Test Type	**Value**	**Range**	**p-value**	**R^2**	**SEE, in**
Hypothesis Test (1): Intercept = 0	-0.01	-0.03 to 0.01	0.28	0.60	0.03
Hypothesis Test (2): Slope = 1	1.00	0.84 to 1.14	NA		
Paired t-test	---	---	0.55		

5.3 JPCP IRI or Smoothness

5.3.1 Regression Equation

IRI is predicted for JPCP using the following regression equation:

$$IRI = IRI_I + J1*CRK + J2*SPALL + J3*FAULT + J4*SF \quad (16)$$

Where:

IRI_I = Initial IRI after construction, in/mile
CRK = JPCP transverse fatigue cracking, percent slabs
$SPALL$ = JPCP joint spalling, percent joints
$FAULT$ = JPCP mean joint faulting, mean of all joints in inches
SF = Site factor (includes subgrade fine content, freezing index, age)
$J1, J2, J3, J4$ = Global calibration coefficients (J1 = 0.82, J2 = 0.44, J3 = 1.49, J4 = 25.24)

5.3.2 Verification of Global Calibration Coefficients

A plot of predicted and measured IRI for the Georgia LTPP sites is shown in Figure 31 as well as the R-Squared term, SEE, and number of observations. These results indicate that goodness of fit was poor with a high SEE (18.6 in./mi.). Even after removal of the obvious outliers the prediction appears biased (under prediction). The predicted IRI versus the residual error of IRI (predicted minus measured value) are included in Figure 32. The residual error versus the predicted value suggests bias in the regression equation.

These results indicate that goodness of fit was poor and the model predictions were biased, so local calibration was required. The IRI values, however, are predicted using the values from the other predicted distresses. If the other distress transfer functions exhibit a significant bias, then it is likely that the IRI regression equation will exhibit bias. As such, the IRI regression equation was evaluated for precision and bias but only after the other JPCP transfer functions had been recalibrated to eliminate any bias or errors from those equations and improve on the goodness-of-fit.

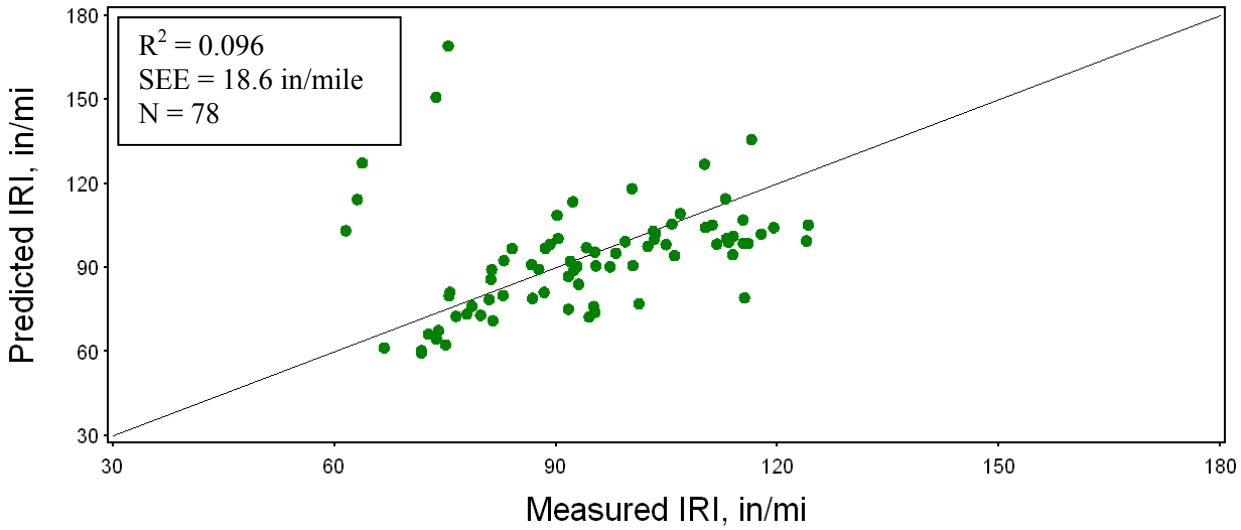

Figure 31—Predicted versus Measured IRI for Georgia LTPP Sections using Global Calibration Coefficients

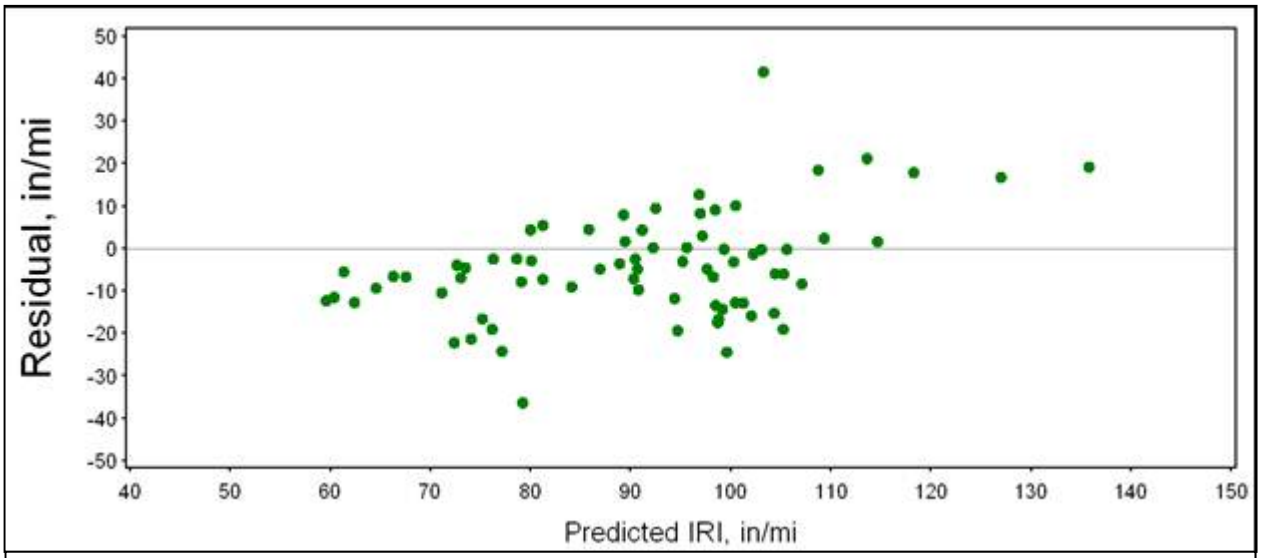

Note: The five data points identified as potential outliers in Figure 44 are not shown in this figure, because the scales for the predicted IRI was set to 150 in./mi. and the maximum residual set at 50 in./mi.

Figure 32—Predicted versus Residuals (Predicted minus Measured Values) for Georgia LTPP Sections

There were several obvious outliers contributing to the poor goodness of fit and bias in the global IRI regression equation. Table 19 summarizes the statistical analysis performed for comparing predicted and measured IRI values. The results are summarized as follows:

- The intercept of the y= x curve was 58.2 (ranging from 32.9 to 83.4) with a corresponding p-value of <0.0001. The p-value less than 0.05 implied the Test 1 null hypothesis was rejected. Thus, the MEPDG predicted IRI does exhibit bias.

- The slope of the y= x curve was 0.981. The corresponding p-value was 0.4389. Thus, the Test 2 null hypothesis is accepted, indicating no bias from a slope standpoint.

- Finally, the p-value from the paired t-test comparison of predicted IRI and measured IRI. The t-test value was 0.9313, thus, the null hypothesis is accepted.

Table 19—Statistical Comparison of Measured and Predicted IRI for Global Calibration Coefficients

Hypothesis Testing and T-Test				**Goodness of Fit**	
Test Type	**Value**	**Range**	**p-value**	**R^2**	**SEE, in/mile**
Hypothesis Test (1): Intercept = 0	58.2	32.9 to 83.4	<0.0001	0.096	18.6
Hypothesis Test (2): Slope = 1	0.981	0.937 to 1.03	0.4389		
Paired t-test	—	—	0.9313		

5.3.3 Georgia Calibration Coefficients

The poor goodness of fit statistics indicates a need to recalibrate the IRI regression equation for Georgia conditions. A few outlier data points were removed and the calibration was rerun and the four new coefficients established which greatly improved the goodness of fit statistics.

A plot of predicted and measured IRI for the Georgia LTPP sites is shown in Figure 33, as well as the R-Squared, SEE, and number of observations. These results indicate that goodness of fit was reasonable and the model predictions appear to be unbiased after local calibration with Georgia data. The SEE of 7.5 in/mile is lower than the SEE for the global regression equation of 18.6 in./mi. The final JPCP calibrated IRI regression equation for Georgia is given by equation 17.

$$IRI = IRI_I + J1*CRK + J2*SPALL + J3*FAULT + J4*SF \qquad (17)$$

Where:

IRI_I = Initial IRI, in/mile (mean of both wheelpaths)
CRK = JPCP transverse fatigue cracking, percent slabs
$SPALL$ = JPCP transverse joint spalling, percent joints
$FAULT$ = JPCP mean transverse joint faulting, in.

SF = Site factor (subgrade fines, freezing index, age)
J1, J2, J3, J4 = Georgia coefficient factors (J1 = 1.05, J2 = 0.5417, J3 = 1.85, J4 = 33.8)

Statistics:

R-Square = 0.74
SEE = 7.5 in/mile
N = 69

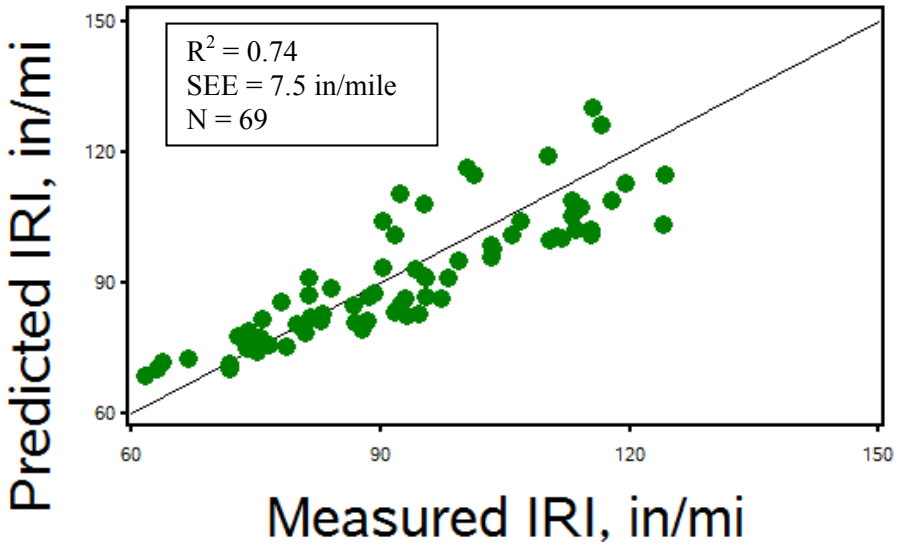

Figure 33—Predicted versus Measured IRI using Georgia Calibration Coefficients

Table 20 summarizes the statistical analysis performed for comparing predicted and measured IRI values. The results are summarized as follows:

- The intercept of the y= x curve was 19 (ranging from 9 to 30) with a corresponding p-value of 0.0005. The p-value less than 0.05 implied the Test 1 null hypothesis was rejected. Thus, the intercept exhibits bias. Since the IRI predictions are typically far above the intercept value of 19 in/mile, this bias is not considered as critical.

- The slope of the y= x curve was 0.98. The 95 percent confidence interval was 0.96 to 1.001 which includes the null hypothesis of 1.00. The corresponding p-value was 0.068 which is greater than 0.05. Thus, the null hypothesis is accepted, indicating no bias of the IRI slope.

- Finally, the p-value from the paired t-test comparison of predicted IRI and measured IRI. The t-test p-value was 0.219, thus, the null hypothesis is accepted indicating no bias.

Figure 34 shows an example plot of IRI versus time for one of Georgia's LTPP sections with both the predicted and measured IRI data points. The GDOT IRI regression equation predicted IRI fairly close to the measured IRI values for most of the calibration sections.

Table 20—Statistical Comparison of Measured and Predicted IRI

Hypothesis Testing and T-Test				Goodness of Fit	
Test Type	**Value**	**Range**	**p-value**	**R^2**	**SEE, in/mile**
Hypothesis Test (1): Intercept = 0	19	9 to 30	0.0005	0.74	7.5
Hypothesis Test (2): Slope = 1	0.98	0.960 to 1.001	0.068		
Paired t-test	—	—	0.219		

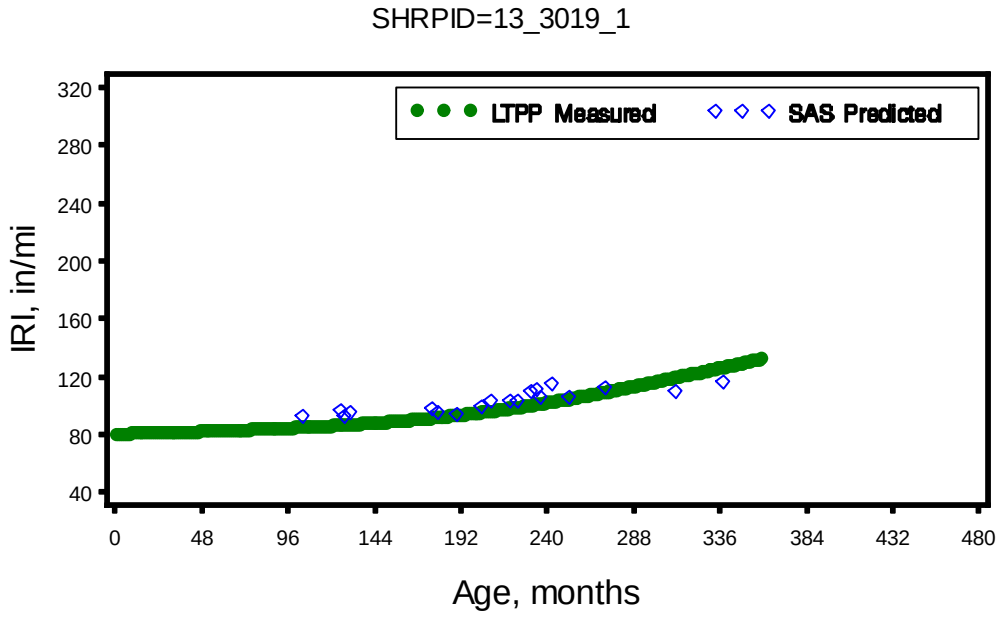

Figure 34—IRI versus Age for a Georgia LTPP JPCP Test Section using the Georgia Calibration Coefficients

VI. CALIBRATION COEFFICIENTS FOR FLEXIBLE PAVEMENTS AND HMA OVERLAYS

Verification of the MEPDG global calibration coefficients of the flexible pavement transfer functions for Georgia conditions consisted of running the *Pavement ME Design* software for the Georgia LTPP and non-LTPP projects and evaluating goodness-of-fit and bias for 32 LTPP test sections. The input values used in predicting pavement distress of each section were discussed and identified under Section II and in the Task 2 interim report.

Appendix A provides the layer and design details of the 22 LTPP and 18 non-LTPP flexible pavement projects used in the verification and calibration analysis. A map illustrating the locations of the LTPP and other Georgia flexible pavement sections was included in Figures 1 and 2. A reasonable spread of sections throughout Georgia and design features was obtained.

The predicted values are compared to the observed or measured values over time to determine if the transfer function exhibits significant bias and poor precision or high SEE values. The AASHTO MEPDG Local Calibration Guide (AASHTO, 2010) recommends both the intercept and slope of the relationship between the predicted and measured values be used to evaluate the null hypothesis (slope = 1 and intercept = 0). If the hypothesis is rejected for either test (the intercept or slope), the results from the confirmation runs are used with additional calibration sites to revise the coefficients of the distress transfer functions (this is part of Task 3, see Section I).

6.1 Rut Depth or Permanent Deformation—HMA Mixtures and Unbound Layers

6.1.1 Transfer Function

Two transfer functions are used to predict the total rut depth of flexible pavements and HMA overlays: one for the HMA layers and the other one for all unbound aggregate base layers and subgrades. Both are discussed and evaluated within this subsection.

Hot Mix Asphalt Mixtures/Layers

The HMA calibrated transfer function was based on laboratory repeated load plastic deformation tests and is shown below.

$$\Delta_{p(HMA)} = \varepsilon_{p(HMA)} h_{HMA} = \beta_{1r} k_z \varepsilon_{r(HMA)} 10^{k_{1r}} n^{k_{2r}\beta_{2r}} T^{k_{3r}\beta_{3r}} \quad (18)$$

Where:

$\Delta_{p(HMA)}$ = Accumulated permanent or plastic vertical deformation in the HMA layer/sublayer, in.

$\varepsilon_{p(HMA)}$ = Accumulated permanent or plastic axial strain in the HMA layer/sublayer, in/in.

$\varepsilon_{r(HMA)}$ = Resilient or elastic strain calculated by the structural response model at the mid-depth of each HMA sublayer, in/in.

$h_{(HMA)}$ = Thickness of the HMA layer/sublayer, in.

n = Number of axle load repetitions.

T = Mix or pavement temperature, °F.
k_z = Depth confinement factor.
$k_{1r,2r,3r}$ = Global field calibration parameters (from the NCHRP 1-40D recalibration; k_{1r} = -3.35412, k_{2r} = 0.4791, k_{3r} = 1.5606).
β_{1r}, β_{2r}, β_{3r}, = Local or mixture field calibration constants; for the global calibration, these constants were all set to 1.0.

$$k_z = (C_1 + C_2 D)0.328196^D \quad (19)$$

$$C_1 = -0.1039(H_{HMA})^2 + 2.4868H_{HMA} - 17.342 \quad (20)$$

$$C_2 = 0.0172(H_{HMA})^2 - 1.7331H_{HMA} + 27.428 \quad (21)$$

D = Depth below the surface, in.
H_{HMA} = Total HMA thickness, in.

Unbound Granular Aggregate Base Layer and Subgrade Soils

Equation 22 shows the rut depth transfer function for the unbound layers and subgrade.

$$\Delta_{p(soil)} = \beta_{s1} k_{s1} \varepsilon_v h_{soil} \left(\frac{\varepsilon_o}{\varepsilon_r} \right) e^{-\left(\frac{\rho}{n}\right)^{\beta}} \quad (22)$$

Where:

$\Delta_{p(Soil)}$ = Permanent or plastic deformation for the layer/sublayer, in.
n = Number of axle load applications.
ε_o = Intercept determined from laboratory repeated load permanent deformation tests, in/in.
ε_r = Resilient strain imposed in laboratory test to obtain material properties ε_o, β, and ρ, in/in.
ε_v = Average vertical resilient or elastic strain in the layer/sublayer and calculated by the structural response model, in/in.
h_{Soil} = Thickness of the unbound layer/sublayer, in.
k_{s1} = Global calibration coefficients; k_{s1}=1.673 for granular materials and 1.35 for fine-grained materials.

β_{s1} = Local calibration constant for the rutting in the unbound layers; the local calibration constant was set to 1.0 for the global calibration effort.

$$Log\beta = -0.61119 - 0.017638(W_c) \quad (23)$$

$$\rho = 10^9 \left(\frac{C_o}{\left(1 - (10^9)^{\beta}\right)} \right)^{\frac{1}{\beta}} \quad (24)$$

$$C_o = Ln\left(\frac{a_1 M_r^{b_1}}{a_9 M_r^{b_9}} \right) = 0.0075 \quad (25)$$

W_c = Water content, percent.
M_r = Resilient modulus of the unbound layer or sublayer, psi.
$a_{1,9}$ = Regression constants; a_1=0.15 and a_9=20.0.
$b_{1,9}$ = Regression constants; b_1=0.0 and b_9=0.0.

6.1.2 Verification of Global Calibration Coefficients

The rut depths for all HMA surfaced pavements (see Appendix A) were calculated with *Pavement ME Design* software using the input values discussed and identified in Section II and in the Task 2 interim report. Two different materials characterization procedures were used for predicting rutting: (1) laboratory measured resilient modulus values at equivalent stress states; and (2) in place volumetric conditions and backcalculated elastic modulus values.

Table 21 compares the bias and standard error for the predicted rut depth of the two sets of data or inputs for characterizing the unbound layers. As shown, there is a significant difference between the two characterization procedures. There is a significant positive bias for the predict rut depths when using the laboratory equivalent resilient modulus values at the in place stress state and volumetric conditions of water content and dry density, and a much lower bias when using the backcalculated elastic modulus values.

Table 21—Comparison of Results from Using Laboratory Measured Resilient Modulus and Backcalculated Elastic Modulus Values for Predicting Rut Depths

Pavement Type	Bias Value, in.		Standard Error, in.	
	Lab Measured Modulus Value	Backcalculated Modulus Value	Lab Measured Modulus Value	Backcalculated Modulus Value
Full Depth Structures	0.412	0.0883	0.0776	0.0523
Pavement with Aggregate Base	0.206	0.0703	0.111	0.130
HMA Overlay of Flexible Pavements	0.0718	-0.0158	0.121	0.0739
SPS-5; HMA Overlay with RAP	0.363	0.0235	0.0731	0.0518
SPS-5; HMA Overlay without RAP	0.366	0.0260	0.0729	0.0526

Figure 35 includes a comparison of the predicted versus measured rut depth using the global calibration coefficients, and a comparison of the predicted rut depth and residual error. As shown in Table 21 and Figure 35, there is a significant bias in the predicted rut depths and the goodness-of-fit is poor. In addition, the residual error is dependent on or related to the predicted rut depths. The bias is significantly lower for the predicted rut depths when using the backcalculated elastic modulus values. Figure 36 includes the same information as graphically presented in Figure 35, except the predicted rut depths are based on using the backcalculated elastic layer modulus values.

The LTPP SPS-5 test sections consistently exhibit higher rut depth rates and magnitudes. The GPS overlay test sections exhibit a significantly lower standard error as compared to the SPS-5 test sections and those sections classified as full-depth and conventional pavement structures. This observation or finding is similar to other local calibration studies. It is expected that the MEPDG is over predicting the rut depth in the unbound layers of new pavement construction and moisture damage is believed to have occurred in the HMA mixtures of the SPS-5 sections. Figure 37 includes some examples comparing the predicted and measured rut depths for four of the LTPP test sections for the flexible pavements and HMA overlays.

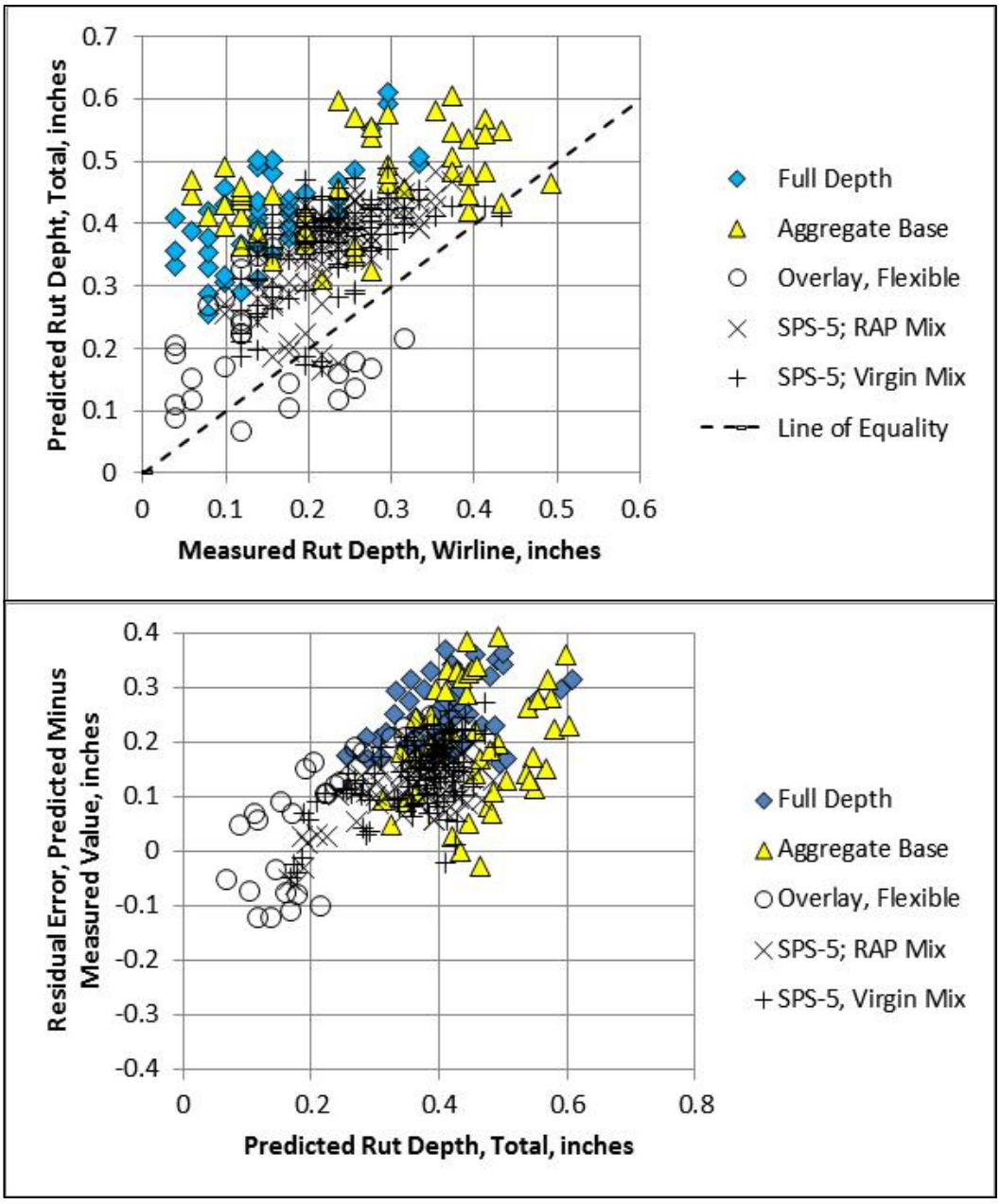

Figure 35—Predicted versus Measured Rut Depth based on Laboratory Measured Resilient Modulus of Unbound Layers using the Global Calibration Coefficients

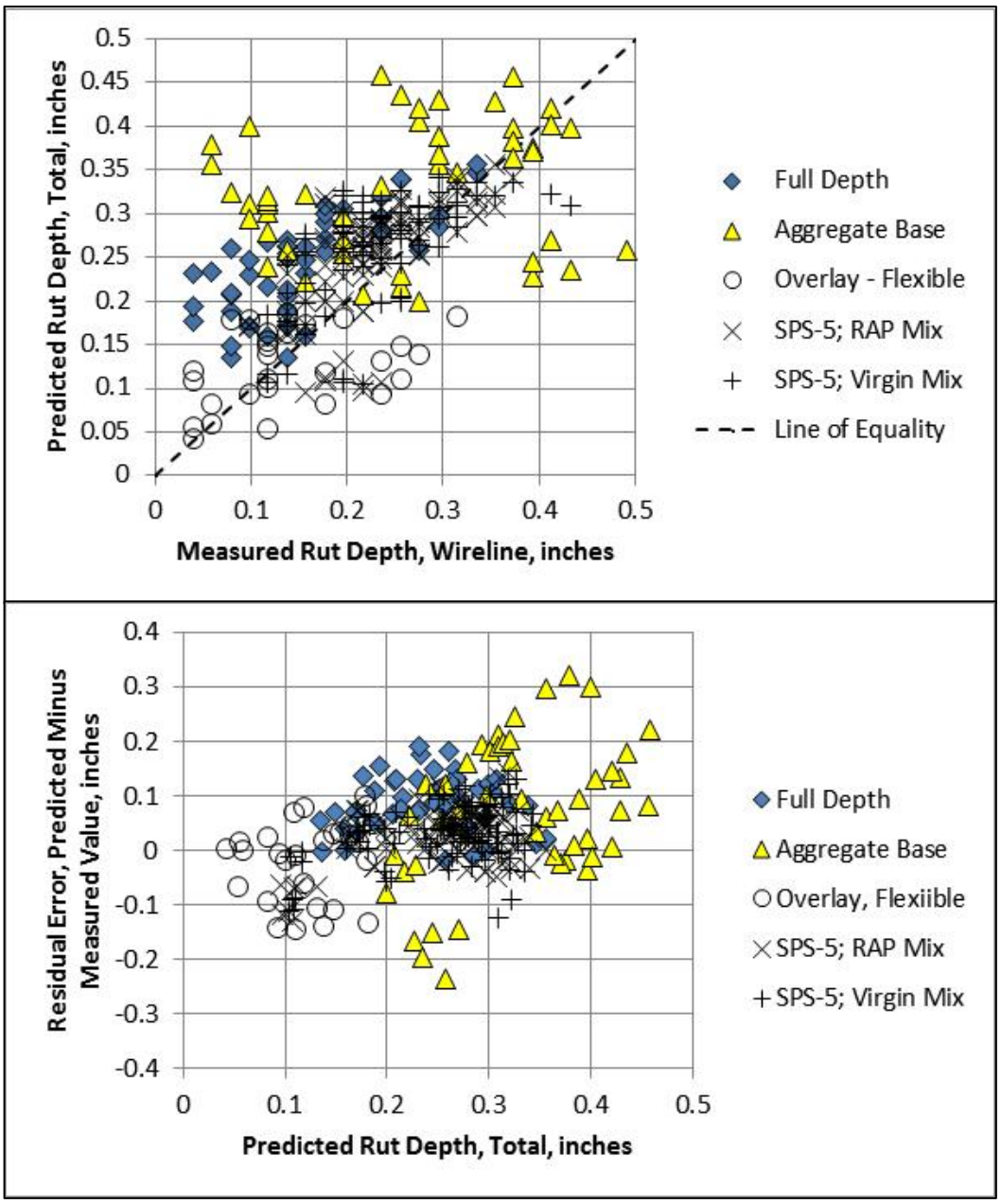

Figure 36—Predicted versus Measured Rut Depth based on Backcalculated Elastic Layer Modulus Values of Unbound Layer using the Global Calibration Coefficients

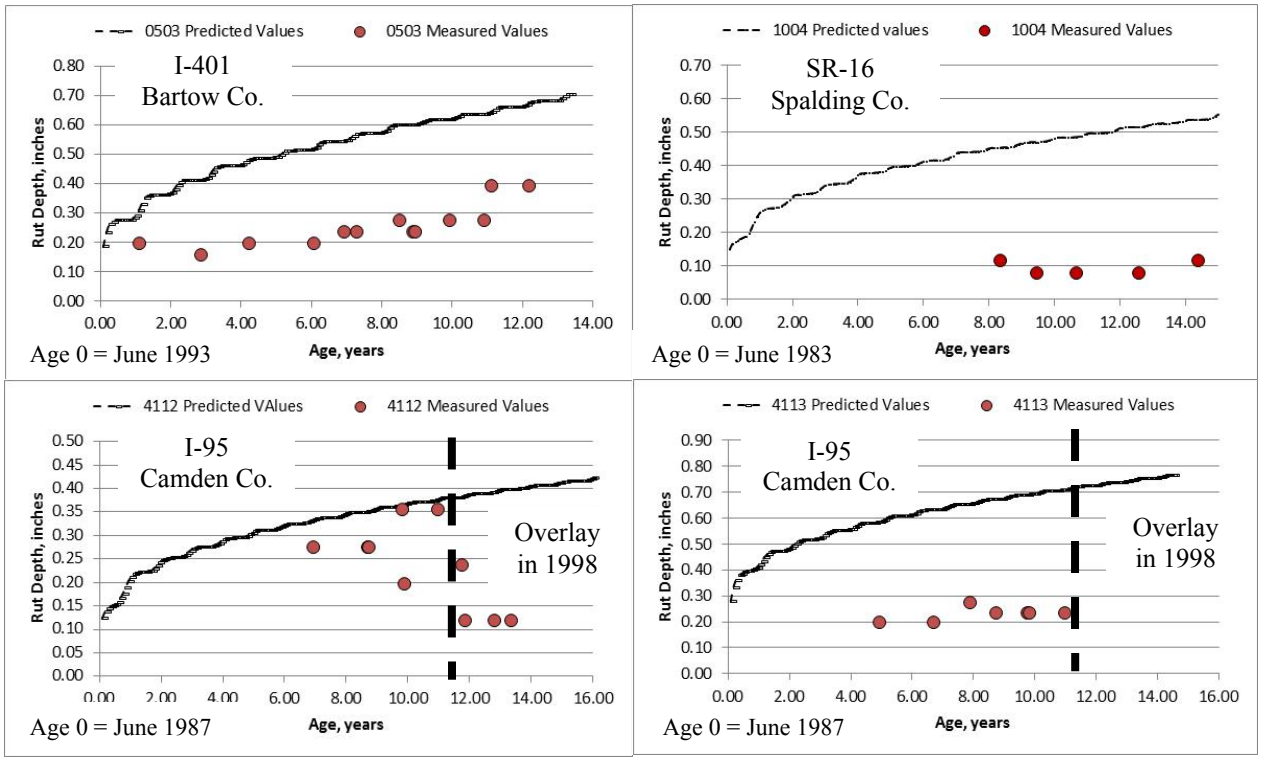

Figure 37—Predicted versus Measured Rut Depth for LTPP Flexible Pavement and HMA Overlay Sections

Removing the SPS-5 test sections from the statistical comparison, however, still results in a significant bias in terms of the intercept. The following lists some of the findings from the comparison of the predicted and measured rut depths.

- The slope of the GPS overlay test sections is significantly different from 1.0.
- The intercept for the full-depth structures are also significantly different from 1.0. The reason for this observation is related to the HMA thickness and resilient modulus of the subgrade soils.
- The conventional flexible pavement structures (HMA over an aggregate base) are highly variable. The reason for this observation is related to the HMA thickness and moisture content of the unbound aggregate base and subgrade.

6.1.3 Georgia Calibration Coefficients

Measured rut depth trends for each calibration section were carefully reviewed. There existed some significant variations over time for some sections. As an example the SPS-5 sections were excluded from the calibration process because the HMA mixtures exhibited stripping or moisture damage. This was explained and illustrated in the Task 2 interim report. The transfer function coefficients recommended for use from NCHRP project 9-30A were used as a starting point in deriving the Georgia calibration coefficients for both the HMA and unbound layers.

The analysis utilized the full Georgia flexible pavement database to establish the goodness of fit and bias in the MEPDG rut depth transfer functions for the HMA and unbound layers. The HMA overlay sections and the semi-rigid pavements were initially used to derive the HMA calibration coefficients that minimize the bias between the predicted and measured rut depths. The conventional, full-depth, and deep strength pavement sections were used to derive the calibration coefficients for the unbound layers. The following summarizes the Georgia calibration coefficients from this analysis, which were found to be dependent on mixture type.

- HMA mixtures calibration parameters:
  - K_1 = -2.45 for neat HMA mixtures and -2.55 for polymer modified mixtures.
  - K_2 = 0.30 for neat and polymer modified mixtures. The K_2 parameter is probably related to mixture type, but laboratory repeated load plastic deformation tests are needed to determine the difference in the K_2 parameter.
  - K_3 = 1.5606; this parameter was found to be the same as the global coefficient and independent of mixture type.
- Unbound layer calibration parameters:
  - Bs1 for coarse-grained soils = 0.50.
  - Bs1 for fine-grained soils = 0.30.

Figure 38 compares the predicted and measured rut depth using the Georgia calibration coefficients for the LTPP and non-LTPP sections. Figure 38 also shows the relationship between the residual error and predicted rutting. As shown, the plots illustrate a good fit and correspondence between the predicted and measured rut depths with an R2 equal to 0.68 and a standard error of the estimate (SEE) of 0.105 inches without obvious bias of under or over prediction of rut depths. Figure 39 shows a similar comparison, but stratified by type of pavement. As shown, pavement type does not result in a biased prediction.

Figure 40 shows a comparison between the measured and predicted rut depths over time for two of the calibration sections.

6.2 Bottom-Up Area Fatigue Cracking

6.2.1 Transfer Function

Two types of load-related cracks are predicted by the MEPDG, alligator cracking and longitudinal cracking. The MEPDG assumes alligator or area cracks initiate at the bottom of the HMA layers and propagate to the surface with continued truck traffic, while longitudinal cracks are assumed to initiate at the surface. The MEPDG Manual of Practice recommends that top-down or longitudinal cracking transfer function not be used to make design revisions, because of the debate and controversy on the appropriateness of the mechanism for surface initiated cracks and field investigations were not used to confirm longitudinal cracks initiated at the surface.

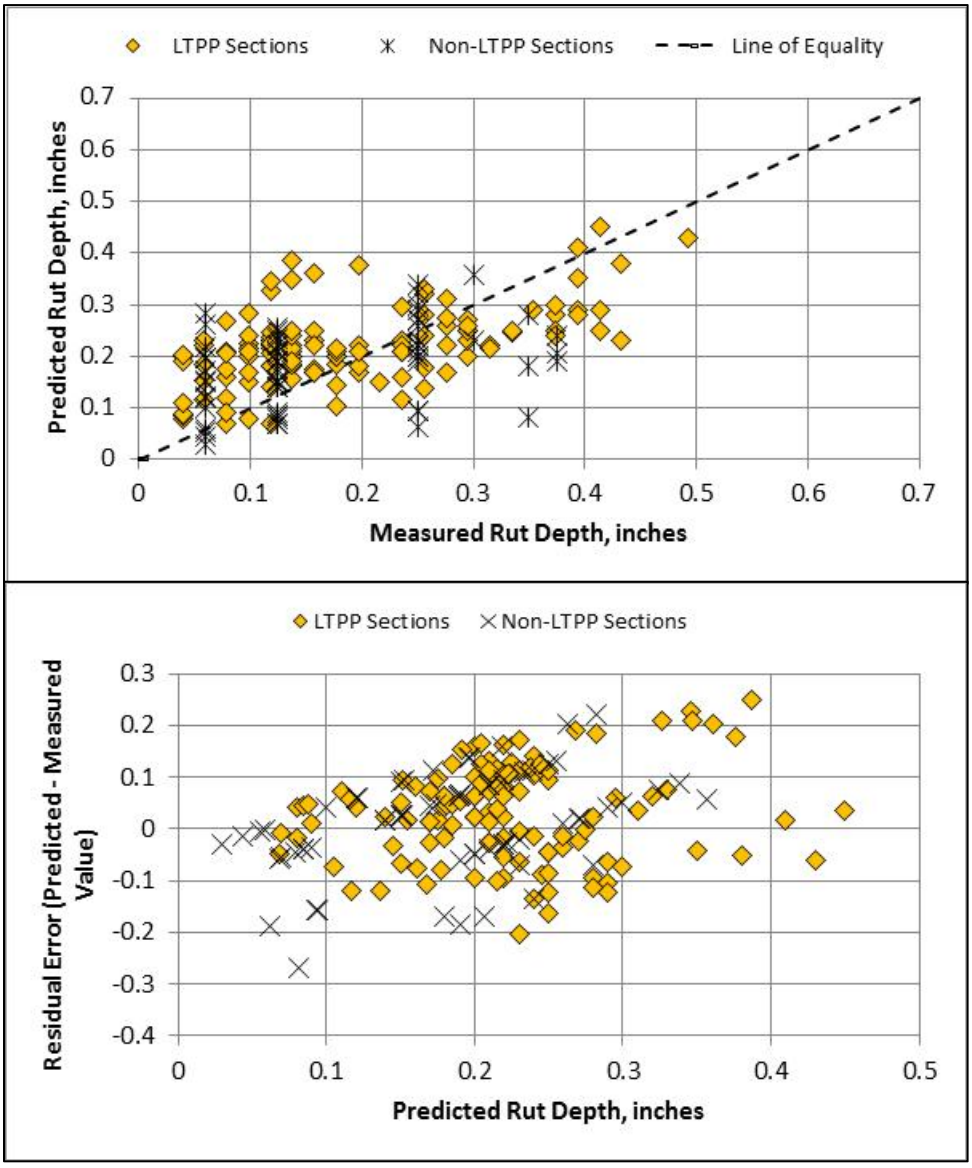

Figure 38—Predicted versus Measured Rut Depth Stratified between LTPP and Non-LTPP Sections using Georgia's Calibration Coefficients

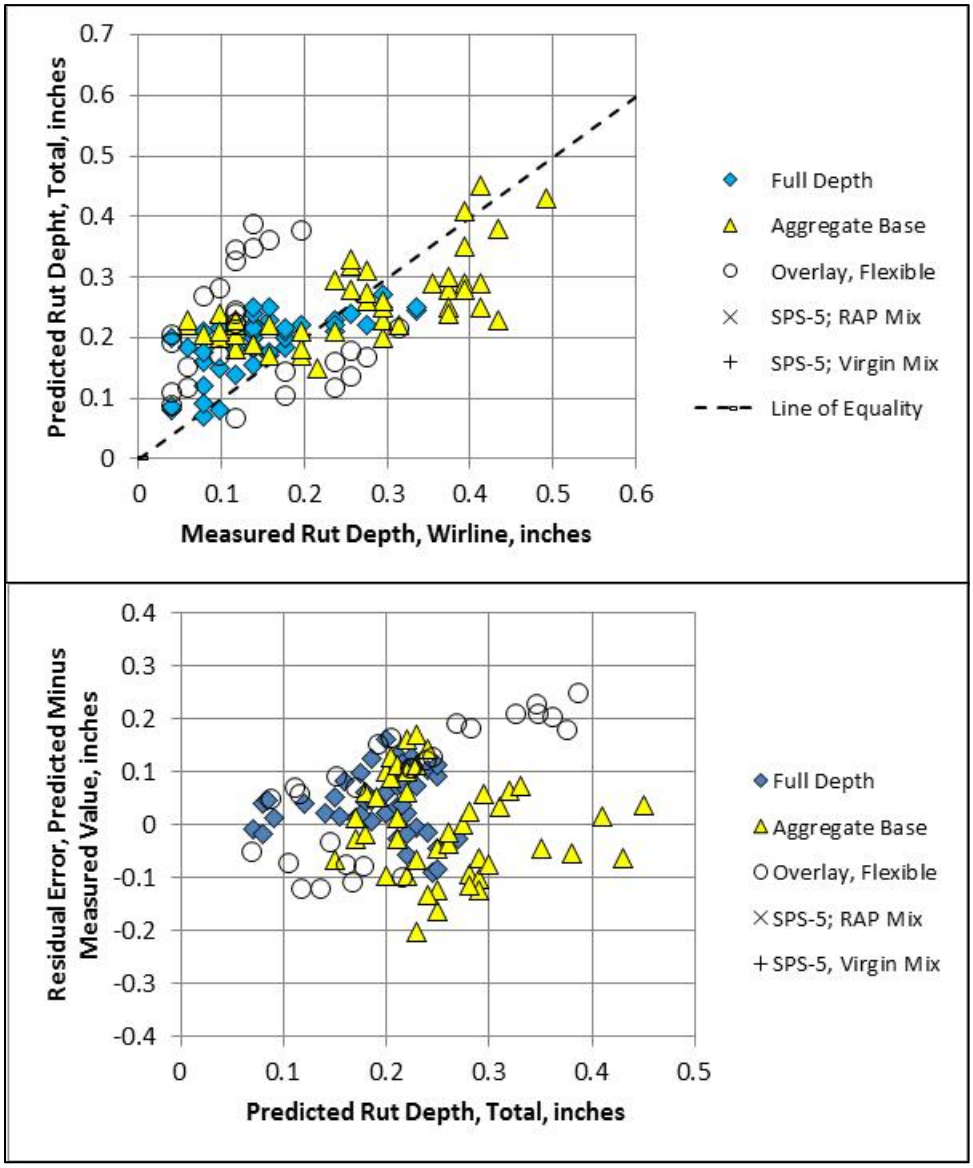

Figure 39—Predicted versus Measured Rut Depth Stratified between Pavement Type using Georgia's Calibration Coefficients

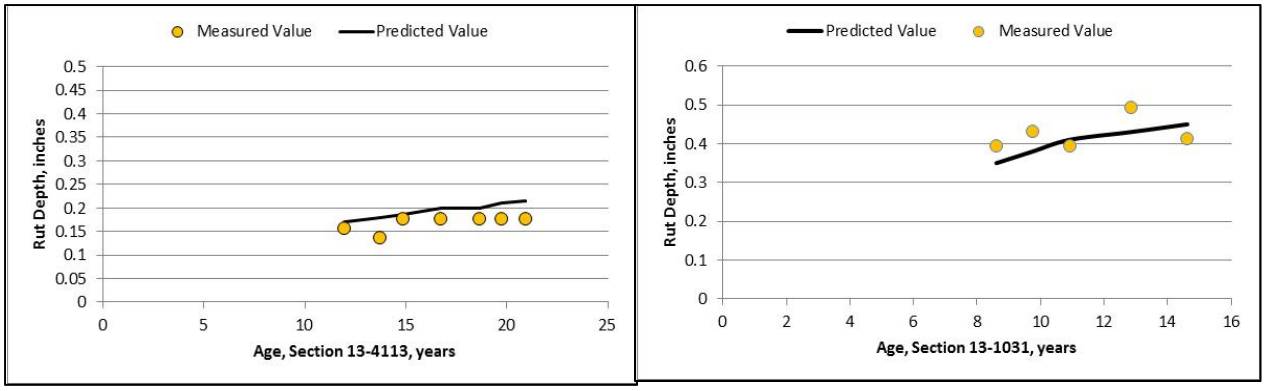

Figure 40—Predicted versus Measured Rut Depth over Time for Two Calibration Sections using Georgia's Calibration Coefficients

The allowable number of axle load applications needed for the incremental damage index approach to predict both types of load related cracks (alligator and longitudinal) is shown below.

$$N_{f-HMA} = k_{f1}(C)(C_H)\beta_{f1}(\varepsilon_t)^{k_{f2}\beta_{f2}}(E_{HMA})^{k_{f3}\beta_{f3}} \quad (26)$$

Where:

$N_{f\text{-}HMA}$ = Allowable number of axle load applications for a flexible pavement and HMA overlays.

ε_t = Tensile strain at critical locations and calculated by the structural response model, in/in.

E_{HMA} = Dynamic modulus of the HMA measured in compression, psi.

k_{f1}, k_{f2}, k_{f3} = Global field calibration parameters (from the NCHRP 1-40D re-calibration; k_{f1} = 0.007566, k_{f2} = -3.9492, and k_{f3} = -1.281).

β_{f1}, β_{f2}, β_{f3} = Local or mixture specific field calibration constants; for the global calibration effort, these constants were set to 1.0.

$$C = 10^M \quad (27)$$

$$M = 4.84\left(\frac{V_{be}}{V_a + V_{be}} - 0.69\right) \quad (28)$$

V_{be} = Effective asphalt content by volume, percent.

V_a = Percent air voids in the HMA mixture.

C_H = Thickness correction term, dependent on type of cracking.

$$C_H = \frac{1}{0.000398 + \frac{0.003602}{1 + e^{(11.02 - 3.49 H_{HMA})}}} \quad (29)$$

H_{HMA} = Total HMA thickness, in.

The cumulative damage index (*DI*) is determined by summing the incremental damage indices over time, as shown below.

$$DI = \sum \left(\Delta DI\right)_{j,m,l,p,T} = \sum \left(\frac{n}{N_{f-HMA}} \right)_{j,m,l,p,T} \quad (30)$$

Where:

n = Actual number of axle load applications within a specific time period.
j = Axle load interval.
m = Axle load type (single, tandem, tridem, quad, or special axle configuration.
l = Truck type using the truck classification groups included in the MEPDG.
p = Month.
T = Median temperature for the five temperature intervals or quintiles used to subdivide each month, °F.

The area of alligator cracking and length of longitudinal cracking are calculated from the total damage over time using different transfer functions. The relationship used to predict the amount of alligator cracking on an area basis, FC_{Bottom}, is shown below.

$$FC_{Bottom} = \left(\frac{1}{60} \right) \left(\frac{C_4}{1 + e^{\left(C_1 C_1^* + C_2 C_2^* Log\left(DI_{Bottom} * 100\right)\right)}} \right) \quad (31)$$

Where:

FC_{Bottom} = Area of alligator cracking that initiates at the bottom of the HMA layers, percent of total lane area.
DI_{Bottom} = Cumulative damage index at the bottom of the HMA layers.
$C_{1,2,4}$ = Transfer function regression constants; C_4= 6,000; C_1=1.00; and C_2=1.00

$$C_1^* = -2C_2^* \quad (32)$$

$$C_2^* = -2.40874 - 39.748\left(1 + H_{HMA}\right)^{-2.856} \quad (33)$$

H_{HMA} = Total HMA thickness, in.

6.2.2 Verification of the Global Calibration Coefficients

Area fatigue cracks for all HMA surfaced pavements (see Appendix A) were calculated with *Pavement ME Design* software using the input values discussed and identified in Section IV and in the Task 2 interim report. As explained for the rut depth transfer function, two different materials characterization procedures were used for predicting rutting: (1) laboratory measured resilient modulus values at equivalent stress states; and (2) in place volumetric conditions and backcalculated elastic modulus values.

Table 22 compares the bias and standard error for the predicted areas of fatigue cracking of the two sets of data or inputs for characterizing the unbound layers. As shown, there is not much of a difference between the two characterization procedures for fatigue cracking predictions. The other important observation is that the bias and standard error for the HMA overlay group of pavements is very low. The reason for the low bias and standard error is the measured areas of fatigue cracking are also very small – few of these test sections exhibit fatigue cracking (see Task 2 interim report).

Table 22—Comparison of Results from Using Laboratory Measured Resilient Modulus and Backcalculated Elastic Modulus Values for Predicting Fatigue Cracks

Pavement Type	Bias Value, in.		Standard Error, in.	
	Lab Measured Modulus Value	Backcalculated Modulus Value	Lab Measured Modulus Value	Backcalculated Modulus Value
Full Depth Structures	-0.662	-0.901	4.06	4.02
Pavement with Aggregate Base	-2.94	-2.41	5.93	5.55
HMA Overlay of Flexible Pavements	-0.45	-0.595	1.14	1.17
SPS-5; HMA Overlay with RAP	0.052	0.019	0.073	0.023
SPS-5; HMA Overlay without RAP	0.036	0.015	0.038	0.016

Figures 41 and 42 show the predicted versus measured fatigue cracking and predicted fatigue cracking versus the residual error for the two characterization methods for the unbound layers. As shown, the MEPDG under predicts the area of fatigue cracking for most of the LTPP test sections with the exception of some of the SPS-5 sections with higher areas of fatigue cracking in the existing HMA layer. The SPS-5 HMA overlay test sections exhibit little to no fatigue cracking, but do exhibit various lengths of longitudinal cracking in the wheel path. Whether these cracks initiated at the surface or not requires the use of cores. Most of the test sections exhibiting area fatigue cracking are the conventional flexible pavement structures, as shown in Figure 43.

Table 22 and Figure 41 illustrate there is a bias in the predicted fatigue cracking and the goodness-of-fit is poor for the conventional flexible pavements. Figure 42 includes the same information as graphically presented in Figure 41, except the predicted fatigue cracking are based on using the backcalculated elastic layer modulus values. As stated in the Task 2 interim report, the LTPP SPS-5 test sections consistently exhibit greater amounts of fatigue cracks even though the magnitudes of fatigue cracks are small. Figure 43 provides some examples of the comparison between the predicted and measured fatigue cracking due to very heavy truck traffic on the SPS-5 section.

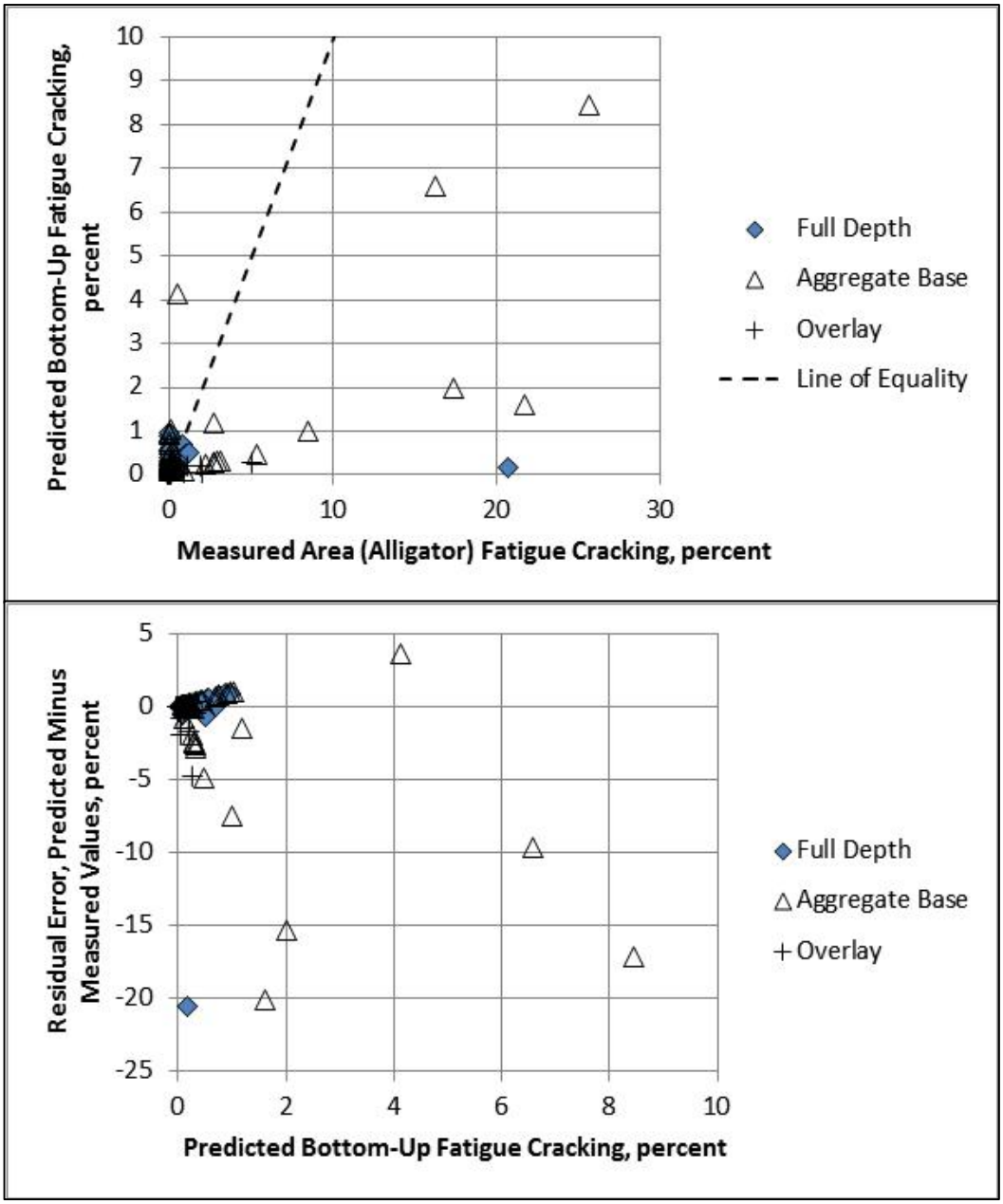

Figure 41—Predicted versus Measured Fatigue Cracking based on Laboratory Measured Resilient Modulus Values of Unbound Layers using the Global Calibration Coefficients

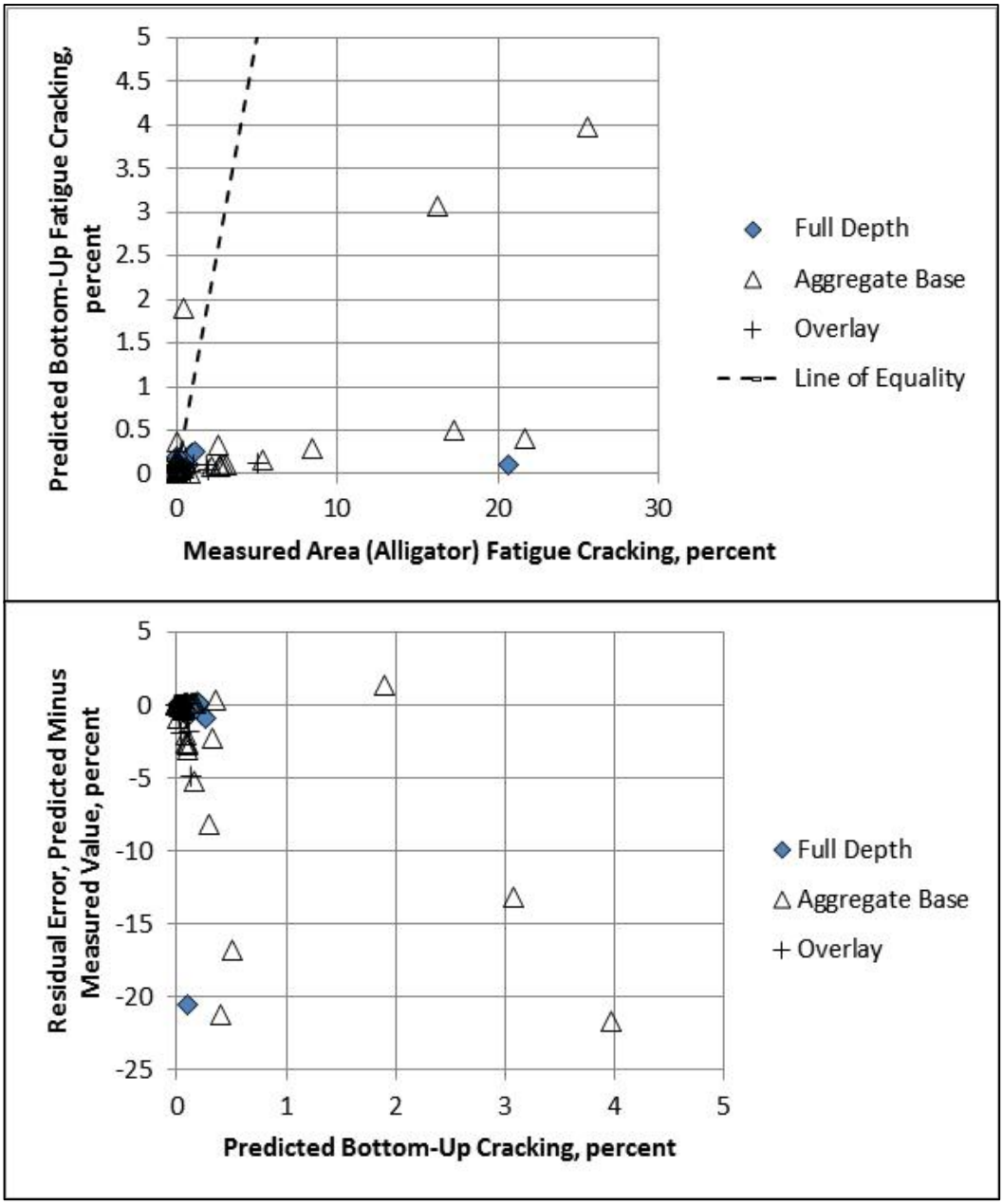

Figure 42—Predicted versus Measured Fatigue Cracking based on Backcalculated Elastic Layer Modulus of Unbound Layers using the Global Calibration Coefficients

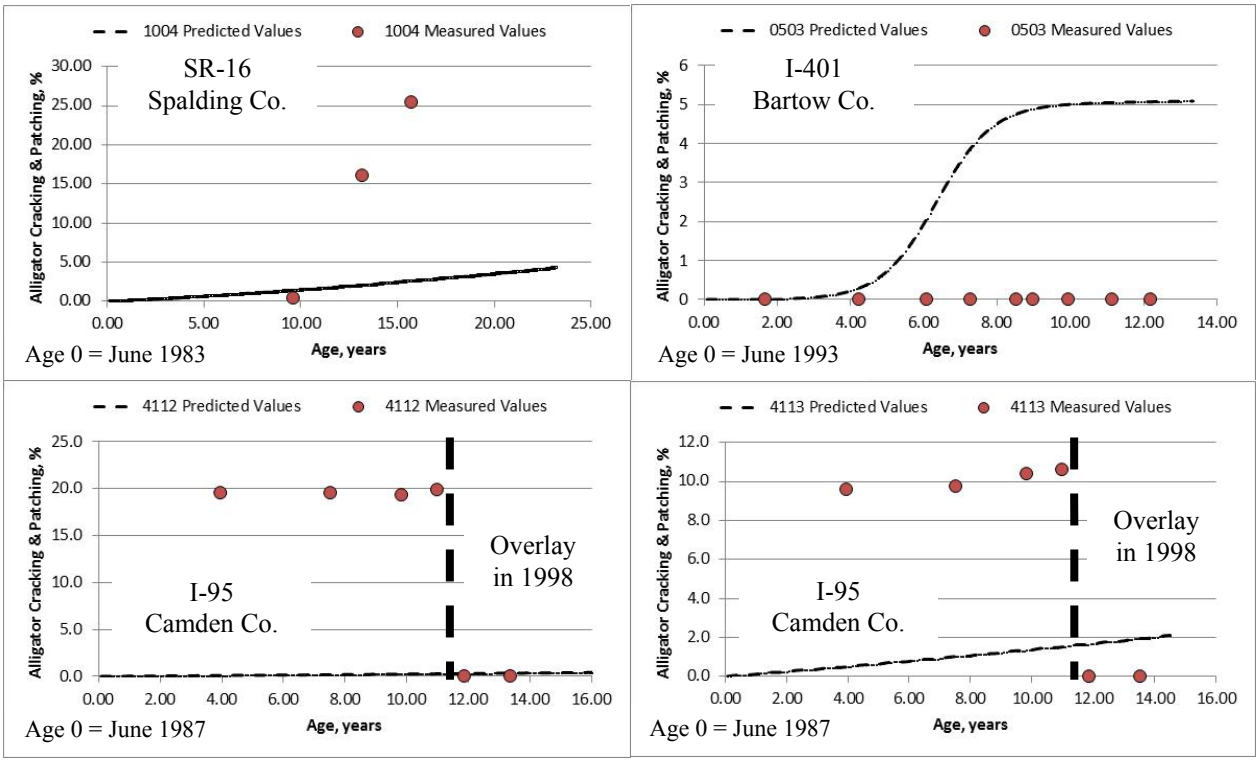

Figure 43—Predicted versus Measured Fatigue Cracking for Selected LTPP Sections

6.2.3 Georgia Calibration Coefficients

Measured fatigue cracking trends for each calibration section were carefully reviewed. There existed some significant variations over time for some sections. As an example, the SPS-5 sections were excluded from the calibration process because the HMA mixtures exhibited stripping or moisture damage. This was explained and illustrated in the Task 2 interim report. The transfer function coefficients recommended for use from NCHRP project 1-40B were used as a starting point in deriving the Georgia calibration coefficients for the HMA.

Figure 44 shows the relationship between damage index as defined from the backcalculated elastic layer modulus from deflection basins and the amount of fatigue cracking in accordance with the MEPDG Manual of Practice. As shown, there is a relationship defined from the damaged elastic modulus which has been found from similar studies in other agencies.

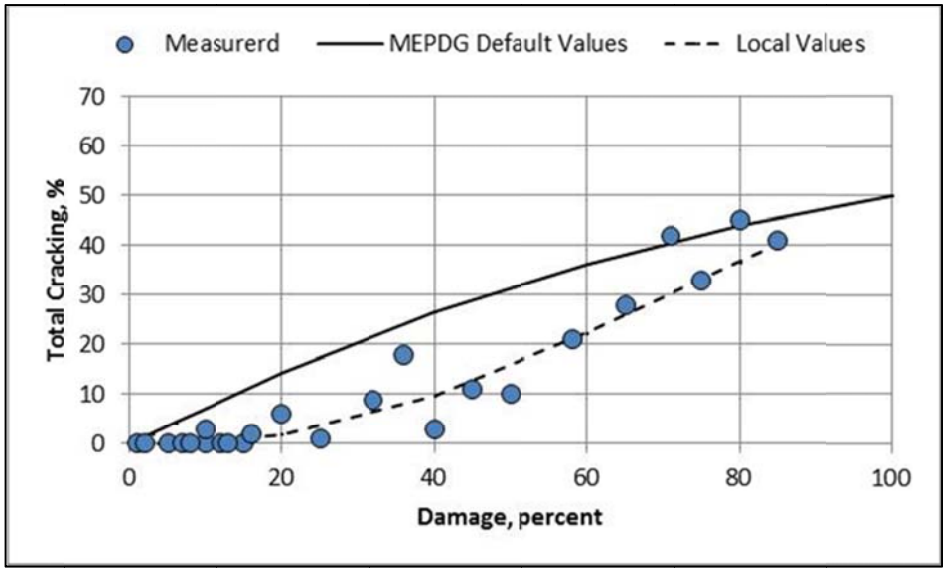

Figure 44—Relationship between In Place Damage and Measured Fatigue Cracking

The analysis utilized the full Georgia flexible pavement database to establish the goodness of fit and bias in the MEPDG fatigue cracking transfer functions for the HMA. The following summarizes the Georgia calibration coefficients from this analysis, which were found to be dependent on mixture type. However, it was decided to not include the sections with RAP because GDOT significantly revised its material specifications for using RAP. The performance of these mixtures with RAP have significantly improved in comparison to the older mixtures included in the LTPP program.

- HMA mixtures calibration parameters for bottom-up fatigue cracking:
  - $K_1 = 0.00075$
  - $K_2 = 3.9491$. The K_2 parameter is probably related to mixture type, but laboratory repeated load flexural fatigue tests are needed to determine the difference in the K_2 parameter.
  - $K_3 = 1.281$; this parameter was found to be the same as the global coefficient and independent of mixture type.
  - $C_1 = 2.2$
  - $C_2 = 2.2$
  - $C_3 = 6{,}000$

Figure 45 compares the predicted and measured fatigue cracking using the Georgia calibration coefficients for the LTPP and non-LTPP sections. Figure 45 also shows the relationship between the residual error and predicted fatigue cracking. As shown, the plots illustrate a good fit and correspondence between the predicted and measured fatigue cracking with an R2 equal to 0.55 and a standard error of the estimate (SEE) of 5.8 percent without obvious bias of under or over prediction of rut depths. Figure 46 shows a similar comparison, but stratified by type of pavement. As shown, pavement type does not result in a biased prediction.

Figure 47 shows a comparison between the measured and predicted fatigue cracking over time for one of the calibration sections.

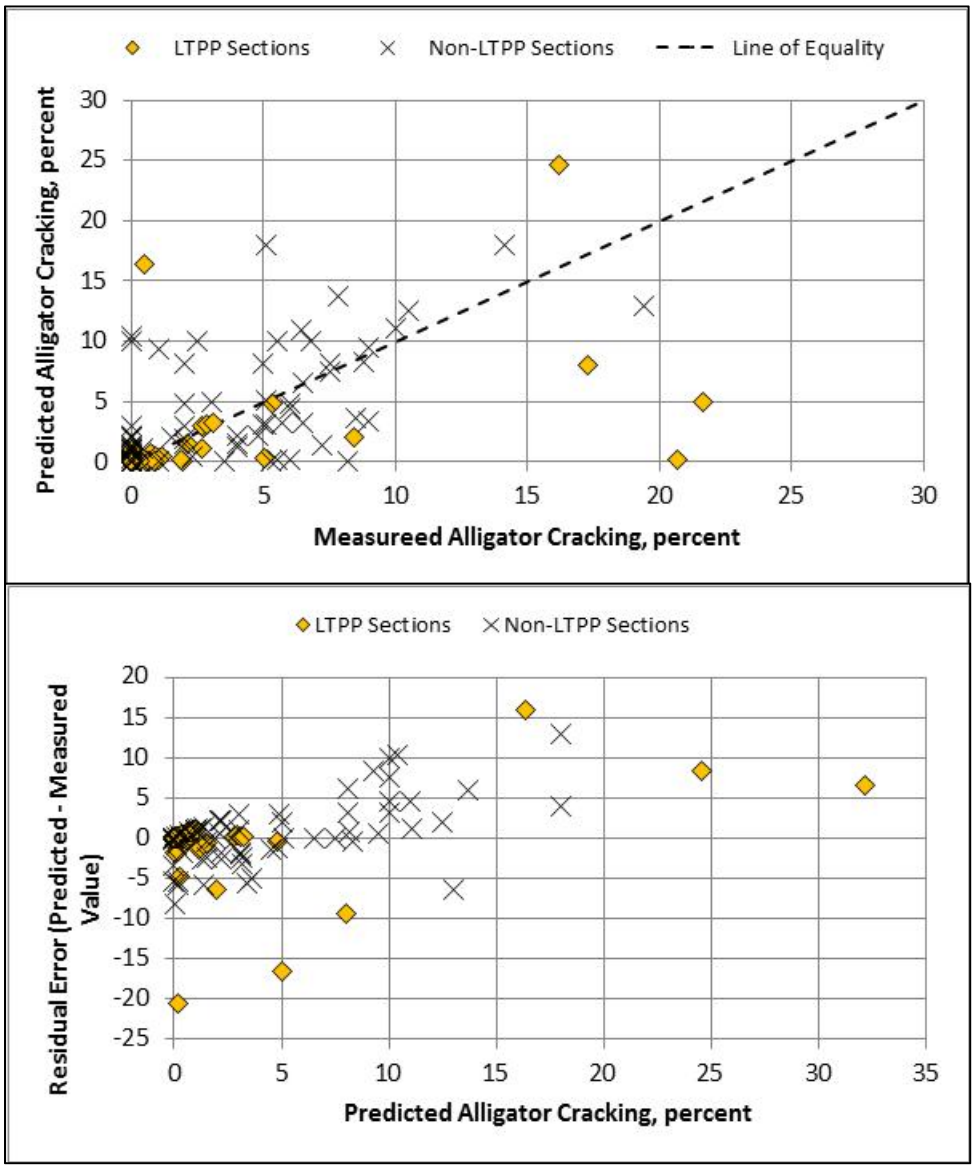

Figure 45—Predicted versus Measured Fatigue Cracking Stratified between LTPP and Non-LTPP Sections using Georgia's Calibration Coefficients

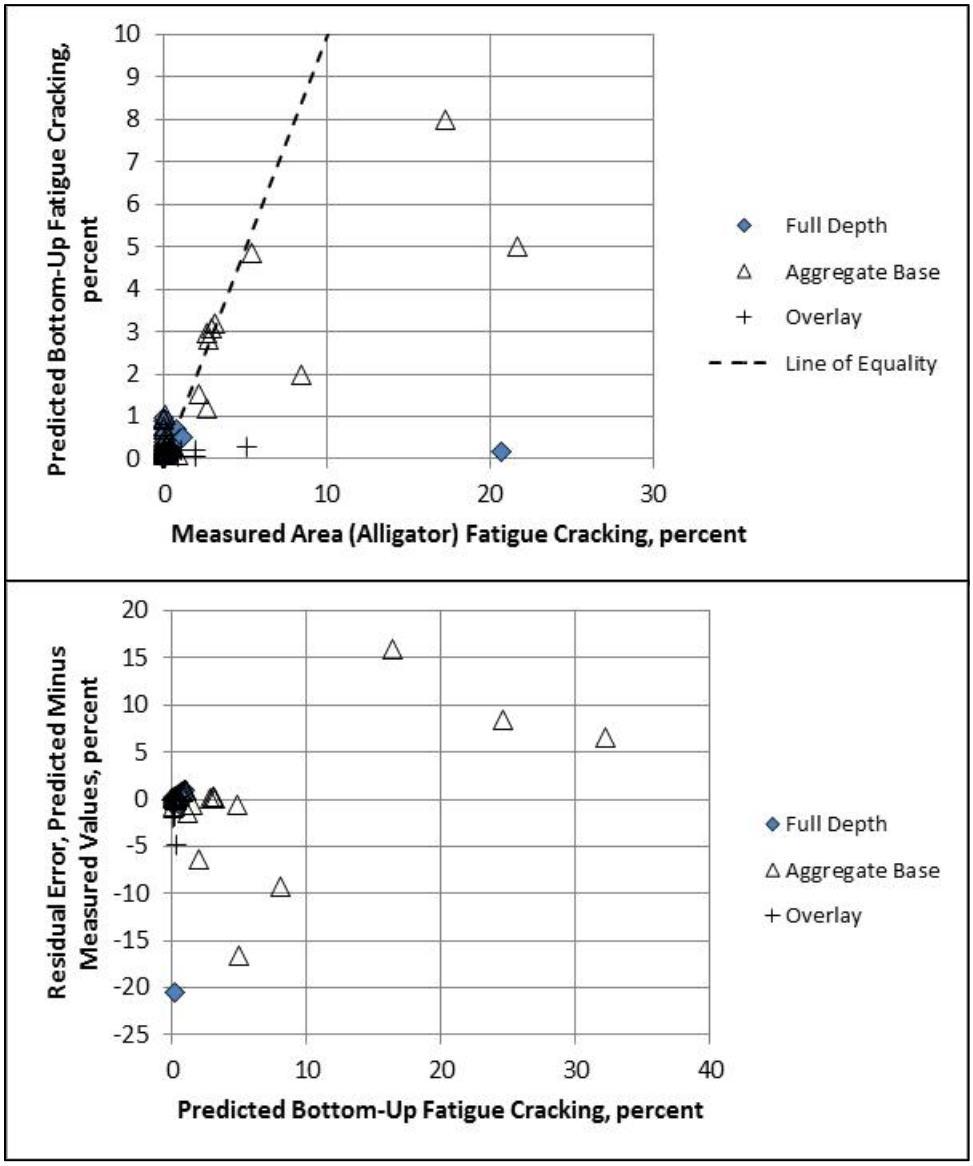

Figure 46—Predicted versus Measured Fatigue Cracking Stratified between Pavement Type using Georgia's Calibration Coefficients

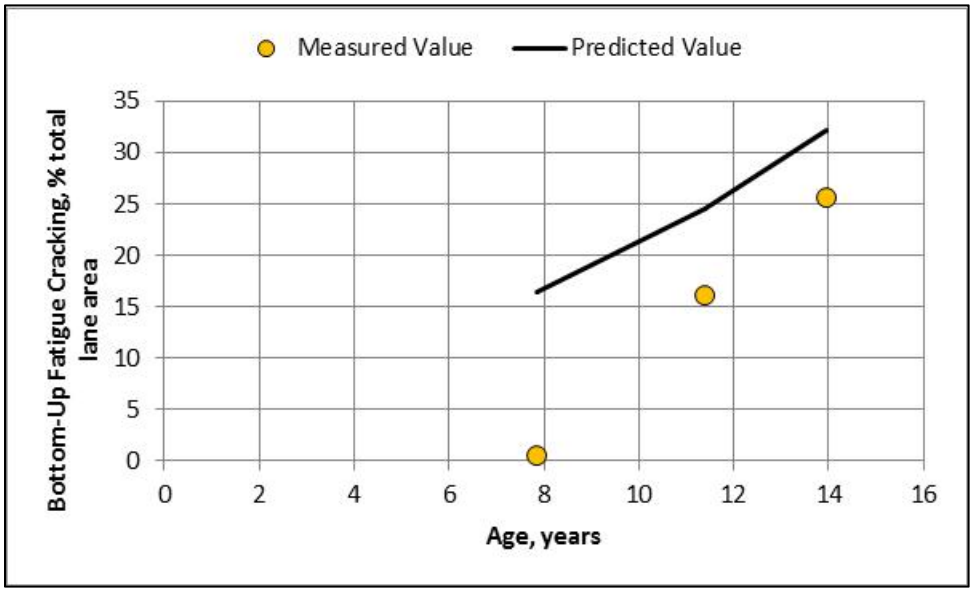

Figure 47—Predicted versus Measured Fatigue Cracking over Time for One Calibration Section using Georgia's Calibration Coefficients

6.3 Fatigue Cracking of Semi-Rigid Pavements

6.3.1 Transfer Function

For fatigue cracks in CTB layers, the allowable number of load applications, $N_{f\text{-}CTB}$, is determined in accordance with equation 34 and the amount or area of fatigue cracking is calculated in accordance with equation 35. These damage and distress transfer functions were never calibrated under any of the NCHRP projects. Montana DOT has completed a local calibration study of fatigue cracking in semi-rigid pavements. The calibration coefficients were found to be highly dependent on the condition or strength of the CTB layer. Thus, the transfer function is provided below, but is not recommended for use until the transfer function has been calibrated to the CTB materials and Georgia's climate.

$$N_{f-CTB} = 10^{\left[\frac{k_{c1}\beta_{c1}\left(\frac{\sigma_t}{M_R}\right)}{k_{c2}\beta_{c2}}\right]} \quad (34)$$

$$FC_{CTB} = C_1 + \frac{C_2}{1 + e^{(C_3 - C_4 Log(DI_{CTB}))}} \quad (35)$$

Where:

$N_{f\text{-}CTB}$ = Allowable number of axle load applications for a semi-rigid pavement.
σ_t = Tensile stress at the bottom of the CTB layer, psi.
M_R = 28-day Modulus of rupture for the CTB layer, psi. (NOTE: Although the MEPDG requires that the 28-day modulus of rupture be entered for all cementitious stabilized layers of semi-rigid pavements, the value used in all

calculations is 650 psi, irregardless of the value entered into the MEPDG software.

DI_{CTB} = Cumulative damage index of the CTB or cementitious layer.

$k_{c1,c2}$ = Global calibration factors – Undefined because prediction equation was never calibrated; these values are set to 1.0 in the software. From other studies, k_{c1}=0.972 and k_{c2}=0.0825.

$\beta_{c1,c2}$ = Local calibration constants; these values are set to 1.0 in the software.

FC_{CTB} = Area of fatigue cracking, sq ft.

$C_{1,2,3,4}$ = Transfer function regression constants; C_1=1.0, C_2=1.0, C_3=0, and C_4=1,000, however, this transfer function was never calibrated and these values will likely change once the transfer function has been calibrated.

The computational analysis of incremental fatigue cracking for a semi-rigid pavement uses the damaged modulus approach. In summary, the elastic modulus of the CTB layer decreases as the damage index, DI_{CTB}, increases. The following equation is used to calculate the damaged elastic modulus within each season or time period for calculating critical pavement responses in the CTB and other pavement layers.

$$E_{CTB}^{D(t)} = E_{CTB}^{Min} + \left(\frac{E_{CTB}^{Max} - E_{CTB}^{Min}}{1 + e^{(-4+14(DI_{CTB}))}} \right) \quad (36)$$

Where:

$E_{CTB}^{D(t)}$ = Equivalent damaged elastic modulus at time t for the CTB layer, psi.

E_{CTB}^{Min} = Equivalent elastic modulus for total destruction of the CTB layer, psi.

E_{CTB}^{Max} = 28-day elastic modulus of the intact CTB layer, no damage, psi.

6.3.2 Verification of the Global Calibration Coefficients

LTPP test sections 4092, 4093, 4096, and 4420 are semi-rigid pavements (see Table 2) and have exhibited little to no fatigue cracking, with the exception of section 4022. Section 4022 exhibited a large amount of fatigue cracking, but after the HMA overlay had been placed on this section. Whether this amount of cracking is a result of damage in the existing HMA layer or a loss of bond between the HMA overlay and existing HMA layers can only be determined through the use of cores. Thus, the LTPP will provide little data in calibrating the fatigue cracking of semi-rigid pavements without additional investigation.

6.3.3 Georgia Calibration Coefficients

Non-LTPP semi-rigid pavements were identified for the sampling matrix. Most of the roadway segments pulled from construction records, however, did not contain sufficient information for estimating the MEPDG inputs. Only one additional roadway segment was added to the sampling matrix so there are too few sections to complete a full or independent local calibration.

The only agency to fully calibrate the semi-rigid transfer function was the Montana DOT so their calibration coefficients were used to verify the applicability of the Montana values to

Georgia semi-rigid pavements. The LTPP and non-LTPP sections were used to confirm the Montana calibration coefficients for Georgia. It should be understood, however, most of the Georgia roadway segments with semi-rigid pavements exhibited little to no fatigue cracking.

The calibration coefficients of the semi-rigid fatigue cracking transfer function are provided in Table 23. These values, however, only confirm little to no fatigue cracking exhibited through the evaluation period. The Georgia calibration coefficients are similar to the values derived from the Montana and Mississippi studies, but are not recommended for use in design until more sections from Georgia confirm the values.

Table 23—Georgia Semi-Rigid Pavement Fatigue Cracking Calibration Coefficients Suggested for Interim Use

Condition or Type of CTB Layer	Coefficient in Semi-Rigid Pavement Fatigue Cracking Equation and Transfer Function (Equations 39 and 40)	
High Strength CTB (intact cores recovered with cement content greater than 6 percent; compressive strength generally greater than 1,000 psi)	B_{C1}	0.85
	B_{C2}	1.10
	C_1	0.00
	C_2	100
	C_3	1.00
	C_4	1,000
Moderate Strength CTB (intact cores recovered with cement contents greater than 4 percent but less than 6 percent; compressive strength generally greater than 300 psi but less than 1,000 psi)	B_{C1}	0.75
	B_{C2}	1.10
	C_1	0.00
	C_2	100
	C_3	1.00
	C_4	1,000
Low Strength CTB (intact cores cannot be recovered with cement content generally less than 4 percent; compressive strength generally less than 300 psi), similar to soil-cement	Semi-Rigid Pavement Simulation not applicable; assume conventional flexible pavement with high stiffness GAB layer.	

6.4 Thermal or Transverse Cracking

6.4.1 Transfer Function

The degree of cracking predicted by the MEPDG uses an assumed relationship between the probability distribution of the log of the crack depth to HMA layer thickness ratio and the percent of cracking. The following equation is used to determine the extent of thermal cracking.

$$TC = \beta_{t1} N \left[\frac{1}{\sigma_d} Log\left(\frac{C_d}{H_{HMA}} \right) \right] \quad (37)$$

Where:

TC = Observed amount of thermal cracking, ft/mi.

β_{t1} = Regression coefficient determined through global calibration (400).
$N[z]$ = Standard normal distribution evaluated at [z].
σ_d = Standard deviation of the log of the depth of cracks in the pavement (0.769), in.
C_d = Crack depth, in.
H_{HMA} = Thickness of HMA layers, in.

The crack depth or amount of crack propagation induced by a given thermal cooling cycle is predicted using the Paris law of crack propagation.

$$\Delta C = A(\Delta K)^n \quad (38)$$

Where:

ΔC = Change in the crack depth due to a cooling cycle.
ΔK = Change in the stress intensity factor due to a cooling cycle.
A, n = Fracture parameters for the HMA mixture, which are obtained from the indirect tensile creep-compliance and strength of the HMA in accordance with the following equations.

$$A = 10^{k_t \beta_t (4.389 - 2.52 Log(E_{HMA} \sigma_m n))} \quad (39)$$

Where:

$$\eta = 0.8\left[1 + \frac{1}{m}\right] \quad (40)$$

k_t = Coefficient determined through global calibration for each input level (Level 1 = 5.0; Level 2 = 1.5; and Level 3 = 3.0).
E_{HMA} = HMA indirect tensile modulus, psi.
σ_m = Mixture tensile strength, psi.
m = The m-value derived from the indirect tensile creep compliance curve measured in the laboratory.
β_t = Local or mixture calibration factor.

The stress intensity factor, K, is defined or estimated by the use of the following simplified equation.

$$K = \sigma_{tip}\left(0.45 + 1.99(C_o)^{0.56}\right) \quad (41)$$

Where:

σ_{tip} = Far-field stress from pavement response model at depth of crack tip, psi.
C_o = Current crack length, feet.

6.4.2 Verification of the Global Calibration Coefficients

Transverse cracks were measured on some of the LTPP test sections (see Figure 21), but many exhibit no transverse cracking. The test sections exhibiting the higher length of transverse cracking (greater than 1,000 ft./mi.) include: all of the semi-rigid pavements (4092, 4093, 4096, and 4420) so these measured cracks are probably reflection cracks from

the CTB layer; and flexible or rigid pavements with HMA overlays (1031 and 7028) so these measured cracks are also probably reflection cracks. Test section 1001 (conventional flexible pavement was the only conventional flexible pavement to exhibit a higher length of transverse cracking.

The MEPDG, however, did not predict any thermal cracks for any of the test sections. Thus, there is a bias of the transfer function. A detailed analysis of the sites with measured transverse cracks using more test sections will be needed to calibrate the thermal cracking transfer function. This observation is not uncommon for the southern climates.

6.4.3 Georgia Calibration Coefficients

New pavement calibration sites (both LTPP and non-LTPP) were used to estimate the Georgia calibration coefficients for the transverse cracking transfer function. The calibration process for the transverse cracking transfer function was restricted to new flexible pavements to exclude the possibility of reflective cracks in HMA overlays and any shrinkage cracks reflecting through the HMA surface of semi-rigid pavements.

A calibration coefficient of 35 was derived to remove the bias for dense-graded mixtures designed in accordance with current HMA mixture design requirements. A coefficient of 45 was derived for dense-graded mixtures with higher amounts of RAP designed in accordance with the older mixture design requirements. However, there is a large dispersion (standard error) between the predicted and measured values. One reason for this high dispersion is the cause of the transverse cracks is probably not from a low temperature event but a combination of shrinkage and lower temperatures. The MEPDG only predicts the length of transverse cracks caused by low temperature events. Thus, it is suggested that a 50 percent reliability level be used in design.

6.5 Reflection Cracking—HMA Overlays

6.5.1 Regression Equation

The MEPDG predicts reflection cracks in HMA overlays or HMA surfaces of semi-rigid pavements using an empirical equation. The empirical equation is used for estimating the amount of fatigue and thermal cracks from a non-surface layer that has reflected to the surface after a certain period of time. This empirical equation predicts the percentage of area of cracks that propagate through the HMA as a function of time using the relationship shown below. This empirical equation, however, was never calibrated under any of the NCHRP Projects.

$$RC = \frac{100}{1 + e^{a(c)+bt(d)}} \quad (42)$$

Where:

RC = Percent of cracks reflected. [NOTE: The percent area of reflection cracking is output with the width of cracks being 1 ft.]
t = Time, years.
a, b = Regression fitting parameters defined through calibration process.

c,d = User-defined cracking progression parameters.

The regression fitting parameters of the above equation (*a* and *b*) are a function of the effective HMA overlay thickness (H_{eff}), the type of existing pavement, and for PCC pavements, load transfer at joints and cracks, as shown below. The effective HMA overlay thickness is provided in Table 24. The user-defined cracking progression parameters can be used by the user to accelerate or delay the amount of reflection cracks, which also are included in Table 24. Non-unity cracking progression parameters (*c* and *d*) could be used with caution, after they have been calibrated locally.

$$a = 3.5 + 0.75\left(H_{eff}\right) \quad (43)$$

$$b = -0.688684 - 3.37302\left(H_{eff}\right)^{-0.915469} \quad (44)$$

The MEPDG predicts the total amount of cracking by combining the reflection cracks with the fatigue cracks predicted in the HMA overlay. Thus, the reflection cracking regression equation is not calibrated separately, but is calibrated concurrently with the other cracking transfer functions based on total cracking measured at the surface of the overlay. Table 24 listed those sections with HMA overlays (the SPS-5 test sections and sections 1031, 4112, 4096, 4113, and 4420).

Table 24—Reflection Cracking Model Regression Fitting Parameters

Pavement Type	**Fitting and User-Defined Parameters**			
	a and b	**C**	**D**	
	H_{eff} of Equations 13.b and 13.c		Delay Cracking by 2 years	Accelerate Cracking by 2 years
Flexible	$H_{eff} = H_{HMA}$	---	---	---
Rigid-Good Load Transfer	$H_{eff} = H_{HMA} - 1$	---	---	---
Rigid-Poor Load Transfer	$H_{eff} = H_{HMA} - 3$	---	---	---
Effective Overlay Thickness, H_{eff}, inches	---	---	---	---
<4	---	1.0	0.6	3.0
4 to 6	---	1.0	0.7	1.7
>6	---	1.0	0.8	1.4

NOTES:
1. Minimum recommended H_{HMA} is 2 inches for existing flexible pavements, 3 inches for existing rigid pavements with good load transfer, and 4 inches for existing rigid pavements with poor load transfer.

6.5.2 Verification of the Global Calibration Coefficients

As noted in the previous section on the thermal cracking transfer function, sections 4092, 4093, 4096, and 4420 are semi-rigid pavements that have exhibited the higher lengths of transverse cracking. These measured cracks are probably reflection cracks from the CTB layer. Unfortunately, the cracking (fatigue or shrinkage) in the CTB layer is unknown, so predicting the reflection of unknown amounts of cracks in the existing layers is difficult. In

addition, the flexible or rigid pavements with HMA overlays (sections 1031 and 7028) have also exhibited transverse cracks which are probably reflection cracks from the cracks or joints in the existing HMA and PCC pavements, respectively.

Table 24 summarized the bias of the total area of fatigue cracking for the HMA overlays. The bias was found to be low, but only because many of the test sections have exhibited no to low areas of fatigue cracking (less than 5 percent). It was observed that the MEPDG under predicted the total area of cracking measured on these sections (see Figure 37 and Table 24). It is expected that additional roadway segments with higher amounts of cracking need to be included in the sampling matrix for recalibration.

6.5.3 Georgia Calibration Coefficients

The Georgia fatigue and transverse cracking calibration coefficients discussed in the previous sections of this chapter were used with the global reflection cracking regression coefficients to predict the total amount of cracks. In summary, the global calibration coefficients were found to be applicable to Georgia conditions and rehabilitation strategies.

6.6 IRI or Smoothness

6.6.1 Regression Equation

The following equations were developed from data collected within the LTPP program and are used to predict IRI over time for HMA-surfaced pavements.

Equation for New HMA Pavements and HMA Overlays of Flexible Pavements:

$$IRI = IRI_o + 0.0150(SF) + 0.400(FC_{Total}) + 0.0080(TC) + 40.0(RD) \quad (45)$$

Where:

IRI_o = Initial IRI after construction, in/mi.
SF = Site factor; as defined below.
FC_{Total} = Area of fatigue cracking (combined alligator, longitudinal, and reflection cracking in the wheel path), percent of total lane area. All load related cracks are combined on an area basis – length of cracks is multiplied by 1 foot to convert length into an area basis.
TC = Length of transverse cracking (including the reflection of transverse cracks in existing HMA pavements), ft/mi.
RD = Average rut depth, in.

The site factor (SF) is calculated in accordance with the following equation.

$$SF = Age(0.02003(PI + 1) + 0.007947(\mathrm{Pr}\,ecip + 1) + 0.000636(FI + 1)) \quad (46)$$

Where:

Age = Pavement age, years.
PI = Percent plasticity index of the soil.
FI = Average annual freezing index, degree F days.
$Precip$ = Average annual precipitation or rainfall, in.

Equation for HMA Overlays of Rigid Pavements:

$$IRI = IRI_o + 0.00825(SF) + 0.575(FC_{Total}) + 0.0014(TC) + 40.8(RD) \quad (47)$$

6.6.2 Verification of the Global Calibration Coefficients

Figure 38 includes a comparison of the predicted and measured IRI values for the Georgia LTPP sites. As shown, there is a significant bias in the predicted IRI values. However, the IRI values are predicted using the other predicted distresses (fatigue cracking, rutting, and thermal cracking). If the other distress transfer functions exhibit a significant bias, then it is likely that the IRI regression equation will exhibit bias. Thus, the IRI regression equation should be revised only after the other flexible pavement transfer functions have been recalibrated to eliminate any bias and improve on the goodness-of-fit.

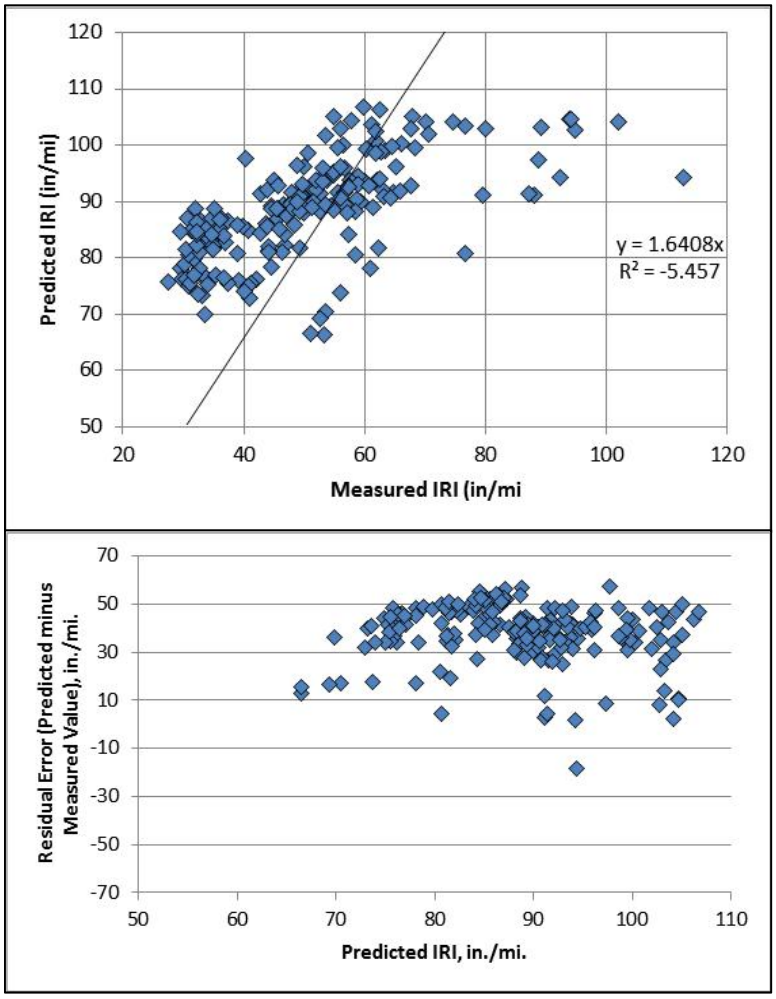

Figure 48—Predicted versus Measured IRI for Flexible, Semi-Rigid, and HMA Overlay Pavements

6.6.3 Georgia Calibration Coefficients

The global calibration coefficients were found to be applicable to the pavement structures used in the Georgia calibration study after the other pavement distress predictions were adjusted to remove any bias. Thus, the global calibration coefficients are recommended for use.

VII. SUMMARY AND CONCLUSIONS

8.1 Major and Appropriate Findings

The number of Georgia LTPP and non-LTPP sites and their developed level of distress are adequate for the calibration process to Georgia conditions and materials from a statistical perspective. The 2010 AASHTO MEPDG Local Calibration Guide includes a general recommendation for a minimum of 18 and 21 flexible and the same for rigid pavement projects. The following summarizes some findings relative to the number of sites.

- The flexible pavements and HMA overlays have a sufficient number of test sections in total, but the SPS-5 project (15 test sections) exhibit significantly different performance characteristics than the other GPS sites located in Georgia. The rutting, fatigue cracking, and longitudinal cracking measured on these sections are believed to be the result of moisture damage or some other material anomaly. These sections were excluded from the local calibration process. A total of 34 flexible pavement sites were used for the calibration.

- There were an insufficient number of semi-rigid pavement sections for the full calibration. As such, the calibration coefficients from other studies were confirmed for use in Georgia.

- The rigid pavements and PCC overlays have a sufficient number of test sections for calibration – a total of 19 were available and used to determine the Georgia calibration coefficients.

The following are some of the other findings:

- Use of the backcalculated elastic layer modulus values significantly reduced the bias of the rut depth transfer function in comparison to the use of laboratory resilient modulus values. Other agencies have reported this same observation. A similar comparison was made between the use of the GDOT default NALS and the global NALS. The use of the GDOT NALS did not significantly lower or increase the bias and standard error of the predicted distresses indicating other factors have a significant impact on performance and the occurrence of distress.

- The resilient modulus of the aggregate base layers is relatively low in comparison to the MEPDG default values for the LTPP test sections, but was higher for the non-LTPP sites. There appears to be a consistent difference between the LTPP and non-LTPP sites which was not explained. The results from the DCP testing confirmed the higher resilient modulus values. Thus, these values were used in setting the default resilient modulus values for use in design.

- The AASHTO C-factor determined for the LTPP subgrade under conventional flexible pavement structures in Georgia are similar to the values recommended for use in the AASHTO Manual of Practice. Conversely, the c-factors for the other

materials and structures are significantly different from the c-factors listed in the MEPDG Manual of Practice (see Table 18).

- The backcalculated mean k-value and the month of measurement for JPCP and CRCP were used iteratively to obtain the input resilient modulus. This input resilient modulus varies between 5,500 to 11,300 psi.

8.2 Georgia Calibration Coefficients

Both LTPP and non-LTPP test sections were used to estimate the precision and bias of the MEPDG transfer functions for predicting the performance indicators (distress and roughness) of GDOT's pavements. The resulting distress prediction models, or transfer functions, can be used to optimize new pavement and rehabilitation design strategies, and used in forecasting of maintenance, repair, rehabilitation, and reconstruction costs.

The remainder of this section lists the GDOT calibration factors for each transfer function for both flexible and rigid pavements. Tables 25 to 28 list the appropriate flexible pavement calibration factors from the GDOT local calibration study, which are included in the baseline files in the GDOT library, and Tables 29 and 31 list the appropriate rigid pavement (JPCP) calibration factors. The calibration coefficients for the IRI regression equation for both the flexible and rigid pavements are not included within this chapter because the local calibration factors are the same as for the global calibration factors – they remained unchanged.

Table 25—GDOT Calibration Coefficients for Asphalt Concrete Rut Depth Transfer Function

Transfer Function Coefficient	Global Value	GDOT Value	
		Neat Mixtures	PMA Mixtures
K1	-3.35412	-2.45	-2.55
K2	1.5606	1.5606	1.5606
K3	0.4791	0.30	0.30
Standard Deviation	$0.24 * Pow(RD, 0.80519) + 0.001$	$0.20 * Pow(RD, 0.55) + 0.001$	
RD = Average rut depth predicted by the Pavement ME Design software.			

Table 26—GDOT Calibration Coefficients for Unbound Layers Rut Depth Transfer Function

Transfer Function Coefficient	Global Value	GDOT Value
Coarse-Grained, Bs1	1.0	0.50
Fine-Grained, Bs1	1.0	0.30
NOTE: The standard deviation equation is unchanged. All of the variance or variability was included in the HMA rut depth prediction equation.		

Table 27—GDOT Calibration Coefficients for Flexible Pavement Bottom-Up Fatigue Cracking Transfer Function

Transfer Function Coefficient	Global Value	GDOT Value (Typical HMA Mixtures)
K1	0.007566	0.00151
K2	3.9492	3.9492
K3	1.281	1.281
C1	1.0	2.2
C2	1.0	2.2
C3	6,000	6,000
Standard Deviation	See Equation 5	See Equation 6
DI_{Bottom} – Damage index for bottom up fatigue or alligator cracking.		

Global Standard Deviation Equation:

$$1.13 + \frac{10}{\left(1 + Exp(7.57 - 15.5 * Log10(DI_{Bottom} + 0.0001)\right)} \quad (48)$$

Where: DI_{Bottom} = Damage index for bottom-up fatigue or alligator cracking

Georgia Standard Deviation Equation:

$$1.0 + \frac{10}{\left(1 + Exp(7.5 - 6.5 * Log10(DI_{Bottom} + 0.0001)\right)} \quad (49)$$

Table 28—GDOT Calibration Coefficients for Asphalt Concrete Thermal Transverse Cracking Transfer Function

Transfer Function Coefficient	Global Value	GDOT Value (Typical HMA Mixtures)
Bt1	1.5	35
Bt3	1.5	35
NOTE: The standard deviation equation remains unchanged because of the high variability and it is recommended that 50 percent reliability be used. If 50 percent reliability is used, the standard deviation has no effect on the final results.		

Table 29—GDOT Calibration Coefficients for JPCP Mid-Slab Cracking Transfer Function

Transfer Function Coefficient	Global Value	GDOT Value
C1	2.0	2.0
C2	1.22	1.22
C4	1.00	0.52
C5	-1.98	-2.17
Standard Deviation	Pow(5.3116*CRACK,0.3903)+ 2.99	3.5522*Pow(CRACK,0.3415)+0.75

Table 30—GDOT Calibration Coefficients for JPCP Faulting Transfer Function

Transfer Function Coefficient	Global Value	GDOT Value
C1	1.0184	0.595
C2	0.91656	1.636
C3	0.0021848	0.00217
C4	0.000883739	0.00444
C5	250	250
C6	0.4	0.47
C7	1.83312	7.3
C8	400	400
Standard Deviation	Pow(0.0097*FAULT,0.5178)+0.014	0.07162*Pow(FAULT,0.368)+0.00806

Table 31—GDOT Calibration Coefficients for CRCP Punchout Transfer Function

Transfer Function Coefficient	Global Value	GDOT Value
C1	2	2
C2	1.22	1.22
C3	216.8421	107.73
C4	33.15789	2.475
C5	-0.58947	-0.785
Standard Deviation	2+2.2593*Pow(PO,0.4882)	2.208*Pow(PO,0.5316)

APPENDIX A—PAVEMENT CROSS SECTION AND STRUCTURE FOR THE LTPP SITES LOCATED IN GEORGIA

Table A.1—New Flexible and Semi-Rigid Pavement Structures for the Georgia LTPP Sites

Section ID	Layer No.	Layer Type	Material Code & Description	Layer Thickness, in.
13-0502	5	Surface	2 – Porous Friction Course	0.9
	4	HMA	1 – Dense Graded HMA	1.9
	3	Stabilized Base	319 – Dense Graded HMA Base	11.2
	2	Aggregate Base	308 – Soil Aggregate Mix; Coarse-Grained; A-1-b	13
	1	Subgrade	215 – Silty Sand with Gravel; A-4	102
13-0503	5	Surface	2 – Porous Friction Course	0.7
	4	HMA	1 – Dense Graded HMA	2.0
	3	Stabilized Base	319 – Dense Graded HMA Base	11.4
	2	Aggregate Base	308 – Soil Aggregate Mix; Coarse-Grained; A-1-b	13
	1	Subgrade	215 – Silty Sand with Gravel; A-4	234
13-0504	5	Surface	2 – Porous Friction Course	0.7
	4	HMA	1 – Dense Graded HMA	2.2
	3	Stabilized Base	319 – Dense Graded HMA Base	11.3
	2	Aggregate Base	308 – Soil Aggregate Mix; Coarse-Grained; A-1-b	13.1
	1	Subgrade	215 – Silty Sand with Gravel; A-4	66
13-0505	5	Surface	2 – Porous Friction Course	1.0
	4	HMA	1 – Dense Graded HMA	2.4
	3	Stabilized Base	319 – Dense Graded HMA Base	11.3
	2	Aggregate Base	308 – Soil Aggregate Mix; Coarse-Grained; A-1-b	13.1
	1	Subgrade	215 – Silty Sand with Gravel; A-4	66
13-0506	5	Surface	2 – Porous Friction Course	0.8
	4	HMA	1 – Dense Graded HMA	2.2
	3	Stabilized Base	319 – Dense Graded HMA Base	11.4
	2	Aggregate Base	308 – Soil Aggregate Mix; Coarse-Grained; A-1-b	13.1
	1	Subgrade	215 – Silty Sand with Gravel; A-4	66
13-0507	5	Surface	2 – Porous Friction Course	0.7
	4	HMA	1 – Dense Graded HMA	2.4
	3	Stabilized Base	319 – Dense Graded HMA Base	11.6
	2	Aggregate Base	308 – Soil Aggregate Mix; Coarse-Grained; A-1-b	13.0
	1	Subgrade	215 – Silty Sand with Gravel; A-4	66
13-0508	5	Surface	2 – Porous Friction Course	0.7
	4	HMA	1 – Dense Graded HMA	1.7
	3	Stabilized Base	319 – Dense Graded HMA Base	11.4
	2	Aggregate Base	308 – Soil Aggregate Mix; Coarse-Grained; A-	13.1

Section ID	Layer No.	Layer Type	Material Code & Description	Layer Thickness, in.
			1-b	
	1	Subgrade	215 – Silty Sand with Gravel; A-4	---
13-0509	5	Surface	2 – Porous Friction Course	0.7
	4	HMA	1 – Dense Graded HMA	1.8
	3	Stabilized Base	319 – Dense Graded HMA Base	11.3
	2	Aggregate Base	308 – Soil Aggregate Mix; Coarse-Grained; A-1-b	13.0
	1	Subgrade	215 – Silty Sand with Gravel; A-4	---
13-0560	5	Surface	2 – Porous Friction Course	0.7
	4	HMA	1 – Dense Graded HMA	1.6
	3	Stabilized Base	319 – Dense Graded HMA Base	15.2
	2	Aggregate Base	308 – Soil Aggregate Mix; Coarse-Grained; A-1-b	15.5
	1	Subgrade	215 – Silty Sand with Gravel; A-4	---
13-0561	5	Surface	2 – Porous Friction Course	0.7
	4	HMA	1 – Dense Graded HMA	1.8
	3	Stabilized Base	319 – Dense Graded HMA Base	15.6
	2	Aggregate Base	308 – Soil Aggregate Mix; Coarse-Grained; A-1-b	15.5
	1	Subgrade	215 – Silty Sand with Gravel; A-4	---
13-0562	5	Surface	2 – Porous Friction Course	0.7
	4	HMA	1 – Dense Graded HMA	1.8
	3	Stabilized Base	319 – Dense Graded HMA Base	15.2
	2	Aggregate Base	308 – Soil Aggregate Mix; Coarse-Grained; A-1-b	15.5
	1	Subgrade	215 – Silty Sand with Gravel; A-4	---
13-0563	5	Surface	2 – Porous Friction Course	0.8
	4	HMA	1 – Dense Graded HMA	2.2
	3	Stabilized Base	319 – Dense Graded HMA Base	15.1
	2	Aggregate Base	308 – Soil Aggregate Mixture; Coarse-Grained	15.5
	1	Subgrade	215 – Silty Sand with Gravel; A-4	36
13-0564	5	Surface	2 – Porous Friction Course	0.7
	4	HMA	1 – Dense Graded HMA	1.7
	3	Stabilized Base	319 – Dense Graded HMA Base	15.2
	2	Aggregate Base	308 – Soil Aggregate Mix; Coarse-Grained; A-1-b	15.5
	1	Subgrade	215 – Silty Sand with Gravel; A-4	---
13-0565	5	Surface	2 – Porous Friction Course	1.0
	4	HMA	1 – Dense Graded HMA	2.0
	3	Stabilized Base	319 – Dense Graded HMA Base	15.6
	2	Aggregate Base	308 – Soil Aggregate Mix; Coarse-Grained; A-1-b	15.5
	1	Subgrade	215 – Silty Sand with Gravel; A-4	60
13-0566	5	Surface	2 – Porous Friction Course	0.6

Section ID	Layer No.	Layer Type	Material Code & Description	Layer Thickness, in.
	4	HMA	1 – Dense Graded HMA	1.7
	3	Stabilized Base	319 – Dense Graded HMA Base	14.4
	2	Aggregate Base	308 – Soil Aggregate Mix; Coarse-Grained; A-1-b	15.5
	1	Subgrade	215 – Silty Sand with Gravel; A-4	---
13-1001	4	HMA	1 – Dense Graded HMA	1.7
	3	HMA	1 – Dense Graded HMA	6.4
	2	Aggregate Base	304 – Crushed Gravel	8.6
	1	Subgrade	145 – Sandy Silt; A-7-6	---
13-1004	4	HMA	1 – Dense Graded HMA	1.9
	3	HMA	1 – Dense Graded HMA	4.9
	2	Aggregate Base	308 – Soil Aggregate Mix; Coarse-Grained; A-1-b	7.6
	1	Subgrade	114 – Sandy Lean Clay; A-5	---
13-1005	4	HMA	1 – Dense Graded HMA	1.4
	3	HMA	1 – Dense Graded HMA	6.2
	2	Aggregate Base	308 – Soil Aggregate Mix; Coarse-Grained; A-1-a	8.8
	1	Subgrade	216 – Clayey Sand; A-4	---
13-1031	5	Surface	2 – Porous Friction Course	0.6
	4	HMA	1 – Dense Graded HMA	2.4
	3	HMA	1 – Dense Graded HMA	8.2
	2	Embankment	309 – Fined-Grained Soil; A-2-4	8.8
	1	Subgrade	214 – Silty Sand; A-1-b	---
13-4092	4	HMA	1 – Dense Graded HMA	1.2
	3	HMA	1 – Dense Graded HMA	4.5
	2	Stabilized Soil	339 – Soil Cement	8.3
	1	Subgrade	216 – Clayey Sand; A-2-4	---
13-4093	4	HMA	1 – Dense Graded HMA	1.2
	3	HMA	1 – Dense Graded HMA	4.6
	2	Stabilized Soil	339 – Soil Cement	7.8
	1	Subgrade	216 – Clayey Sand; A-2-4	156
13-4096	4	HMA	1 – Dense Graded HMA	1.3
	3	HMA	1 – Dense Graded HMA	2.8
	2	Stabilized Soil	339 – Soil Cement	6.3
	1	Subgrade	216 – Clayey Sand; A-3	---
13-4111	4	Surface	2 – Porous Friction Course	0.7
	3	HMA	1 – Dense Graded HMA	8.1
	2	Aggregate Base	308 – Soil Aggregate Mix; Coarse-Grained; A-1-a	8.2
	1	Subgrade	113 – Sandy Clay; A-6	---
13-4112	4	Surface	72 – Slurry Seal Coat	0.1
	3	HMA	1 – Dense Graded HMA	3.1

Section ID	Layer No.	Layer Type	Material Code & Description	Layer Thickness, in.
	2	HMA	319 – Dense Graded HMA Base	12.7
	1	Subgrade	202 – Poorly Graded Sand; A-3	---
13-4113	4	Surface	71 – Chip Seal/Seal Coat	0.1
	3	HMA	1 – Dense Graded HMA	3.6
	2	Stablized Base	321 – Asphalt Stabilized/Treated Base	11.5
	1	Subgrade	204 – Poorly Graded Sand with Silt; A-3	---
13-4119	5	Surface	2 – Porous Friction Course	0.8
	4	HMA	1 – Dense Graded HMA	1.8
	3	HMA	319 – Dense Graded HMA Base	13.8
	2	Aggregate Base	308 – Soil Aggregate Mix; Coarse-Grained; A-1-a	16.4
	1	Subgrade	145 – Sandy Silt; A-4	48
13-4420	4	HMA	1 – Dense Graded HMA	1.7
	3	HMA	1 – Dense Graded HMA	2.9
	2	Stabilized Soil	339 – Soil Cement	7.9
	1	Subgrade	214 – Silty Sand; A-2-4	---

Table A.2—Rehabilitated Flexible and Semi-Rigid Pavement Structures for the Georgia LTPP Sites

[NOTE: The layers for the existing pavement structure are provided in Table A.1; the information included in this table is only for the rehabilitation.]

Section ID	Layer No.	Layer Type	Material Code & Description	Layer Thickness, in.
13-0502	7	Overlay	2 – Porous Friction Course	1.0
	6	Overlay	1 – Dense Graded HMA with RAP	1.6
			No milling of the existing pavement structure	---
13-0503	8	Overlay	2 – Porous Friction Course	1.1
	7	Overlay	1 – Dense Graded HMA with RAP	1.4
	6	Overlay	1 – Dense Graded HMA with RAP	3.8
			Milling used to remove surface	---
	5	Surface	2 – Porous Friction Course	0.0
	4	HMA	1 – Dense Graded HMA	1.4
13-0504	8	Overlay	2 – Porous Friction Course	0.9
	7	Overlay	1 – Dense Graded HMA	1.4
	6	Overlay	1 – Dense Graded HMA	3.9
			Milling used to remove surface	---
	5	Surface	2 – Porous Friction Course	0.0
	4	HMA	1 – Dense Graded HMA	1.6
13-0505	7	Overlay	2 – Porous Friction Course	1.0
	6	Overlay	1 – Dense Graded HMA	1.4
			Milling used to remove surface	---
	5	Surface	2 – Porous Friction Course	0.0
	4	HMA	1 – Dense Graded HMA	1.8
13-0506	8	Overlay	2 – Porous Friction Course	1.0
	7	Overlay	1 – Dense Graded HMA	1.8
	6	Overlay	1 – Dense Graded HMA	2.4
			Milling used to remove surface	---
	5	Surface	2 – Porous Friction Course	0.0
	4	HMA	1 – Dense Graded HMA	0.0
13-0507	8	Overlay	2 – Porous Friction Course	0.8
	7	Overlay	1 – Dense Graded HMA	1.3
	6	Overlay	1 – Dense Graded HMA	4.6
			Milling used to remove surface	---
	5	Surface	2 – Porous Friction Course	0.0
	4	HMA	1 – Dense Graded HMA	1.6
13-0508	8	Overlay	2 – Porous Friction Course	0.9
	7	Overlay	1 – Dense Graded HMA with RAP	1.3
	6	Overlay	1 – Dense Graded HMA with RAP	5.4
			Milling used to remove surface	---
	5	Surface	2 – Porous Friction Course	0.0
	4	HMA	1 – Dense Graded HMA	0.0

Table A.2—Rehabilitated Flexible and Semi-Rigid Pavement Structures for the Georgia LTPP Sites (Continued)

[NOTE: The layers for the existing pavement structure are provided in Table A.1; the information included in this table is only for the rehabilitation.]

Section ID	Layer No.	Layer Type	Material Code & Description	Layer Thickness, in.
13-0509	8	Overlay	2 – Porous Friction Course	1.0
	7	Overlay	1 – Dense Graded HMA with RAP	2.0
	6	Overlay	1 – Dense Graded HMA with RAP	2.1
			Milling used to remove surface	---
	5	Surface	2 – Porous Friction Course	0.0
	4	HMA	1 – Dense Graded HMA	0.4
13-0560	8	Overlay	2 – Porous Friction Course	0.7
	7	Overlay	1 – Dense Graded HMA with RAP	1.2
	6	Overlay	1 – Dense Graded HMA with RAP	1.1
			Milling used to remove surface	---
	5	Surface	2 – Porous Friction Course	0.0
	4	HMA	1 – Dense Graded HMA	1.3
13-0561	8	Overlay	2 – Porous Friction Course	1.1
	7	Overlay	1 – Dense Graded HMA with RAP	1.1
	6	Overlay	1 – Dense Graded HMA with RAP	1.9
			Milling used to remove surface	---
	5	Surface	2 – Porous Friction Course	0.0
13-0562	8	Overlay	2 – Porous Friction Course	0.9
	7	Overlay	1 – Dense Graded HMA	1.4
	6	Overlay	1 – Dense Graded HMA	2.1
			Milling used to remove surface	---
	5	Surface	2 – Porous Friction Course	0.0
	4	HMA	1 – Dense Graded HMA	1.6
13-0563	7	Overlay	2 – Porous Friction Course; Inlay	1.1
	6	Overlay	1 – Dense Graded HMA; Inlay	2.3
			Milling used to remove surface	---
	5	Surface	2 – Porous Friction Course	0.0
	4	HMA	1 – Dense Graded HMA	0.0
13-0564	7	Overlay	1 – Dense Graded HMA with RAP; Inlay	1.0
	6	Overlay	1 – Dense Graded HMA with RAP; Inlay	2.3
			Milling used to remove surface	---
	5	Surface	2 – Porous Friction Course	0.0
	4	HMA	1 – Dense Graded HMA	0.0
13-0565	8	Overlay	2 – Porous Friction Course	0.9
	7	Overlay	1 – Dense Graded HMA; with RAP; Inlay	1.2
	6	Overlay	1 – Dense Graded HMA; with RAP; Inlay	3.3
			Milling used to remove surface	---
	5	Surface	2 – Porous Friction Course	0.0
	4	HMA	1 – Dense Graded HMA	1.9

Table A.2—Rehabilitated Flexible and Semi-Rigid Pavement Structures for the Georgia LTPP Sites (Continued)

[NOTE: The layers for the existing pavement structure are provided in Table A.1; the information included in this table is only for the rehabilitation portion.]

Section ID	Layer No.	Layer Type	Material Code & Description	Layer Thickness, in.
13-0566	8	Overlay	2 – Porous Friction Course	0.8
	7	Overlay	1 – Dense Graded HMA; Inlay	1.3
	6	Overlay	1 – Dense Graded HMA; Inlay	4.2
			Milling used to remove surface	---
	5	Surface	2 – Porous Friction Course	0.0
	4	HMA	1 – Dense Graded HMA	0.0
13-1001			Maintenance activity applied.	
13-1004			Maintenance activity applied.	
13-1005			Maintenance activity applied.	
13-1031	6	Overlay	2 – Porous Friction Course	0.9
			Milling used to remove surface	---
	5	Surface	2 – Porous Friction Course	0.0
13-4092			Maintenance activity applied.	
13-4093			Maintenance activity applied.	
13-4096	6	Overlay	13 – RAP Overlay; Plant Produced	1.4
	5	Overlay	71 – Seal Coat/Chip Seal	0.3
13-4112			Maintenance activity applied.	
13-4113	5	Overlay	1 – Dense Graded HMA	1.8
13-4119			Maintenance activity applied.	
13-4420	6	Overlay	1 – Dense Graded HMA	1.1
	5	Overlay	1 – Dense Graded HMA	0.7

Table A.3—New Rigid Pavement Structures for the Georgia LTPP Sites

Section ID	Layer No.	Layer Type	Material Code & Description	Layer Thickness, in.
13-3007	3	PCC	4 – Jointed Plain Concrete	9.3
	2	Aggregate Base	308 – Soil Aggregate Mix; Coarse-Grained; A-1-b	9.0
	1	Subgrade	145 – Sandy Silt; A-2-4	---
13-3011	4	PCC	4 – Jointed Plain Concrete	10.1
	3	Treated Base	319 – Dense Graded HMA Base	0.9
	2	Treated Soil	339 – Soil Cement	4.7
	1	Subgrade	214 – Silty Sand; A-2-4	---
13-3015	4	PCC	4 – Jointed Plain Concrete	10.0
	3	Treated Base	78 – Asphalt Concrete Inerlayer	1.0
	2	Treated Soil	339 – Soil Cement	5.7
	1	Subgrade	202 – Poorly Graded Sand; A-2-4	---
13-3016	4	PCC	4 – Jointed Plain Concrete	11.1
	3	Treated Base	319 – Dense Graded HMA Base	1.4
	2	Aggregate Base	308 – Soil Aggregate Mix; Coarse-Grained; A-1-a	5.0
	1	Subgrade		60
13-3017	3	PCC	4 – Jointed Plain Concrete	9.9
	2	Treated Base	331 – Cement Treated Base	6.1
	1	Subgrade	214 – Silty Sand; A-5	144
13-3018	3	PCC	4 – Jointed Plain Concrete	9.9
	2	Treated Base	331 – Cement Treated Base	5.8
	1	Subgrade	216 – Clayey Sand; A-4	---
13-3019	3	PCC	4 – Jointed Plain Concrete	9.1
	2	Aggregate Base	308 – Soil Aggregate Mix; Coarse-Grained; A-1-a	7.2
	1	Subgrade	114 – Sandy Lean Clay; A-7-5	---
13-3020	3	PCC	4 – Jointed Plain Concrete	9.1
	2	Treated Soil	339 – Soil Cement	5.4
	1	Subgrade	216 – Clayey Sand; A-6	---
13-4118	2	PCC	4 – Jointed Plain Concrete	7.8
	1	Subgrade	216 – Clayey Sand; A-4	---
13-5023	3	PCC	6 – Continuously Reinforced Concrete	8.4
	2	Treated Soil	339 – Soil Cement	5.5
	1	Subgrade	202 – Poorly Graded Sand; A-3	---

Table A.4—Rehabilitated Rigid Pavement Structures for the Georgia LTPP Sites
[NOTE: The layers for the existing pavement structure are provided in Table A.3; the information included in this table is only for the rehabilitation.]

Section ID	Layer No.	Layer Type	Material Code & Description	Layer Thickness, in.
13-3017			Maintenance activity applied.	
13-3020			Maintenance activity applied.	
13-4118	3	Overlay, PCC	6 – Continuously Reinforced Concrete	8.4
13-7028	This PCC pavement already had an HMA overlay when it was included in the LTPP database			
13-7028	7	Overlay	1 – Dense Graded HMA	3.4
	6	Overlay	72 – Chip Seal/Seal Coat	0.1
	5	Overlay	1 – Dense Graded HMA	2.6
	4	PCC	4 – Jointed Plain Concrete	9.1
	3	Treated Base	321 – Asphalt Treated Base	3.1
	2	Aggregate Base	310 – Other Base Material; A-1-b	3.9
	1	Subgrade	216 – Clayey Sand; A-4	---
13-7028			Maintenance activity applied.	
13-7028	8	2nd Overlay	1 – Dense Graded HMA	2.5
			Milling used to remove surface	---
	7	Overlay	1 – Dense Graded HMA	1.9

REFERENCES

AASHTO, Mechanistic-Empirical Pavement Design Guide, Interim Edition: A Manual of Practice, Publication Number AASHTO MEPDG-1, Washington, DC, 2008.

AASHTO, Guide for the Local Calibration of the Mechanistic-Empirical Pavement Design Guide, Publication Number AASHTO LCG-1, Washington, DC, 2010.

AASHTO, Pavement ME Design™ website: http://www.me-design.com/MEDesign/Index.html.

Darter, Michael I., Leslie Titus-Glover, and Harold L. Von Quintus, *Implementation of the Mechanistic-Empirical Pavement Design Guide in Utah: Validation, Calibration, and Development of the UDOT MEPDG User's Guide*, Report No. UT-09.11, Utah Department of Transportation, Research and Materials Division, Salt Lake City, Utah, October 2009.

Darter, Michael I., Jagannath Mallela, Leslie Titus-Glober, Biplab Bhattacharya, and Harold L. Von Quintus, *Calibration and Implementation of the AASHTO Mechanistic-Empirical Pavement Design Guide in Arizona*, Report Number FHWA-AZ-14-606, Project Number SPR 606, Arizona Department of Transportation, Phoenix, Arizona, September 2014.

Federal Highway Administration, Distress Identification Manual for Long Term Pavement Performance Program, Fourth Revised Edition, Publication Number FHWA-RD-03-031, Federal Highway Administration, Washington, DC, 2003.

Kim, Sung-Hee, *Measurements of Dynamic and Resilient Moduli of Roadway Test Sites*, Final Report, Research Project Number 12-07, Georgia Department of Transportation, Office of Materials and Research, Research and Development Branch, Forest Park, Georgia, December 2013.

Kim, Sung-Hee, *Determination of Coefficient of Thermal Expansion for Portland Cement Concrete Pavements for MEPDG Implementation*, Final Report, Research Project Number 10-04, Georgia Department of Transportation, Office of Materials and Research, Research and Development Branch, Forest Park, Georgia, October 2012.

Mallela, Jagannath, M.I. Darter, C. Rao, S. Sadasivam, L. Titus-Glover, H.L. Von Quintus, and M. Stanley, *Implementing the AASHTO Mechanistic-Empirical Pavement Design Guide in Missouri: Volume I—Study Findings, Conclusions, and Recommendations; Volume II—MEPDG Model Validation and Calibration*, MODOT Study #R104-002, Missouri Department of Transportation, Pavement Section Investigation Report, Jefferson City, Missouri, March 2009.

NCHRP, *Refining the Calibration and Validation of Hot Mix Asphalt Performance Models: An Experimental Plan and Database*, Research Results Digest 284, National Cooperative Highway Research Program, Transportation Research Board, Washington, DC, 2003.

NCHRP, *Jackknife Testing—An Experimental Approach to Refine Model Calibration and Validation*, Research Results Digest Number 283, National Cooperative Highway Research Program, Transportation Research Board, Washington, DC, 2003.

National Cooperative Highway Research Program (NCHRP), MEPDG reports: http://onlinepubs.trb.org/onlinepubs/archive/mepdg/guide.htm.

NCHRP, *Guide for Mechanistic-Empirical Design of New and Rehabilitated Structures*, NCHRP Report 01-37A, National Cooperative Highway Research Program, Transportation Research Board, Washington, DC, 2004.

National Cooperative Highway Research Program, *Changes to the Mechanistic-Empirical Pavement Design Guide Software Through Version 0.900,* NCHRP Research Results Digest 308, NCHRP Project 1-40D, Transportation Research Board, National Research Council, Washington, DC, 2006.

Sachs, S., J. Vandenbossche, M. Snyder, *Developing Recalibrated Concrete Pavement Performance Models for the Mechanistic-Empirical Pavement Design Guide*, NCHRP Project 20-07, Task 327, Transportation Research Board, 2014.

Selezneva, Olga and Harold L. Von Quintus, *Traffic Load Spectra for Implementing and Using the Mechanistic-Empirical Pavement Design Guide in Georgia*, Final Report, Research Project #10-09, Georgia Department of Transportation, Office of Materials and Research, Research and Development Branch, Forest Park, Georgia, January 2014.

Von Quintus, Harold L. and Brian Killingsworth, *Analyses Relating to Pavement Material Characterization and Their Effects on Pavement Performance*, Report No. FHWA-RD-97-085, Federal Highway Administration, Office of Engineering R&D, McLean, Virginia, January 1998.

Von Quintus, H.L. and J.S. Moulthrop, *Mechanistic-Empirical Pavement Design Guide Flexible Pavement Performance Prediction Models*, Report No. FHWA/MT-07-008/8158-1, Submitted to Montana Department of Transportation, Helena, MT, 2007. http://www.mdt.mt.gov/research/docs/research_proj/pave_model/volumei.pdf

Von Quintus, Harold L. and Rohan Perera, *Extending the Life of Asphalt Pavements*, Report #RC-1551, Michigan Department of Transportation, Office of Research and Best Practices, Lansing, Michigan; May 2011.

Von Quintus, H.L., J. Mallela, R. Bonaquist, C.W. Schwartz, R.L. Carvalho, *Calibration of Rutting Models for Structural and Mix Design*, NCHRP Report No. 719, National Cooperative Highway Research Program, Transportation Research Board, Washington, DC, 2012. http://onlinepubs.trb.org/onlinepubs/nchrp/nchrp_rpt_719.pdf

Von Quintus, Harold L., et al., *Calibration of Rutting Models for HMA Structural and Mixture Design*, NCHRP Report #719 (NCHRP Project Number 9-30A), National

Cooperative Highway Research Program, Transportation Research Board, Washington, DC, August 30, 2012.

Yau, Amber, and Harold L. Von Quintus, *Study of LTPP Laboratory Resilient Modulus Test Data and Response Characteristics*, Publication Number FHWA-RD-02-051, Federal Highway Administration, Washington, DC, 2002.

[This Page Intentionally left blank.]